FAKULTÄT FÜR MEDIZIN DER TECHNISCHEN UNIVERSTÄT MÜNCHEN

STUDY OF ALPHA-SYNUCLEIN FRAGMENTS AND THEIR INVOLVEMENT IN SPREADING OF PATHOLOGY:

NEW INSIGHTS FOR IMMUNOTHERAPIES

TASNIM CHAKROUN

Vollständiger Abdruck der von der Fakultät für Medizin der Technischen Universität München zur Erlangung des akademischen Grades einer Doktorin der Naturwissenschaften (Dr.rer.nat) genehmigten Dissertation.

Vorsitzender: Prof. Dr. Mikael Simons

Prüfer der Dissertation:

1. Prof. Dr. Stefan Lichtenthaler
2. Prof. Dr. Aphrodite Kapurniotu

Die Dissertation wurde am 20.07.2020 bei der Technischen Universität München eingereicht und durch die Fakultät für Medizin am 16.03.2021 angenommen.

To my parents, my husband, and my Adam

Contents

Abbreviations 7
ABSTRACT 8
Zusammenfassung 9
1. INTRODUCTION 10
1.1. Synucleinopathies 10
1.1.1. Parkinson's disease 10
1.1.2. Dementia with Lewy bodies 11
1.1.3. Multiple system atrophy 11
1.2. The alpha-synuclein protein 12
1.2.1. The synuclein family 12
1.2.2. The *SNCA* gene 13
1.2.3. Structure and biophysical properties 15
1.2.4. Physiological functions 16
1.2.5. Post-translational modifications 18
1.2.6. Role in neurodegenerative diseases 20
1.3. The LUHMES cell model 24
2. SPECIFIC AIMS 26
3. EXPERIMENTAL PROCEDURES 27
3.1. Cell culture 27
3.2. Transduction with adenoviral vectors 27
3.3. Treatments with recombinant αSyn 27
3.4. Generation of αSyn knockout LUHMES cell line by CRISPR-Cas9 genome editing 28
3.5. Western blotting 29
3.6. LC-MS analysis 31
3.7. Proteomic data analysis 31
3.8. Human protease array 32
3.9. *In vitro* cleavage assay 32
3.10. *In vitro* Protease inhibition 32
3.11. Conditioned medium uptake assay 33
3.12. Recombinant protein labeling and uptake assays 33
3.13. LDH assay 34
3.14. Cell-free aggregation assays 34
3.15. Dynamic light scattering measurements 35
3.16. Proteinase K digestion 35
3.17. Toxicity blocking with antibodies 36
3.18. Statistical Analysis 36
4. RESULTS 37
4.1. Analysis of αSyn species released from αSyn-overexpressing neurons 37
4.2. Extracellular αSyn fragments result from multiple truncation events 37
4.3. Fragments result from extracellularly processed full-length αSyn 39
4.4. Several proteases are present in the conditioned medium of LUHMES cells 41
4.5. The serine protease plasmin is involved in the cleavage of αSyn in the extracellular space 41
4.6. Extracellularly generated αSyn fragments can be taken up by naïve αSyn knockout cells 44
4.7. Recombinant αSyn fragments differentially influence the aggregation of FL-αSyn .. 46
4.8. Aggregates generated with αSyn recombinant fragments have distinct seeding properties in a second aggregation cycle 49
4.9. Recombinant αSyn fragments are taken up by LUHMES neurons 49

4.10. αSyn fragments 1-95 and 61-140 result in different intracellular aggregation patterns 52
4.11. Fragment-seeded intracellular aggregation requires endogenous αSyn 53
4.12. αSyn fragments 61-140 and 1-95 induce toxicity that can be prevented with domain-specific antibodies 55
5. DISCUSSION 58
5.1. Biological fragments versus recombinant fragments 58
5.2. Biological relevance of αSyn fragments 59
5.3. Spreading of αSyn fragments versus fibrils 60
5.4. Proteolytic cleavage of αSyn 61
5.5. Aggregation characteristics of αSyn fragments 62
5.6. αSyn fragments and implications for strains 62
5.7. Immunoreactivity of fragment-induced aggregates: implications for immunotherapeutical approaches 63
6. SUMMARY AND SIGNIFICANCE 65
7. ACKNOWLEDGEMENT 66
8. DECLARATION OF CONTRIBUTIONS 67
9. REFERENCES 68
10. LIST OF PUBLICATIONS 83

List of Figures

Introduction

Figure 1.1: Immunohistochemistry stainings of αSyn inclusions in different synucleinopathies…… 12
Figure 1.2: Phylogenetic tree and sequence alignment of the synuclein family members……... 13
Figure 1.3: The SNCA gene and the αSyn splicing isoforms…….. 14
Figure 1.4: Structural features of monomeric αSyn…… 16
Figure 1.5: Overview of most known αSyn PTMs……. 19
Figure 1.6: Aggregation pathway of αSyn…….. 20
Figure 1.7: Release and uptake pathways of αSyn…….. 22
Figure 1.8: Intracellular processes disrupted by pathological αSyn…… 24
Figure 1.9: Characterization of LUHMES cells as dopaminergic neurons……. 25

Results

Figure 4.1: αSyn fragments in the conditioned medium of αSyn-overexpressing LUHMES neurons……... 38
Figure 4.2: Identification of extracellular αSyn fragments…… 39
Figure 4.3: Extracellular generation of αSyn fragments and screening of proteases present in LUHMES cells CM…… 40
Figure 4.4: Identification of the protease responsible for extracellular cleavage of αSyn…… 43
Figure 4.5: The αSyn knockout (KO) LUHMES cell line and uptake of CM-generated αSyn fragments…… 45
Figure 4.6: Recombinant αSyn fragments show distinct effects on aggregation of full-length αSyn in a cell-free aggregation assay……... 47
Figure 4.7: Seeding properties of aggregates generated with recombinant αSyn fragments in the second aggregation cycle……. 50
Figure 4.8: Uptake of recombinant αSyn fragments by naïve WT LUHMES neurons.. 51
Figure 4.9: αSyn fragments induce different aggregation patterns in LUHMES neurons..... 52
Figure 4.10: αSyn fragments recruit endogenous αSyn and induce long lasting aggregation…….. 54
Figure 4.11: Intracellular seeding-potent αSyn fragments also induce toxicity..…… 56
Figure 4.12: αSyn fragments-mediated toxicity can be rescued by domain specific antibodies……. 57

Discussion

Figure 5.1: Summary of fragment generation and spreading model in LUHMES cells. 59

List of Tables

Table 1: Overview of used recombinant αSyn…….. 28
Table 2: Overview of antibodies used for Western blotting……. 30
Table 3: Overview of used protease inhibitors……. 33
Table 4: List of Proteases detected in CM of untreated control and αSyn-overexpressing cells……... 42
Table 5: Plasmin cleavage sites on αSyn…….. 44

Abbreviations

AV	Adenovirus
CM	Conditioned medium
DAPI	4′,6-diamidino-2-phenylindole
DIV	Days *in vitro*
DPT	Days post transduction
DLB	Dementia with Lewy bodies
DLS	Dynamic light scattering
FL-αSyn	Full-length alpha-synuclein
FRU	Relative fluorescence unit
GCI	Glial cytoplasmic inclusion
GFP	Green fluorescent protein
KO	Knockout
LB	Lewy bodie
LC-MS	Liquid chromatoghraphy-mass spectrometry
LDH	Lactate dehydrogenase
LN	Lewy neurite
LUHMES	Lund human mesencephalic
MSA	Multiple system atrophy
NAC	Non amyloid component
PD	Parkinson's disease
PFFs	Pre-formed fibrils
PIC	Protease inhibitor cocktail
PK	Proteinase K
PTM	Post translational modification
ThT	Thioflavin T
WB	Western Blot
WT	Wild-type
αSyn	Alpha-synuclein
βSyn	Beta-synuclein
γSyn	Gamma-synuclein

ABSTRACT

Synucleinopathies affect a considerable part of the aging population, and lead to severe symptoms mainly related to progressive neurodegeneration. Due to their highly complex etiology, disease-modifying therapies remain so far unavailable. Alpha-synuclein (αSyn) accumulation is considered a common pathophysiological event of all synucleinopathies. αSyn itself is, however, one of main challenges standing in the way of developping efficient therapies. First, its functions in health and disease continue to be largely unknown despite several decades of research. Secondly, the ability of αSyn to form various intra and extracellular species during aggreation and spreading makes identifiying and targeting neurotoxic species difficult.

The present work aimed to gain a deeeper understanding of relevant αSyn species that are involved in disease spreading. I particularly focused on αSyn fragments, and used a systematic approach to determine their implication in pathological events. Through a comparative and proof-of-principle methodology, I showed that two different αSyn fragments, αSyn 1-95 and 61-140, fulfill all the criteria of a spreading species. Furthermore, they efficiently instigated the aggregation of full-length αSyn, both in a human dopaminergic neurons cell model, and in a cell-free assay. Interestingly, these fragments seem to have the ability to determine specific aggregation pathways. Indeed, fragment-seeded aggregates had distinct aggregation kinetics and patterns, as well as an enhanced proteinase K resistance in comparison to full-length αSyn. Furthermore, they induced a slow-onset toxicity that could be reduced with domain specific antibodies. Additionally, these aggregates were only detectable by specific antibodies. The results presented in this this work suggest that αSyn fragments might be relevant not only for spreading, but also for aggregation-fate determination and differential strain formation. The present thesis describes new insights on the nature of such aggregates and on the possible pivotal role of proteases in the pathogenesis of synucleinopathies.

Zusammenfassung

Synucleinopathien betreffen einen beträchtlichenTeil der alternden Bevölkerung und führen zu schweren Symptomen, die sich hauptsächlich auf eine fortschreitende Neurodegeneration zurückzuführen lassen. Aufgrund ihrer hochkomplexen Ätiologie sind krankheitsmodifizierende Therapien bislang nicht verfügbar. Die Anreicherung des Proteins Alpha-Synuclein (αSyn) wird als häufiges pathophysiologisches Ereignis aller Synucleinopathien angesehen. αSyn selbst ist jedoch eine der Hauptherausforderungen, die der Entwicklung effizienter Therapien im Wege stehen. Erstens sind seine Funktionen in Bezug auf Gesundheit und Krankheit trotz jahrzehntelanger Forschung weitgehend unbekannt. Zweitens erschwert die Fähigkeit von αSyn, während der Aggreation und Ausbreitung verschiedene intra- und extrazelluläre Spezies zu bilden, die Identifizierung und gezielte Bekämpfung neurotoxischer Spezies.

Die vorliegende Arbeit zielte darauf ab ein besseres Verständnis der relevanten αSyn-Arten, die an der Ausbreitung von Synucleinopathien beteiligt sind, zu erlangen. Ich habe mich besonders auf αSyn-Fragmente konzentriert und einen systematischen Ansatz verwendet, um ihre Bedeutung für pathologische Ereignisse zu bestimmen. Durch eine Vergleichs- und 'Proof-of-Principle'-Methode habe ich gezeigt, dass zwei verschiedene αSyn-Fragmente, αSyn 1-95 und 61-140, alle Kriterien einer sich ausbreitenden Spezies erfüllen. Darüber hinaus initiierten sie effizient die Aggregation von αSyn, sowohl in einem Zellmodell mit humanen dopaminergen Neuronen als auch in einem zellfreien Versuchsansatz. Interessanterweise scheinen diese Fragmente die Fähigkeit zu haben spezifische Aggregationswege zu bestimmen. In der Tat zeigten Fragment-Seed-Aggregate unterschiedliche Aggregationskinetiken und -muster sowie eine erhöhte Proteinase-K-Resistenz im Vergleich zu αSyn. Darüber hinaus induzierten sie eine langsam einsetzende Toxizität, die mit domänenspezifischen Antikörpern verringert werden konnte. Außerdem waren die gebildeten Aggregate nur durch spezifische Antikörper nachweisbar. Die in dieser Arbeit vorgestellten Ergebnisse legen nahe, dass αSyn-Fragmente nicht nur für die Ausbreitung, sondern auch für die Bestimmung des Aggregationsschicksals und die Bildung differenzieller Stämme relevant sein könnten. Die vorliegende Arbeit beschreibt neue Erkenntnisse über die Natur solcher Aggregate und über die möglicherweise zentrale Rolle von Proteasen bei der Pathogenese von Synucleinopathien.

1. INTRODUCTION

1.1. Synucleinopathies

Synucleinopathies are a group of neurodegenerative diseases that include Parkinson's disease (PD), dementia with Lewy bodies (DLB), and multiple system atrophy (MSA). They have several characteristics in common such as the affection of the motor and cognitive neurological spheres, as well as progression from one brain region to another in a stereotyped fashion (Alegre-Abarrategui et al., 2019). Such progression is pathologically marked by neuronal cell death, coinciding with abnormal accumulation and deposition of insoluble, alpha-synuclein-(αSyn)-rich, intracellular inclusions (Papp et al., 1989, Spillantini et al., 1998b). Synucleinopathies affect primarily the aging population, and with the increased life expectancy world-wide, the prevalence of such neurodegenerative disorders is expected to increase in the next decades (Bach et al., 2011, Savica et al., 2013). Notably, there are currently no disease-modifying therapies available for these devastating disorders.

1.1.1. Parkinson's disease

A complete description of the shaking palsy was first provided in 1817 by James Parkinson (Parkinson, 1817). The disease was later renamed after him by the French neurologist Jean-Martin Charcot (Charcot et al., 1878). PD is the most common synucleinopathy, and is characterized by the selective and progressive loss of dopaminergic neurons in the midbrain. The resulting depletion of dopamine levels leads to characteristic motor symptoms that include muscle rigidity, resting tremors, bradykinesia and impaired posture and balance (Lim et al., 2002). Non motor symptoms such as autonomic dysfunction, cognitive decline, sensory abnormalities, and sleep disorders can either precede the motor symptoms or develop as the disease progresses (Jankovic, 2008). Symptomatic therapies like dopamine replacement and deep brain stimulation have proven to be relatively successful in ameliorating the motor symptoms. However, their benefits are limited in time and dissipate at advanced stages of the disease (Hauser, 2010). The PD pathology is characterized on the cellular level by the presence of neuronal cytoplasmic inclusions called Lewy bodies (LBs) and neuritic threads called Lewy neurites (LNs), which consist mainly of filamentous αSyn aggregates (Figure1.1) (Spillantini et al., 1997, Spillantini et al., 1998b, Braak et al., 2003).

The majority of PD cases are considered sporadic, and are strongly linked to environmental factors including exposure to pesticides (Franco et al., 2010). Genetic causes on the other hand account for 5 to 10% of total diagnosed PD cases (Lesage and Brice, 2009). They can have, either dominantly or recessively inherited disease forms deriving from mutations on several specific

genes. The number of risk-genes associated with PD is consistantly increasing and includes so far 15 well-established candidates (Chang et al., 2017, Billingsley et al., 2018).

1.1.2. Dementia with Lewy bodies

DLB is the second most common synucleinopathy (Peng et al., 2018b). And after Alzheimer's disease (AD), the most common cause of neurodegenerative dementia (McKeith et al., 1996). Histologically, DLB is mainly characterized by the presence of LBs. In most DLB cases however, LBs can coexist with other lesions such as LNs, and AD pathology, predominantly β-amyloid deposition and diffuse plaques (Halliday et al., 2011). Cortical and midbrain regions are affected in DLB, which cause a progressive decline in mental faculties. Most common clinical symptoms include visual hallucinations, parkisonian movement disorder, sensory alteration and autonomic failure (McKeith et al., 1996). Most DLB cases are sporadic, nevertheless, some familial cases were reported in the past. Recently, the first genome wide association study in DLB revealed common genetic risk factors with both AD and PD (Orme et al., 2018).

1.1.3. Multiple system atrophy

MSA is classified as an orphan disease (Bower et al., 1997). It is by far more aggressive in disease progression than PD, with an average survival of 6 to 9 years (Ben-Shlomo et al., 1997, Fanciulli and Wenning, 2015). MSA presents as two distinct clinical and pathological subtypes with different clinical symptoms. The parkinsonian type (MSA-P; 80% of total MSA cases), and the cerebellar type (MSA-C; 20% of total MSA cases). The parkinsonian type is usually associated with motor symptoms similar to PD but respond poorly to dopamine replacement therapy, whereas the cerebellar type presents with problems in movement and coordination, impaired speech, visual disturbances and difficulties in swallowing or chewing. Most likely, the different symptoms are related to the distinct affected brain regions: striatonigral degeneration in MSA-P and olivopontocerebellar atrophy in MSA-C (Fanciulli and Wenning, 2015).

MSA is histologically distinct from PD and DLB and is characterised by the abundance of αSyn pathology in oligodendrocytes as glial cytoplasmic inclusions (GCIs) (Tu et al., 1998), and to a much lesser extent, neuronal inclusions (Figure 1.1). MSA is mainly considered a sporadic disease, but genetic risk factors were recently associated with an increased susceptibility to develop MSA (Soma et al., 2006, Multiple-System Atrophy Research, 2013).

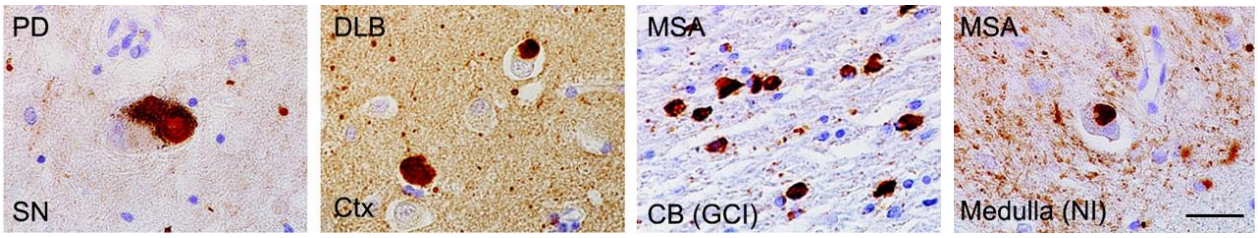

Figure 1.1. Immunohistochemistry stainings of αSyn inclusions in different synucleinopathies. PD: Parkinson's disease; SN: substantia nigra; DLB: dementia with Lewy bodies; Ctx: cortex; MSA: multiple system atrophy; CB: cerebellum; GCI: glial cytoplasmic inclusion; NI: neuronal inclusion. Scale bar: 25 μm. [Taken from from (Peng et al., 2018b)]

1.2. The alpha-synuclein protein

The discovery that αSyn is the main component of LBs, LNs, and GCIs (Spillantini et al., 1997, Spillantini et al., 1998a, Tu et al., 1998), effectively linked it to a multitude of poorly understood disorders. This marked the beginning of great efforts to understand the properties and functions of αSyn in health and disease. Over two decades later, many aspects of the physiological and pathophysiological functions of αSyn remain still largely unknown.

1.2.1. The synuclein family

αSyn was first isolated from the fish *Torpedo californica* in 1988. The distribution of its localization between the nuclear envelope and the presynaptic terminals prompted the name synuclein which refers to its abundance in both synapses and nuclei. (Maroteaux et al., 1988). Later on, two other proteins were discovered and determined to be a second and a third member of the synuclein family, and thereafter named β-synuclein (βSyn) and γ-synuclein (γSyn), respectively (Tobe et al., 1992, Shibayama-Imazu et al., 1993, Jakes et al., 1994, Ji et al., 1997, Lavedan et al., 1998).

Synucleins have only been identified in vertebrates so far (Clayton and George, 1999). They have a highly conserved primary sequence (Figure 1.2), and are natively unfolded proteins (George, 2002). All synucleins were found to be abundant in the brain, but with different distributions. αSyn and βSyn are mostly localised to nerve terminals, with a very sparse presence in the cytoplasm and dendrites, whereas γSyn is more evenly distributed throughout neurons. Moreover, while αSyn is most abundant in the telencephalon and the diencephalon regions, βSyn is more evenly distributed throughout the whole brain, and γSyn is predominantly present in peripheral and sensory neurons (Nakajo et al., 1994, Iwai et al., 1995, Ji et al., 1997).

The physiological functions of the synuclein proteins are not fully understood. αSyn and βSyn were proposed to have similar physiological functions due to their similar ultrastructural distributions. On the other hand, γSyn has been tightly linked with tumorigenesis-related cell migration and mictrotubule regulation (George, 2002).

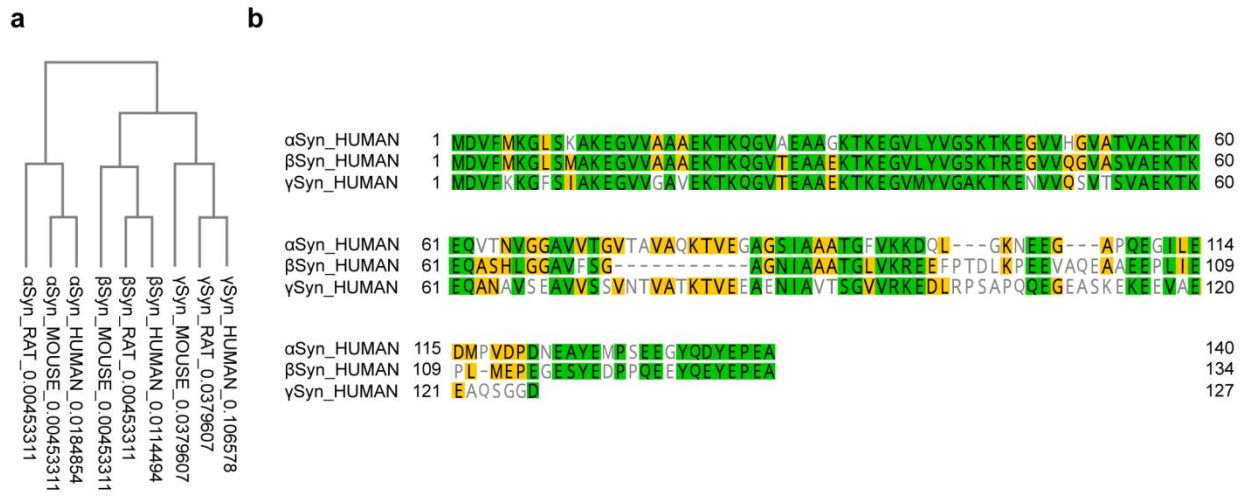

Figure 1.2. Phylogenetic tree and sequence alignment of the synuclein family members. (a) Phylogenetic tree and branch length of the human, rat, and mouse synuclein family members (Produced with the phylogeny tool [www.phylogeny.fr]). (b) Sequence alignment of the three synucleins. Highly conserved residues (green) and similar residues (yellow) are represented (produced with the alignment tool [www.uniprot.org])

1.2.2. The *SNCA* gene

1.2.2.1. Properties of *SNCA*

αSyn is encoded by the *SNCA* gene, located on chromosome 4q22.1. It contains 114 kb and consists of six exons, only five of which are coding since the transcription start codon ATG is located on exon 2 and the stop codon TAA is located on exon 6 (Xu et al., 2015). Transcription of the *SNCA* gene in dopaminergic neurons is regulated by multiple factors such as the GATA-1 and GATA-2 motifs located on intron 1 and intron 2 respectively (Scherzer et al., 2008). Likewise, methylation levels of a CpG island (DNA regions enriched in CG nucleotides), also located on intron 1 were linked with expression levels of *SNCA* (Matsumoto et al., 2010). Moreover, REP1, a complex polymorphic microsatellite repeat located on the 5'UTR of the *SNCA* gene seems to be strongly regulating the expression levels of *SNCA* (Chiba-Falek and Nussbaum, 2001). Interestingly, the *SNCA* gene undergoes various and complex splicing events (Gamez-Valero and

Beyer, 2018). At least five different alternative splicing isoforms of *SNCA* were so far confirmed, namley isoforms *SNCA140*, *SNCA126*, *SNCA112*, *SNCA98*, and *SNCA41*. The numbers represent the amino acid content of each resulting protein (Figure 1.3). The messenger RNA (mRNA) of *SNCA140* includes all coding exons (2 to 6), whereas isoforms *SNCA126* and *SNCA112* are lacking exons 3 and 5 respectively, and isoform *SNCA98* is lacking both exons 3 and 5 (Bungeroth et al., 2014). Isoform *SNCA41* is the only alternative splicing isoform of *SNCA* that lacks exon 4 in addition to exon 3 (Vinnakota et al., 2018).

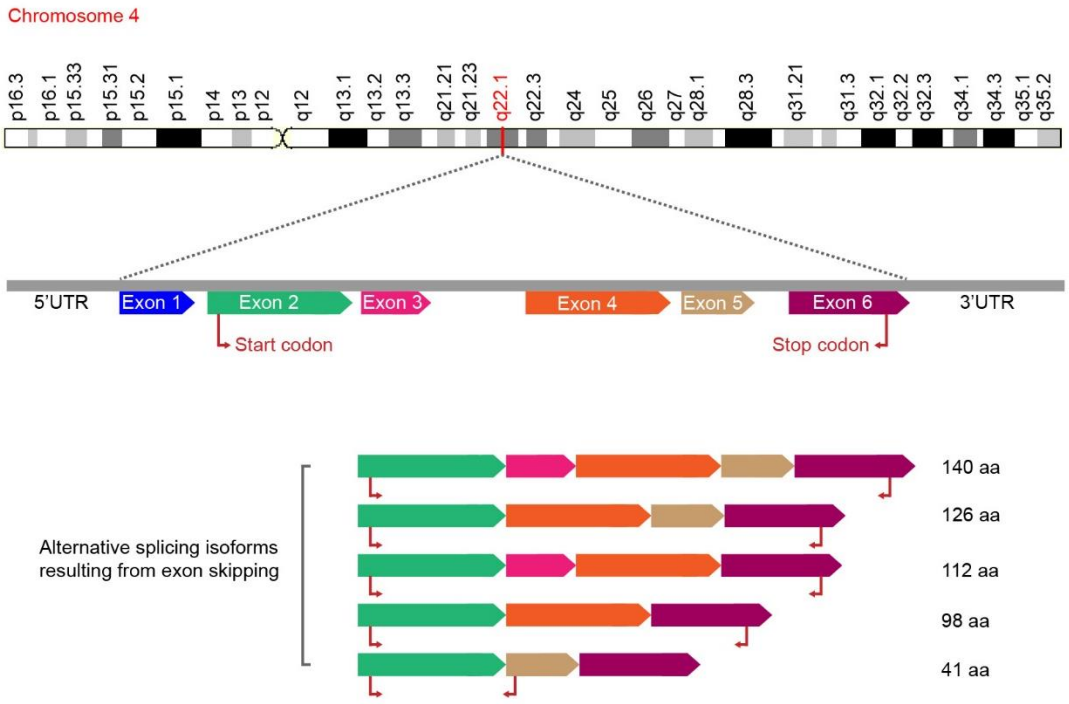

Figure 1.3. The *SNCA* gene and the αSyn splicing isoforms. Schematic depiction of the *SNCA* gene and its various alternative splicing isoforms. (Chromosome 4 illustration was taken from from [genecards.org])

1.2.2.2. Genetics and epigenetics of *SNCA* in synucleinopathies

The discovery of αSyn as a major component in LBs led to a particular focus on the *SNCA* gene. It was soon thereafter identified as an important risk factor. Three missense point mutations were first identified, A30P and A53T in familial PD (Polymeropoulos et al., 1997, Krüger et al., 1998), and E46K in familial DLB (Zarranz et al., 2004). Later, duplication and triplication on the *SNCA* locus were linked to increased αSyn levels and a higher risk for developing LB diseases (Chartier-Harlin et al., 2004, Ibanez et al., 2004, Hofer et al., 2005). More recently, additional point

mutations of the *SNCA* gene were identified, namely H50Q and G51D in familial PD cases (Appel-Cresswell et al., 2013, Kiely et al., 2013), as well as A53E as the first mutation related to MSA (Pasanen et al., 2014) (Figure 1.4b). Apart from point mutations and gene dose-related genetic factors, various single nucleotide polymorphisms (SNPs) were linked to a higher risk of developing synucleinopathies (McCarthy et al., 2011). Moreover, the expression pattern of different *SNCA* splicing isoforms was directly associated with several synucleinopathies. For instance, alternative splicing activation can be triggered by several parkinsonism-inducing factors, including toxins like MPTP (Kalivendi et al., 2010). The highly aggregation prone *SNCA*112 isoform was found to be highly overexpressed in cortical regions of DLB patients, and slightly upregulated in patients with PD (Beyer et al., 2004, Beyer et al., 2008).

More importantly, accumulating evidence indicates that αSyn forms the center of a very complex network, where it is not only tightly regulated, but also plays an important role as a gene expression regulator (van Heesbeen and Smidt, 2019). This role is achieved through interactions with transcription and translation factors, histones, and even direct interaction with DNA and RNA molecules. Furthermore, the ability to regulate gene expression by direct binding to nucleic acid is emerging as a common feature of several amyloidogenic proteins, such as amyloid beta and prion proteins (Hedge et al. 2010). Evidently, the genetic and epigenetic regulation of *SNCA* are complex and closely intertwined in the etiology of synucleinopathies.

1.2.3. Structure and biophysical properties

αSyn is a very abundant protein, and is estimated to account for approximatively up to 1% of total protein in the brain (Iwai et al. 2005). It is a highly soluble, acidic, and thermally stable small protein of 140 amino acids (Drescher, 2012). Its primary structure can be divided into three functional domains (Figure 1.4):

1) The N-terminal domain spanning between residues 1 to 60 is the most conserved region of the protein. It contains four imperfect KTKEGV motif repeats (George, 2002), which contribute to the formation of stable amphipathic α-helix structures and confer to its ability of binding to lipids (Eliezer et al., 2001). Interestingly, all known point mutations implicated in familial synucleinopathies are located in the N-terminal region of αSyn, which indicates the importance of this domain in the regulation of αSyn function (Gamez-Valero and Beyer, 2018).
2) The central region comprises residues 61 to 95, and is highly hydrophobic and amyloidogenic. Two imperfect KTKEGV motif repeats are found within this region of αSyn,

commonly called the non-amyloid-component or NAC domain, which is considered the main contributor to αSyn's aggregation prone characteristics (Giasson et al., 2001).

3) The C-terminal domain contains residues 96 to 140. It is rich in negatively charged amino acids and remains therefore unstructured under physiological conditions. This region contains most of the interaction sites with other proteins as well as the majority of known post translational modifications (PTMs) sites. It also confers a chaperone-like activity to αSyn and plays a role as an aggregation inhibitor (Eliezer et al., 2001, Oueslati et al., 2010).

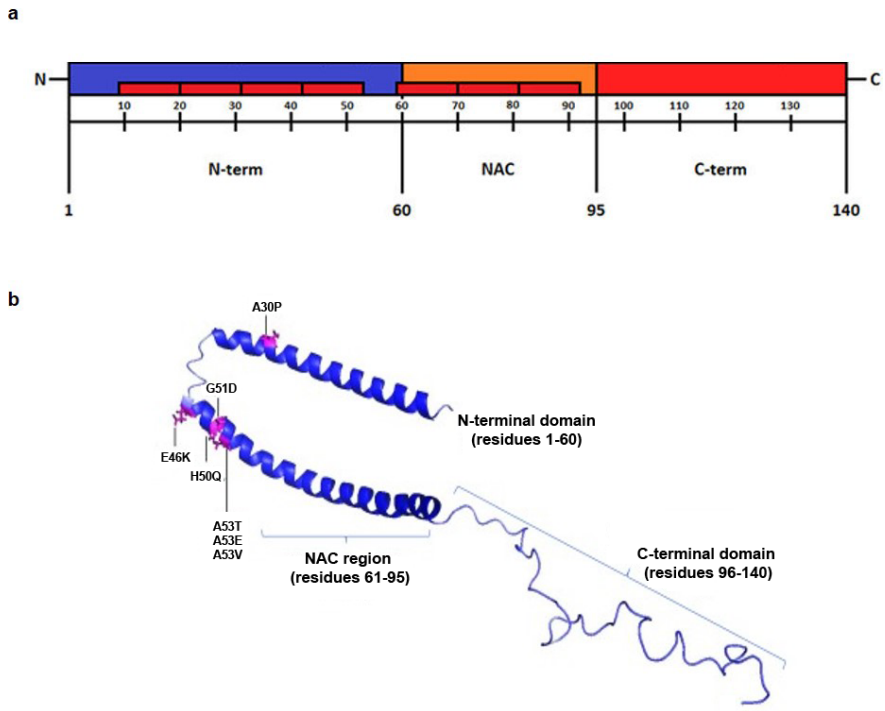

Figure 1.4. Structural features of monomeric αSyn. (a) Schematic diagram of αSyn primary structure and domains. Red boxes represent the KTKEGV motif repeats. (b) structure of the membrane-bound form of αSyn. The positions of point mutations associated with Parkinson's disease are indicated with arrows and in pink. [upper panel taken from (Gallegos et al., 2015), lower panel taken from (Whittaker et al., 2017)]

1.2.4. Physiological functions

The exact physiological functions of αSyn are still poorly understood but it is widely accepted to play very versatile roles in various cellular processes. This versatility is due to the unique biophysical properties of its different domains. Under physiological conditions, αSyn exists either as soluble natively unfolded protein, or as membrane-bound protein with α-helical conformation. αSyn was proposed to dynamically convert between these two states in order to fulfil its putative functions (Uversky, 2003).

Because of its abundant presence at presynaptic termini, αSyn involvement in the organization and recycling of neurotrasmitters was suggested (Lotharius and Brundin, 2002). Indeed, it was shown to regulate several aspects of neurotransmitter release, as well as the metabolism of dopamine via reduction of enzymatic activity of tyrosine hydroxylase and dopa decarboxylase (Masliah et al., 2000, Kirik et al., 2002, Tehranian et al., 2006). A direct interaction with dopamine transporter was also described, however the resulting effects of this interaction are conflicting (Lee et al., 2001, Wersinger and Sidhu, 2003). More recently, a role in regulation of synaptic vesicles pools and presynaptic architecture was proposed (Scott and Roy, 2012, Vargas et al., 2017). Also, an involvement in vesicle docking was proposed since αSyn seems to play a role as molecular chaperone in soluble *N*-ethylmaleimide-sensitive factor attachement protein receptor (SNARE)-complex assembly via direct binding to synaptobrevin-2 (Burre et al., 2010), or via direct binding to membranes (DeWitt and Rhoades, 2013, Lai et al., 2014) .

A molecular chaperone role for αSyn was first speculated based on the biophysical properties of its C-terminal domain (Weinreb et al., 1996, Uversky, 2003). Later on, αSyn was shown to form a chaperone machine complex with other molecular chaperones to control and maintain the integrity of neurotransmission processes (Emamzadeh, 2016).

αSyn was implicated in neuroprotection as well, since it was shown to modulate apoptotic responses to oxidative stress and exposure to neurotoxins via a concomitant increase of anti-apoptotic factors and decrease of pro-apoptotic factors (Jin et al., 2011, Alves da Costa et al., 2017).

Furthermore, αSyn has been reported to interact with several mitochondrial components and regulate mitochondrial morphology and fusion, electron transport chain, and cytosolic protein import (Martin et al., 2006, Kamp et al., 2010, Nakamura et al., 2011, Di Maio et al., 2016). At the nucleus, αSyn fosters several interactions with epigenetic and genetic regulation components (Goncalves and Outeiro, 2013, Ma et al., 2014). αSyn was also discovered in vesicular transport organelles such as the endoplasmic reticulum, golgi apparatus, and the endolysosomal system. Specific roles of αSyn in these compartments are unknown so far (Bernal-Conde et al., 2019).

Overall, αSyn seems to be strongly implicated in multiple cellular processes. However, assessing its normal functions is particularly challenging because of its conformational plasticity as well as the staggering number of its interaction partners (Longhena et al., 2019). This presents a considerable obstacle since understanding the physiological roles of αSyn is very important to discern its pathophysiological functions in relation to synucleinopathies.

1.2.5. Post-translational modifications

The physiological and pathophysiological functions of αSyn are greatly influenced by several PTMs. αSyn is known to undergo various types of PTMs (Figure 1.5), including phosphorylation, ubiquitination, nitration and oxidation, sumoylation, O-GlcNAcylation, and truncations. (Zhang et al., 2019).

Phosphorylation, especially at S129, has emerged as a hallmark for pathological αSyn since it was found to be highly abundant in LBs (Fujiwara et al., 2002, Anderson et al., 2006). This phosphosite is by far the most studied PTM of αSyn, and was shown to implicate various kinases, which might lead to distinct outcomes. For instance, phosphorylation at S129 by polo-like kinase 2 (PLK2) seems to promote αSyn degradation, while phosphorylation at the same site by casein kinase II (CKII) promotes αSyn fibrillation (Oueslati, 2016). αSyn can also be phosphorylated at several other serine and tyrosine sites, including: S87, Y125, Y133, and Y136. The impact of phosphorylation at most of these site, as well the responsible kinases remain unknown (Zhang et al., 2019).

Another common PTM of αSyn that is also abundant in LBs, is ubiquitination (Gomez-Tortosa et al., 2000). E3 ubiquitin-protein ligases have been particulary implicated in ubiquitination of αSyn: the C-terminal U-box domain of co-chaperone Hsp70-interaction protein (CHIP), seven in absentia homolog (SIAH), and neuronal precursor cell-expressed, developmentally downregulated gene 4 (Nedd4) (Liani et al., 2004, Shin et al., 2005, Tofaris et al., 2011). While ubiquitination via SIAH seems to induce intracellular aggregation of αSyn (Rott et al., 2008), CHIP and Nedd4 were associated with inhibition of aggregation as well as increased degradation of αSyn through the proteasomal and lysosomal pathways (Shin et al., 2005, Tofaris et al., 2011). αSyn can also be conjugated to small ubiquitin-like modifier (SUMO) at lysine residues. Some studies showed that sumoylation can result in different outcomes regarding aggregation and pathology, depending on the modified residue (Rott et al., 2017).

Oxidative stress, and more specifically oxygen and nitric oxide species and their respective products, lead to the nitration of tyrosine residues of αSyn. Nitrated forms of αSyn were found in LBs and all four tyrosine residues of αSyn (Y39, Y125, Y133, and Y136) are very susceptible to nitration (Sevcsik et al., 2011, Burai et al., 2015). Nitration was shown to have a great impact on the aggregation properties of monomeric and dimeric αSyn. Moreover, the aggregation properties seem to highly depend on the residue that undergoes nitration (Burai et al., 2015).

Besides the full-length protein, truncated forms αSyn were found in LBs and appear to make up 15% of total αSyn in pathological inclusions (Breydo et al., 2012, Beyer and Ariza, 2013). Several studies have shown that at least five different truncated forms, or fragments, of αSyn are present in LBs, including both N- and C-terminally truncated species (Anderson et al., 2006, Baba et al., 1998, Campbell et al., 2001, Crowther et al., 1998, Spillantini et al., 1998b, Okochi et al., 2000, Li et al., 2005, Liu et al., 2005). Moreover, the truncation of αSyn seems to correlate with its aggregation propensity and toxicity in cell models, and has also been shown to induce a severe motor phenotype in mice models (Tofaris et al., 2006, Periquet et al., 2007, Daher et al., 2009). Furthermore, several proteases such as neurosin (Iwata et al., 2003), plasmin (Kim et al., 2012), calpain (Mishizen-Eberz et al., 2005, Games et al., 2014), cathepsin D (Sevlever et al., 2008), metalloproteases (Levin et al., 2009) and caspase 1 (Wang et al., 2016) have been implicated in the cleavage of αSyn. Also, autoproteolysis of αSyn has been suggested (Vlad et al., 2011). Interestingly, fragmentation is currently emerging as a potential common feature observed also for other neurodegeneration-related proteins, such as amyloid precursor protein and tau (Mazzitelli et al., 2016).

PTMs are evidently key regulators of αSyn function. However, most of the available insights on this topic were obtained in an *in vitro* setting, whereas the *in vivo* effects of PTMs are still poorly understood. The complexity of the interplay between αSyn PTMs and pathophysiology is amplified by the fact that the same modifications can have opposite effects when carried out by different effectors. Likewise, the picture gets even more complicated when interactions between different PTMs are taken into consideration. An interplay between phosphorylation and ubiquitination (Hasegawa et al., 2002), as well as between phosphorylation and truncation were previously studied (Kasai et al., 2008) . It is not yet known whether interactions between more than two PTMs can occur and whether it might act as multi-layered regulation network for αSyn.

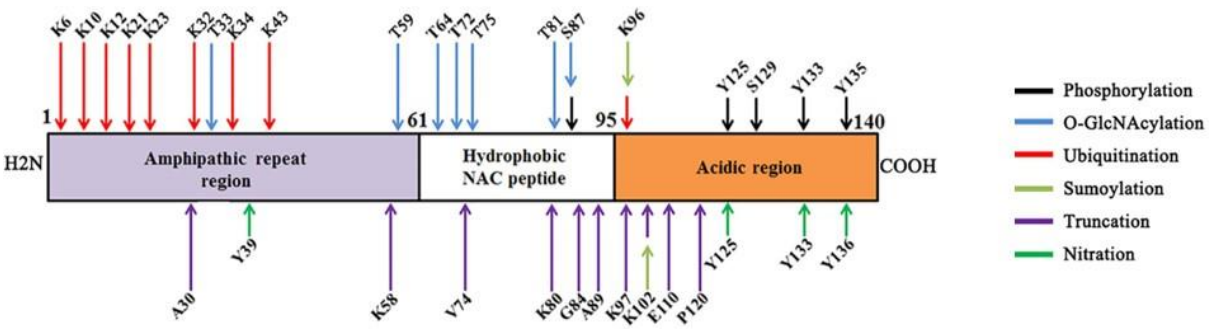

Figure 1.5. Overview of most known αSyn PTMs. [Modified from (Zhang et al., 2019)]

1.2.6. Role in neurodegenerative diseases

1.2.6.1. General mechanisms of αSyn aggregation

Since LBs, LNs and CGIs are mainly composed of aggregated αSyn (Spillantini et al., 1998b, Tu et al., 1998, Braak et al., 2003), aggregation is considered as a key event in the pathogenesis of synucleinopathies. Therefore, it is crucial to understand the specific mechanisms that lead to an accelerated aggregation of αSyn (Figure 1.6).

The exact molecular events that result in initial intracellular aggregation of αSyn are still unknown. There is however a consensus on the fact that natively unfolded αSyn undergoes a conformational shift and subsequently acquires nucleation and aggregation properties (Narhi et al., 1999, Uversky et al., 2001a). Fibrillar forms of αSyn result from a multistep aggregation process where a misfolding event leads to the exposure of hydrophobic stretches of the protein, and subsequently to initial aggregation events. Many intermediate forms of αSyn are formed during this aggregation process, including small oligomers, large oligomers, protofibrils, and fibrils (Hoyer et al., 2002, Caughey and Lansbury, 2003). Oligomers especially were found to greatly accelerate the aggregation kinetics, they are therefore called on-pathway oligomers. Intermediate species that do not lead to further aggregation, namely off-pathway oligomers, were also described but whether they play a protective or a toxic role is under debate (Cappai et al., 2005, Ehrnhoefer et al., 2008).

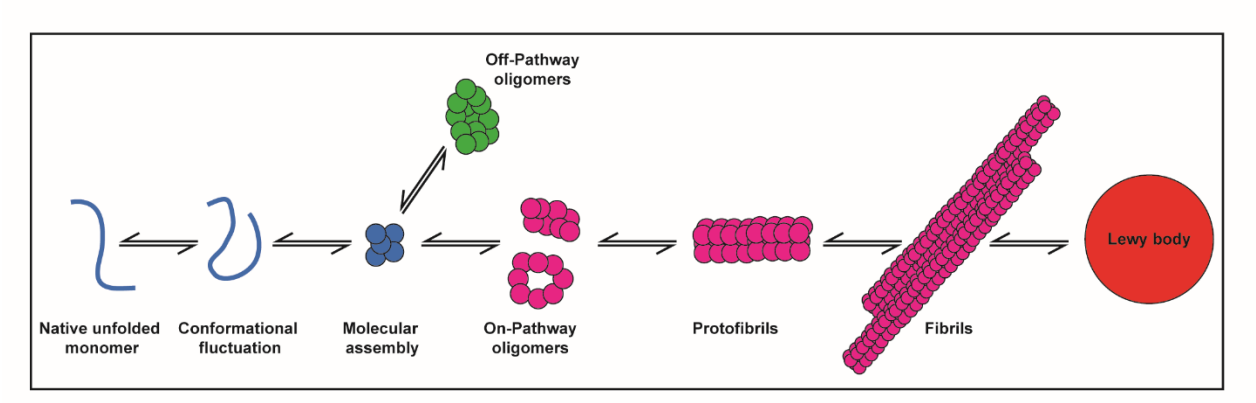

Figure 1.6. Aggregation pathways of αSyn.

Aggregation properties and kinetics can be modulated by several factors. Among those factors, an increased concentration of αSyn, increased temperature, decreased pH, or an increased ionic strength in the cellular environment were described as aggregation-inducing or enhancing events (Narkiewicz et al., 2014). Exposure to environmental factors such as pesticides, metal ions, and organic solvents proved very efficient to accelerate αSyn aggregation as well (Uversky et al.,

2001b, Uversky et al., 2001c, Manning-Bog et al., 2002, Janeczek and Lewohl, 2013). In addition, binding partners of αSyn such as histones were able to mediate aggregation in a dose-dependent manner (Goers et al., 2003). Likewise, most of the known synucleinopathy related point mutations of αSyn are also implicated in an increased aggregation rate in comparison to WT αSyn. Moreover, PTMs such as phosphorylation, nitration and truncation of αSyn seem to lead to a faster aggregation of αSyn (Oueslati et al., 2010). On the other hand, heat shock proteins, βSyn, and γSyn have the ability to inhibit αSyn aggragation (Uversky et al., 2002, Bruinsma et al., 2011), along with several classes of small chemical compounds such as polyphenols, benzothiazoles, and flavonoids (Masuda et al., 2006, Meng et al., 2010).

1.2.6.2. Cell-to-cell spreading of αSyn

The spreading of αSyn pathology was first consolidated by the observation of 'host-to-graft' transmission of LBs (Kordower et al., 2008a, Kordower et al., 2008b, Li et al., 2008, Li et al., 2010). Currently, there is a growing body of evidence supporting the hypothesis that cell-to-cell transmission of pathological αSyn species underlies spreading of the pathology from one brain area to another and thus, disease progression (Braak et al., 2003, Muller et al., 2005). The spreading process depends first on the release of αSyn species from a diseased cell into the extracellular space, followed by their uptake into healthy neighbouring cells (Figure 1.7).

The sequence of αSyn does not contain a secretion signal, which implicates that this protein is not destined to be secreted. It is nonetheless found in measurable amounts in biological fluids such as CSF and plasma, as well as in cell culture supernatants (El-Agnaf et al., 2006, Mollenhauer et al., 2008). Interestingly, the amount of extracellular αSyn seems to correlate with intracellular levels (Reyes et al., 2015), which might be related to the impairment of intracellular clearance mechanisms when αSyn concentration increases.

The exact release mechanisms of pathological species of αSyn are not yet fully understood. Numerous studies showed that αSyn can be released from donor cells either via active or passive mechanisms. Passive release mechanisms such as diffusion seem to involve monomeric αSyn but not its aggregated forms. The ability of αSyn monomers to pass the cell membrane boundaries through diffusion is well established (Ahn et al., 2006, Lee et al., 2008a). However, exact diffusion mechanisms are still unknown because αSyn can not simply pass through the lipid bilayer (Lee et al., 2005). Monomers and aggregated forms can be passively released in the extracellular space when the cell membrane integrity is compromised. Active release on the other hand comprises several distinct mechanisms, including non classical exocytosis, ER-Golgi-dependent exocytosis,

and exosomal secretion. Both monomeric and aggregated forms of αSyn can be released from cells via non classical exocytosis and via exosomes (Grozdanov and Danzer, 2018).

Uptake mechanisms of αSyn, especially pathological forms thereof, have been intensively studied over the last years. Uptake can also take place through passive or active mechanisms. Similar to passive release, passive uptake mainly involves monomeric forms. Contrarily, aggregated αSyn species are mainly taken up via active mechanisms. The endocytosis pathways of αSyn aggregates and/or fibrils vary considerably depending on the cell type. Indeed, microglia were demonstrated to internalize extracellular αSyn more efficiently than neurons and astrocytes (Lee et al., 2008b). Moreover, uptake via receptor-mediated endocytosis was proposed. The lymphocyte-activation gene 3 (LAG-3) surface receptor was shown to have a high binding affinity to αSyn aggregates and to facilitate their uptake into cells leading to subsequent toxicity (Deng et al., 2016). Besides, several forms of αSyn can traffic between cells in association with exosomes, and effectively initiate seeding and toxicity in recipient cells (Danzer et al., 2009, Danzer et al., 2012).

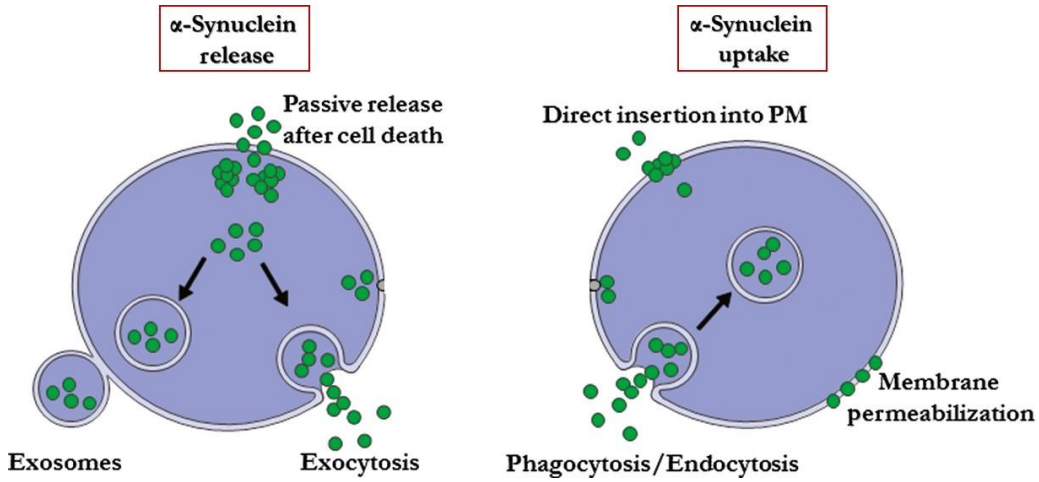

Figure 1.7. Release and uptake mechanisms of αSyn. PM: plasma membrane [modified from (Ottolini et al., 2017)]

1.2.6.3. Seeding properties and strains

At the molecular level, aggregated forms of αSyn were shown to have the capacity to act as a template, commonly called seed, and recruit endogenous αSyn for misfolding and aggregation. This process leads to an amplification of pathological aggregates, which can subsequently further spread to other cells (Hardy, 2005). Templated- or seeded aggregation is able to produce aggregates that faithfully replicate the conformational and structural properties of the seed itself.

αSyn strains are currently emerging as a potential explanation to the differences between brain areas and cell types affected by αSyn pathology in various synucleinopathies like PD, DLB and MSA. The discovery that recombinant αSyn monomers can form aggregates with variable conformations and biological activities (Guo et al., 2013) led the way to more findings showing that different αSyn strains can have very distinct physical and structural properties. More importantly, different strains have the ability to impose their structural and conformational properties on a new cycle of aggregation. They are also able to induce different levels of toxicity in cells (Bousset et al., 2013) and revealed different spreading and toxicity potentials in a mouse model (Peelaerts et al., 2015). Even more strikingly, different strains resulted in the formation of αSyn deposits in different cell types (Peelaerts et al., 2015). More recently, the examination of αSyn aggregates extracted from PD and MSA brains revealed distinct seeding characteristics that were conserved even after several cycles of aggregation (Yamasaki et al., 2019), further showing that αSyn strains underlie the vast pathophysiological and clinical disparities between synucleinopathies.

1.2.6.4. Interference with intracellular processes and underlying toxicity

While monomeric αSyn is mainly located in presynaptic terminals, aggregated forms are localized throughout the cell body, suggesting that take part in pathological functions via disruption of normal cellular processes. Indeed, αSyn-mediated cytotoxicity was correlated with functional impairment of multiple organelles, as well as inter-organelle communication and axonal transport (Figure 1.8).

Oligomeric species of αSyn were shown to disrupt membranes and interfere with synaptic functions and dopamine release (Abeliovich et al., 2000, Mosharov et al., 2009, Burre et al., 2012). Aggregated αSyn also interferes with mithochondrial homeostasis and morphology via increased calcium uptake and impairement of cytosolic protein import (Kamp et al., 2010, Rostovtseva et al., 2015, Di Maio et al., 2016).

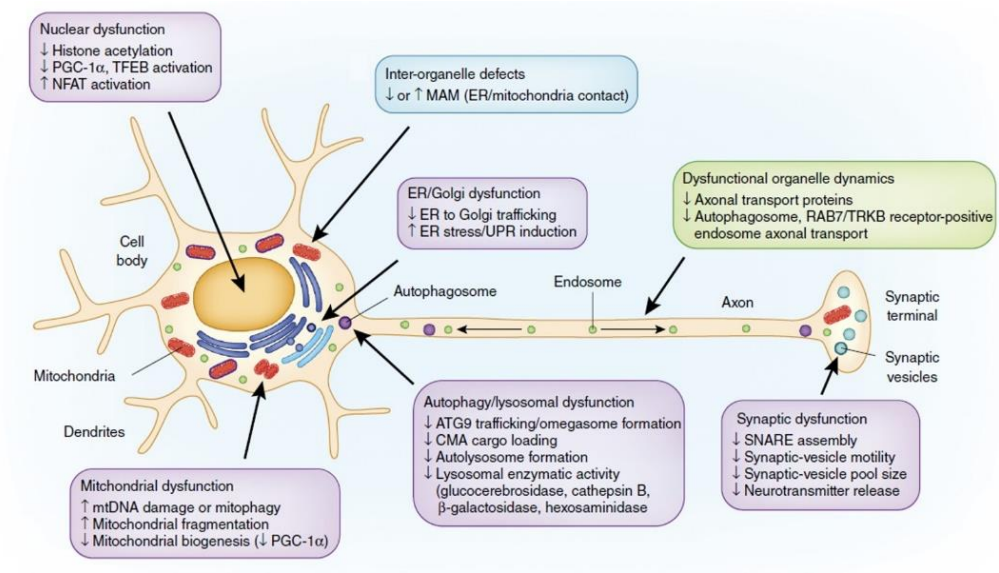

Figure 1.8. Intracellular processes disrupted by pathological αSyn. [taken from (Wong and Krainc, 2017)]

The endoplasmic reticulum and golgi functions are affected by αSyn pathology as well. Recent evidence points towards a disruption of traffic between the two organelles, resulting in ER stress and secretory pathways dysfunction (Hampton, 2000, Colla et al., 2012, Wong and Krainc, 2017). Interestingly, pathological forms of αSyn were shown to disrupt cellular pathways responsible for clearance of abnormal protein aggregates and damaged organelles, such as the unfolded protein response (UPR), the proteasome, and the autophagy-lysosomal pathway, thus effectively leading to pathology accumulation and exacerbation (Cuervo et al., 2004, Winslow et al., 2010, Volpicelli-Daley et al., 2014, Wong and Krainc, 2016).

1.3. The LUHMES cell model

Lund human mesencephalic (LUHMES) were used throughout this study to model synucleinopathy. LUHMES cells originated from Lund University. First trimester human embryonic mesencephalic cells were conditionally immortalized using a myc oncogene. They proliferate continuously in culture, and conditionally differentiate into morphologically and biochemically postmitotic human dopaminergic neurons upon addition of low concentrations of tetracycline (Figure 1.9) (Lotharius et al., 2002).

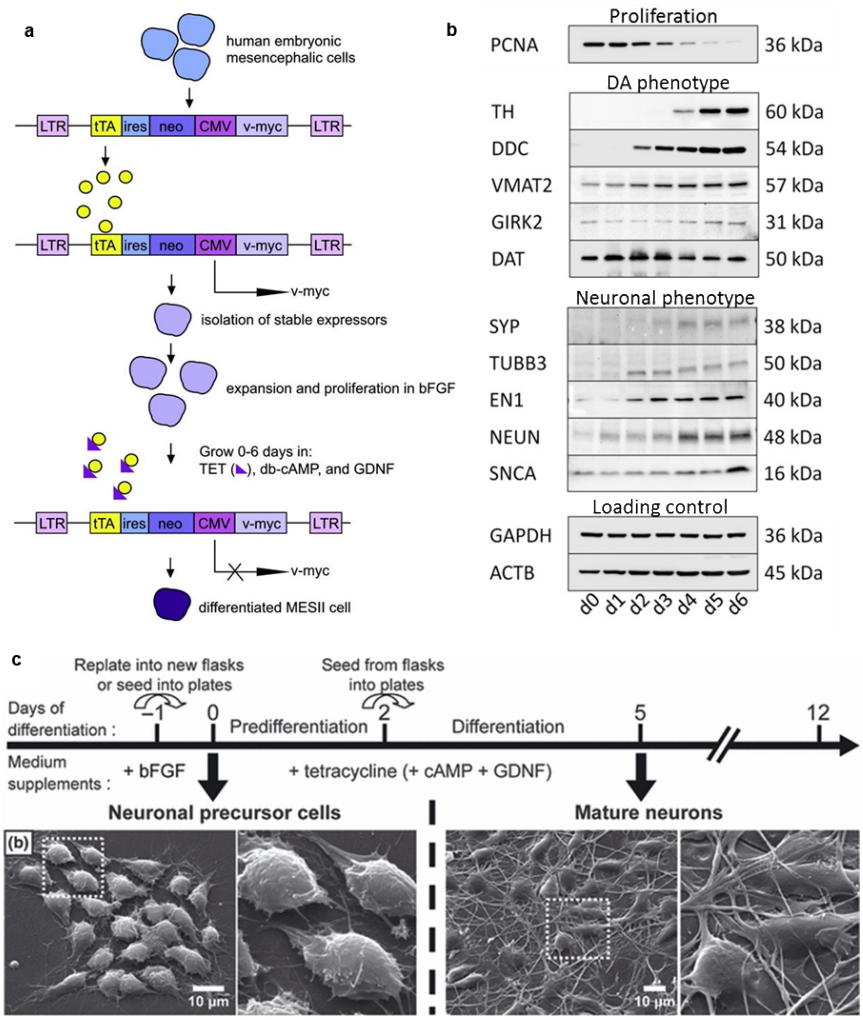

Figure 1.9: Characterization of LUHMES cells as dopaminergic neurons. a) Human embryonic mesencephalic cells were conditionally immortalized with Tet-off v-myc overexpression under the CMV promotor. Once tetracycline is added to the medium, v-myc is no longer espressed and the cells differenciate into dopaminergic-like neurons. **b)** LUHMES cells display a progressive decline in proliferation markers and increase of neuronal and dopaminergic markers throughout differentiation. **c)** Once fully differentiated, LUHMES cells present a neuronal phenotype with a dense neuronal network. [a) taken from (Lotharius et al., 2002); b) taken from (Höllerhage et al., 2014); c) taken from (Scholz et al., 2011)]

LUHMES cells present an advantage on other immortalized cell lines and primary cell cultures in terms of phenotype adaptability and rapid differentiation. It is a robust human dopaminergic cell model that offers high population homogeneity, which gives this model a high value for disease modelling, toxicology, and neuropharmacology studies. In addition, LUHMES cells express stable levels of αSyn protein, which makes them highly relevant in studying αSyn-related pathology (Lotharius et al., 2005, Schildknecht et al., 2013, Höllerhage et al., 2014).

2. SPECIFIC AIMS

The aim of my doctoral thesis was to investigate specific αSyn species that are mediating the spreading, seeding and toxicity in synucleionpathies. By a systematic approach, I focused on the four main events of the spreading process, and addressed the following questions:

- Which αSyn species are released into the extracellular space under pathological conditions?
- What are the mechanisms underlying the formation of these species?
- Can the αSyn species detected in the extracellular space be taken up by naïve cells?
- Upon uptake, do they seed aggregation into healthy cell endogenous αSyn?
- Do these species result in a measurable toxicity in the recipient cells?
- Is a toxicity in recipient cells the direct consequence of the uptake and the subsequent seeding activity of these αSyn species?

3. EXPERIMENTAL PROCEDURES

3.1. Cell culture

Proliferating Lund human mesencephalic (LUHMES) cells (Lotharius et al., 2002) were expanded on T75 flasks (EasYFlasks, Nunclon DELTA, VWR, Darmstadt, Germany) coated with 50 µg/mL poly-L-ornithine (Sigma-Aldrich, St. Louis, MO) . Proliferation medium consisted of DMEM/F12 (Sigma-Aldrich) supplemented with 1% N2 supplement (Life Technologies, Carlsbad, CA) and 0.04 µg/mL basic fibroblast growth factor (bFGF; PeproTech, Rocky Hill, CT).

Cells were plated on either T25 flasks or multi-well-plates (Nunc MicroWell plates, Thermo Fisher Scientific, Waltham, MA) sequentially coated with 50 µg/mL poly-L-ornithine (Sigma-Aldrich) and 5 µg/mL bovine fibronectin (Sigma-Aldrich) for experiments. Differentiation into dopaminergic neurons was triggered with a differentiation medium consisting of DMEM/F12 with 1% N2 supplement, 1 µg/mL tetracycline, 0.49 µg/mL dibutyryl cyclic-AMP (Sigma-Aldrich) and 2 ng/mL glial cell-derived neurotrophic factor (GDNF; R&D Systems, Minneapolis, MN). Cell density was 100,000 cells/cm^2 across all flasks and well plate formats, and the cells were kept at all times in standard cell culture conditions at 37 °C, 5% CO_2, and water-saturated air. Mycoplasma contamination tests were routinely performed.

3.2. Transduction with adenoviral vectors

For overexpression experiments, adenoviral vectors expressing human wild-type alpha synuclein (αSyn) or green fluorescent protein (GFP) under a cytomegalovirus promoter (BioFocus DPI, Leiden, Netherlands) were added to 2 dans differentiated LUHMES cells with a multiplicity of infection (MOI) of 2, as previously described (Fussi et al., 2018, Höllerhage et al., 2019). Untreated controls were supplemented with differentiation medium without adenoviral vectors. After 24 h, the adenoviral overexpression vectors were removed and cells were thouroughly washed with PBS (Life Technologies, Carlsbad, CA, USA) to remove virus particles, then supplemented with fresh differentiation medium and kept in culture until indicated readout times.

3.3. Treatments with recombinant αSyn

Cells were treated with 3 µM recombinant full-length and fragmented wild-type human αSyn (rPeptide, Watkinsville, GA; see table below) after 4 days of differentiation. Unless otherwise indicated, cells were treated for 48 h. Cells were then washed 3 times with PBS and treated with trypsin-EDTA (Life Technologies) for 45 s at 37 °C followed by a wash with DMEM/F12 medium

supplemented with 10% fetal calf serum (FCS; Gibco Life Sciences, Carlsbad, CA), then a final wash in PBS to ensure appropriate removal of extracellular αSyn and avoid artefact in the analysis of intracellular αSyn. Cells were either harvested immediately after washing or kept in culture with fresh differentiation medium until indicated readout times.

Table 1. Overview of used recombinant αSyn.

Recombinant αSyn	Source	Treatment concentration
Alpha-Synuclein (1mg)	rPeptide	3 µM
Alpha-Synuclein, 1-60 (0.5mg)	rPeptide	3 µM
Alpha-Synuclein, 1-95 (0.5 mg)	rPeptide	3 µM
Alpha-Synuclein, 61-140 (0.5 mg)	rPeptide	3 µM
Alpha-Synuclein, 96-140 (0.5 mg)	rPeptide	3 µM
Alpha-Synuclein, NAC peptide (2 mg)	JPT peptide	3 µM

3.4. Generation of αSyn knockout LUHMES cell line by CRISPR-Cas9 genome editing

The exon 4 of *SNCA* gene was targeted to ensure silencing of all known spilincg isoforms and to exclude the possibility of alternative translation initiation. The 3' portion of *SNCA* exon 4 and part of its adjacent intron were replaced with an autonomous puromycin resistance cassette on one allele and a frame shift-inducing indel was introduced in the same exon on the second allele. Small guide RNAs (sgRNAs) were designed using Benchling Biology Software 2016 (Benchling, San Francisco, CA, https://benchling.com) against *SNCA* exon 4 (5'-AGTAGCCCAGAAGACA GTGG-3') and the adjacent 3' intron (5'-GGAGCAAGATACTTACTGTG-3'). They were then cloned into the pbs-U6-chimaric_RNA sgRNA expression plasmid. A fragment harboring the was amplified with PCR from LUHMES and inserted into a pCR-Blunt-II vector (Invitrogen, Carlsbad, CA). The portion between guide RNA-binding positions was consecutively substituted by the puromycin selection cassetteto produce the final homologous donor vector. The pCAG-Cas9v2-bpA vector was used to express the SpCas9 nuclease. All plasmids were amplified in E. coli DH5-α and isolated using PureLink HiPure plasmid purification kits (Invitrogen, Carlsbad, CA, USA). LUHMES cells were cultured in proliferation medium at 37 °C / 5% CO_2. Flasks and multi-well plates we coated with 1% Geltrex (Gibco Life Sciences) in DMEM/F12 (Sigma-Aldrich, St. Louis, MO, USA) at 37 °C overnight prior to seeding. At 70% confluency, undifferentiated cells were washed once with PBS and then detached using Accutase (Sigma-Aldrich) for 15 min at 37 °C. Detached cells were washed in pre-warmed (37 °C) proliferation medium supplemented with 10%

FCS. Two million cells were resuspended in 100 µL nucleofection solution (Amaxa Basic Nucleofector Kit Primary Neurons; Lonza, Basel, Switzerland) supplemented with the appropriate plasmids (10 µg for 10^6 cells at a mass ratio of 2:1:1:1 [Cas9 : homologous donor : exonic sgRNA : intronic sgRNA]). Cells were then immediately transferred into cuvettes and transfected using program C-013 on a Nucleofector 2b device (Lonza, Basel, Switzerland) according to the manufacturer's protocol (Schildknecht et al., 2013). Finally, the cells were allowed to recover in 900 µL of pre-warmed RPMI medium with 20% B27 (Gibco Life Sciences) at 37 °C for 10 min and added to 5 mL of pre-warmed proliferation medium in a T25 flask. On the following day, cells were washed once with PBS, supplemented with fresh medium and allowed to expand further for 2 to 3 days. They were then supplemented with an intial dose of 0.2 µg/mL puromycin for 3 days. Cells were allowed to recover for 3 more days and then treated with an icreased dose of 0.8 µg/mL puromycin, and allowed to recover again after 3 days. They were then seeded at 300 cells per 1.5 mL growth medium supplemented with 8% B27 and 10 µg/mL ciprofloxacin in 6-well plates and grown for a week at 37 °C, 5% CO_2 and 3% O_2. After clonal expansion, the clones were incubated in 0.02% EDTA/PBS (Sigma-Aldrich) for 4 min at 37 °C, PBS was added and individual cell patches were transferred by pipette into 300 µL pre-warmed growth medium supplemented with 6% B27 in 48-well plates. Individual clones were expanded and passaged, using a portion of the cell mass for genotyping. Selection criteria were integration of the resistance cassette into one allele and frame shift-inducing indels in the second allele of the *SNCA* gene. Absence of α-synuclein protein was confirmed by Western blot.

3.5. Western blotting

Cell harvesting and sample preparation:

Cells were harvested in M-PER lysis buffer (Thermo Scientific Pierce Protein Biology, Waltham, MA) supplemented with protease and phosphatase inhibitors cocktail (Roche, Basel, Switzerland). Lysis was carried out by incubation on ice for 15 min, followed by one freeze-thaw cycle. Cell debris was then cleared by centrifugation at 13,000 x g for 10 min at 4 °C. Concentration of the supernatant was determined by BCA protein assay kit (Thermo Scientific Pierce Protein Biology) according to the manufacturer's instructions.

Conditioned medium samples harvesting and preparation:

Conditioned medium was collected and centrifuged at 2,000 x g for 10 min to remove cell debris. Medium was then concentrated for Western blot analysis with a 3 kDa molecular weight cut-off

filter vivaspin columns (Vivaspin; Sartorius, Göttingen, Germany). The protein content in the medium was quantified using the 660 nm Protein Assay Reagent (Thermo Scientific Pierce Protein Biology).

Gel elecrophoresis and Western blotting:

Proteins from cell homogenates were loaded on 4-12% Bis-Tris precast protein gels (Bio-Rad Laboratories, Hercules, CA) and electrophoresis was carried out with MES running buffer. For CM samples, proteins were loaded on 16.5% Tris-Tricine precast protein gels (Bio-Rad Laboratories) and electrophoresis carried out with Tris-Tricine running buffer. Proteins were transferred on 0.2 µm PVDF membranes (Bio-Rad Laboratories) and immediately fixed with 0.4% formaldehyde as previously described (Lee and Kamitani, 2011). Membranes were blocked with a 30% RotiBlock solution (Carl Roth, Karlsruhe, Germany) or 5% skimmed milk in Tris-buffered saline (TBS) supplemented with 0.05% Tween-20 (Sigma-Aldrich) (TBST) and incubated overnight with primary antibodies at 4 °C. Correspondent HRP-coupled secondary antibodies were incubated for 1 h at room temperature, followed by incubation in Clarity Western ECL Substrate (Bio-Rad Laboratories) for visualization. Images were taken with Odyssey Fc (LI-COR Biotechnology, Lincoln, NE) imaging system.

Table 2. Overview of antibodies used for Western blotting

Antigen	**Clone**	**Species**	**Dilution**	**Source**
Alpha-synuclein, C-terminal	Polyclonal	Rabbit	1:500	Cell signaling technology (Danvers, MA)
Alpha-synuclein, N-terminal	EP1646Y	Rabbit	1:500	Abcam (cambridge, UK)
Plasminogen	Polyclonal	Rabbit	1:1000	Cell signaling technology
GAPDH	Plyclonal	Rabbit	1:3000	Merck Millipore, Billerica, MA
B-actin, HRP conjugate	13E5	Rabbit	1:2000	Cell signaling technology
Rabbit IgG, HRP conjugate secondary antibody	Polyclonal	Goat	1:5000	Vector Laboratories, Burlingame, CA

3.6. LC-MS analysis

Gel slices (2 mm) were excised from a Colloidal Coomassie stained SDS-polyacrylamide gel at the regions between 5 and 18 kDa (fragments and monomer). Gel slices were further cut into small cubes and transferred into individual vials for subsequent protein cleavage by trypsin and chymotrypsin. First, gel pieces were destained with 50 mM ammonium bicarbonate (Ambic) (Sigma-Aldrich) in water containing 50% acetonitrile (ACN) (Sigma-Aldrich). Next, 200 ng of trypsin was added for the first digestion step and the samples were incubated for 12 h at 37 °C. The supernatant was transferred into a fresh vial and the gel cubes were washed once with 50 µL of a 100 mM Ambic solution and the wash was combined with the supernatant from the tryptic cleavage. Subsequently, 300 ng of chymotrypsin were added to the gel cubes and samples were incubated for 4 h at 30 °C. All samples were then acidified using 10% formic acid (FA) and corresponding supernatants of trypsin and chymotrypsin digestion were combined. Peptides were finally eluted twice with 50 µL of 50% ACN containing 0.1% FA (Sigma-Aldrich). All samples were vacuum-dried before desalting on a C18 stage tip column (Thermo Fisher Scientific). Desalted samples were then reconstituted in 0.05% trifluoroacetic acid (Sigma-Aldrich) and chromatographically separated on an U3000 nano-chromatography system (Thermo Fisher Scientific) which was directly coupled to an LTQ orbitrap mass spectrometer (Thermo Fisher Scientific) for online detection of peptides. Peptides were directly loaded on the RP-C18 nano-column packed into an ESI emitter (120 x 0.075 mm, filled with ReproSil-Pur C18-AQ 2.4 µm, Dr. Maisch AG, Ammerbuch-Entringen, Germany) and subsequently separated via a linear gradient from 3% ACN to 35% ACN in 50 min. Peptides eluting from the chromatography column were transferred into the mass spectrometer via nano-electrospray ionization. The mass spectrometer was run in data-dependent acquisition mode, acquiring one survey scan to detect ionized peptide ions and performing 6 fragment ion scans of selected precursor peptide for sequence determination.

3.7. Proteomic data analysis

All raw data files for excised αSyn gel slices were searched in parallel against a human protein database (uniprot, vs 11/2017) using the MaxQuant/Andromeda search algorithm (vs. 1.6.0.6, www.maxquant.org (Tyanova et al., 2016).

For comparison with calculated peptide masses, a mass deviation of 20 ppm was allowed for the first search step, for the main search it was adjusted to 6 ppm. For MS/MS data a mass accuracy for 0.6 Da was selected. Protein N-terminal acetylation, methionine oxidation and cysteine carbamidomethylation were enabled as post-translational modifications. All obtained results were

filtered for 1% FDR on the peptide level and 5% on the protein level. Furthermore, at least two peptide sequences had to be associated with reported protein sequences.

For αSyn, N-terminal and C-terminal regions were not covered by the proteomics data. In order to guarantee correct annotation of the covered areas, identified peptides were loaded into Skyline (vs. 18, University of Seattle, www.skyline.ms (MacLean et al., 2018) and the peptide peak areas were annotated manually. Peptide abundance was compared between all samples.

3.8. Human protease array

To identify proteases present in LUHMES cells conditioned medium, the Proteome Profiler human protease array kit (R&D systems, Minneapolis, MN) was used according to the manufacturer's instructions. Briefly, membranes dotted with different protease antibodies were activated in assay buffer, then incubated overnight with either conditioned medium supplemented with the provided protease detection antibody cocktail. On the next day, the membranes were incubated with an HRP-coupled secondary antibody and developed with ECL. The transparency overly provided with the kit was used to identify the proteases corresponding to each dot.

3.9. *In vitro* cleavage assay

To monitor protolytic events in conditioned medium, recombinant FL-αSyn (1 µg) was added to 100 µL of various unconcentrated media conditions, then the mixture was incubated at 37 °C for 24 h. Next, 30 µL were taken out of the reaction, mixed with reducing XT sample loading buffer (Bio-Rad Laboratories) and heated at 95 °C for 5 min. Samples were loaded on in-house casted 16% Bis-tris gels prior to Western blotting as described before.

3.10. *In vitro* Protease inhibition

Protease inhibitors (see table below) were added to 100 µL of unconcentrated medium conditioned with untreated LUHMES cells followed by an incubation of 1h at 37 °C. 1 µg of recombinant FL-αSyn was then added and a further incubation at 37 °C for 24 h was performed. Next, 30 µL were taken out of the reaction, mixed with reducing XT sample loading buffer (Bio-Rad Laboratories) and heated at 95 °C for 5 min. Samples were loaded on in-house casted 16% Bis-tris gels prior to Western blotting as described before.

Table 3. Overview of used protease inhibitors.

Protease inhibitor	Target	Source	Treatment concentration
EDTA	Metalloproteases	Thermo Fisher	5 mM
Protease inhibitor cocktail 1	General	Roche	1X
Protease inhibitor cocktail 2	General	Thermo Fisher	1X
NNGH	Metalloproteases 3 and 9	Selleckchem	100 µM
Calpastatin	Calpain inhibitor	Selleckchem	1 µM
Pepstatin A	Cathepsin inhibitor	Selleckchem	50 µM
Z-VAD-FMK	Caspases	Selleckchem	100 µM
AEBSF	Serine proteases	Roth	2 mM
Aprotinin	Serine proteases	Roth	2 µM
Bestatin	Amino-peptidases	Selleckchem	100 µM
E64	Cystein proteases	Selleckchem	30 µM
Leupeptin	Serine and Cystein proteases	Roth	40 µM
PKSI-527	Kallikreins	Enzo life sciences	10 µM

3.11. Conditioned medium uptake assay

Wild-type LUHMES were transduced with αSyn overexpressing AV and the resulting conditioned medium (CM) was harvested at DIV8 as described before. Briefly, the medium was first spun at 2,000 x g for 10 min to remove cell debris, then concentrated using 3 kDa molecular weight cut-off Vivaspin clumns (Vivaspin; Sartorius, Göttingen, Germany) to achieve the desired concentration factors (2X, 5X and 10X) accordingly. DIV8 αSyn knockout LUHMES cells were treated with different concentrations of the conditioned medium at 37 °C for 6 h. Cells were afterwards thoroughly washed, harvested and cell lysates were used for Western blotting.

3.12. Recombinant protein labeling and uptake assays

Protein Fluorescent labeling:

For protein uptake, recombinant proteins were labeled with ATTO-488-NHS ester fluorescent dye (ATTO-TEC, Siegen, Germany) according to the manufacturer's instructions. Briefly, protein concentrations were adjusted to 2 mg/mL and reconstitution buffer was exchanged from Tris to PBS with dialysis. The pH of the coupling reactions was adjusted to 8.3 with a 0.2 M sodium bicarbonate solution (Sigma-Aldrich). The fluorescent dye was reconstituted with dimethyl sulfoxide (Sigma-Aldrich) to a final concentration of 5 mg/mL and added to the proteins with a three to ten folds molar excess, and the mixture was incubated at room temperature for 1 h in the dark. Tris buffer contained in Bio-Spin 6 size exclusion spin columns (Bio-Rad Laboratories) was exchanged with PBS before their use to remove excess unbound dye. Labeling was verified with gel electrophoresis followed by fluorescence imaging. An approximate degree of labeleing was determined with photospectrometry.

Confocal imaging:

Cells were seeded on 8-well ibidi µ-slides (ibidi, Gräfelfing, Germany) and allowed to differentiate for 4 daysThey were then treated with 3 µM of FL-αSyn or fragments for 48 h. The treatment was removed and cells were washed as described above. CellTrace Calcein red-orange (Thermo Fisher Scientific) was used as a cell filling dye prior to fixing with 4% paraformaldehyde (Sigma-Aldrich). 4′,6-diamidino-2-phenylindole (DAPI; Invitrogen) was used as a nuclear counterstain. Z-stack images were taken using an inverted laser scanning confocal microscope (Zeiss LSM 880, Carl Zeiss, Oberkochen, Germany) using a 40x oil immersion objective with a digital zoom of 2.5. Orthogonal projections were made using the Fiji software (https://imagej.net/fiji).

Automated uptake assay:

For automated uptake kinetics assays, cells were seeded on 48 well-plates and treated with labeled αSyn for the indicated amounts of time , then washed twice with PBS and treated with a 0.5 M trypan blue solution diluted in extracellular buffer to quench extracellular green fluorescence as previously described (Karpowicz et al., 2017). Intracellular fluorescence in live cells at each time point was assessed with a CLARIOstar plate reader (BMG Labtech, Offenburg, Germany) using a well-scanning protocol with a 10 x 10 matrix.

3.13. LDH assay

Cytotoxicity was was mesured via lactate dehydrogenase (LDH) activity in the culture medium at the indicated readout times using the fluorescence based CytotoxONE Membrane Integrity Assay (Promega, Fitchburg, WI) according to the manufacturer's instructions. Fluorescence levels were determined with a fluorescence microplate reader CLARIOstar plate reader (BMG Labtech). Cells lyzed with 1% triton X (Sigma-Aldrich) were used as a positive control and were considered as the 100% cell death reference.

3.14. Cell-free aggregation assays

Aggregation reactions preparation

The different fragments used as seeds were mixed with monomeric FL-αSyn with a molar ratio of 1:10, respectively, with a final concentration of 20 µM in 50 mM tris-HCl buffer at pH 7.0 and 25 µM thioflavine T (ThT; Sigma-Aldrich). Each sample was prepared in three technical repeats in black-walled clear bottom 384 well plates (Thermo Fisher Scientific) with a final volume of 45 µL. The plates were sealed and allowed to shake at 700 rpm at 37 °C for 230 h. Aggregation

kinetics were monitored by measuring ThT fluorescent signal every hour in relative fluorescence units (RFU). The experiment was repeated at least 3 times.

Apparent lag time and growth rate detemination

To determine the apparent lag time, each data set was normalized by subtraction of its lowest value and division by its highest value. Apparent lag times were determined as the time at which the curves reached 10% of the elongation phase ($T_{10\%}$). Growth rate was calculated as follows:

$$Growth\ rate\ (RFU/hour) = \frac{F50 - F10}{T50 - T10}$$

Where F_{50} and F_{10} are the fluorescence values in RFU when the curves reached 50% and 10% of the elongation phase, respectively. T_{50} and T_{10} are the time points at which the curves reached 50% and 10% of the elongation phase, respectively.

3.15. Dynamic light scattering measurements

Particle size distributions and zeta potential measurements were perfomed with dynamic light scattering (DLS) using a Malvern Zetasizer Nano ZSP (Malver Instruments, Malvern, UK). An estimation of the hydrodynamic radius (r_h) was obtained with the Stokes-Einstein relation:

$$D = \frac{k_B T}{6\pi\eta r_h}$$

Where D is the measured particle diffusion constant, k_B is the Bolzmann constant, T is the absolute temperature and the viscosity of the measurment medium. The particle diameter ($2xr_h$) was calculated from the Z-average size from the cumulants fit, using the software provided by Malvern Instruments.

3.16. Proteinase K digestion

Cell-free produced aggregates:

3 µg of previously described aggregateswere digested at 37 °C with 0.1 µg/mL of proteinase K (Thermo Fisher Scientific, Waltham, MA, USA) for the indicated amounts of time. The enzymatic reaction was stopped by mixing with preheated 1X sample loading buffer followed by immediate incubation at 95 °C for 5 min. The samples were loaded on 12% Bis-Tris criterion gels (Bio-Rad Laboratories) for electrophoresis, then stained with Pierce silver staining kit (Thermo Fisher

Scientific) according to the manufacturer's instructions. Pictures of the stained gels were acquired with the Gel Doc™ XR imaging system (Bio-Rad Laboratories) and the optical density of bands was quantified with the Image Lab™ software (Bio-Rad Laboratories).

Cell lysates:

20 µg of total cell lysates were digested at 37 °C with increasing concentrations of proteinase K for 30 min. The digestion reaction was stopped by mixing with preheated sample loading buffer followed by immediate incubation at 95 °C for 5 min. The samples were then loaded on 12% Bis-Tris criterion gels (Bio-Rad Laboratories) and Western blots were carried out as described above.

3.17. Toxicity blocking with antibodies

At DIV 4, LUHMES cells were pretreated with anti αSyn N-terminal (Syn303; 25µg/mL; Biolegend, San Diego, CA) or C-terminal (Syn211; 25µg/mL; Thermo Fisher Scientific) antibodies for for 1h at 37 °C, 5% CO_2, and water-saturated air.. 3 µM of recombinant αSyn fragments 61-140 and 1-95 were then added and the treatment was carried on for 48h. Cells were washed at DIV 6, and medium was changed at DIV9. Toxicity measurement was performed at DIV 12 with an LDH assay as described above.

3.18. Statistical Analysis

Statistical analysis was performed using GraphPad Prism 7.01 (GraphPad Software, La Jolla, CA). The GraphPad Prism 'identify outliers' tool with the ROUT method (Q=1%) was used and data determined as outliers were excluded from statistical analysis Data are shown as means with error bars representing the standard error of the mean (SEM). Two-way ANOVA and one-way ANOVA were used followed by Tukey's *post hoc* test, p-values < 0.05 were considered as statistically significant.

4. RESULTS

4.1. Analysis of αSyn species released from αSyn-overexpressing neurons

Adenoviral (AV) overexpression of αSyn in differentiated LUHMES cells provides a robust and reproducible model for αSyn-mediated pathology (Höllerhage et al., 2014). Here, I used this model to study the release of αSyn into the extracellular space under pathological conditions. Transduction with AVs was performed at day *in vitro* (DIV) 2 and readouts for toxicity, intracellular and extracellular αSyn were performed at DIV4, DIV6 and DIV8 (Figure 4.1a). αSyn-mediated toxicity was measured as lactate dehydrogenase (LDH) activity in cell culture medium, and related a 100% cell lysis positive control (Figure 4.1b). While GFP overexpression yielded a very mild toxicity in comparison to untreated controls, αSyn overexpression induced consistently increasing toxicity over time and reached approximately 50% at DIV8.

Next, I monitored intracellular αSyn species in whole cell homogenates (Figure 4.1c). As expected, αSyn overexpression led to a stable increase in αSyn levels, as well as a marked intracellular aggregation.

To explore the release of αSyn into the extracellular space, I analyzed cell conditioned medium (CM) for different αSyn species (Figure 4.1d). Several forms of αSyn appeared in the CM at DIV6; an oligomeric species at approximatively 37 kDa, monomeric FL-αSyn at 15 kDa and several αSyn fragments ranging between 13 and 6 kDa in molecular size. At this time point, cytoplasmic content leakage, as shown by GAPDH level, was very minimal. At DIV8, however, the level of all αSyn species increased considerably with concomitant increase of cytoplasmic leakage as indicated by the increase of GAPDH in the CM, pointing towards an accumulation of αSyn in the medium as a result of cell death. Interestingly, no intracellular αSyn fragments lower in molecular weight than FL-αSyn (15 kDa) were detectable in cell homogenates at any time after transduction.

4.2. Extracellular αSyn fragments result from multiple truncation events

To better characterize the αSyn fragments detected in the medium (Figure 4.1d), I aimed first to confirm that the αSyn-immunoreactive bands smaller than 15 kDa in the extracellular space are indeed αSyn fragments, and secondly to uncover their cleavage sites. Hence, the CM of αSyn-overexpressing cells at DIV8 was analyzed by liquid chromatography mass spectrometry (LC-MS) (Figure 4.2). This analysis revealed the presence of peptides corresponding to αSyn sequence in all investigated gel sections, except gel section #7.

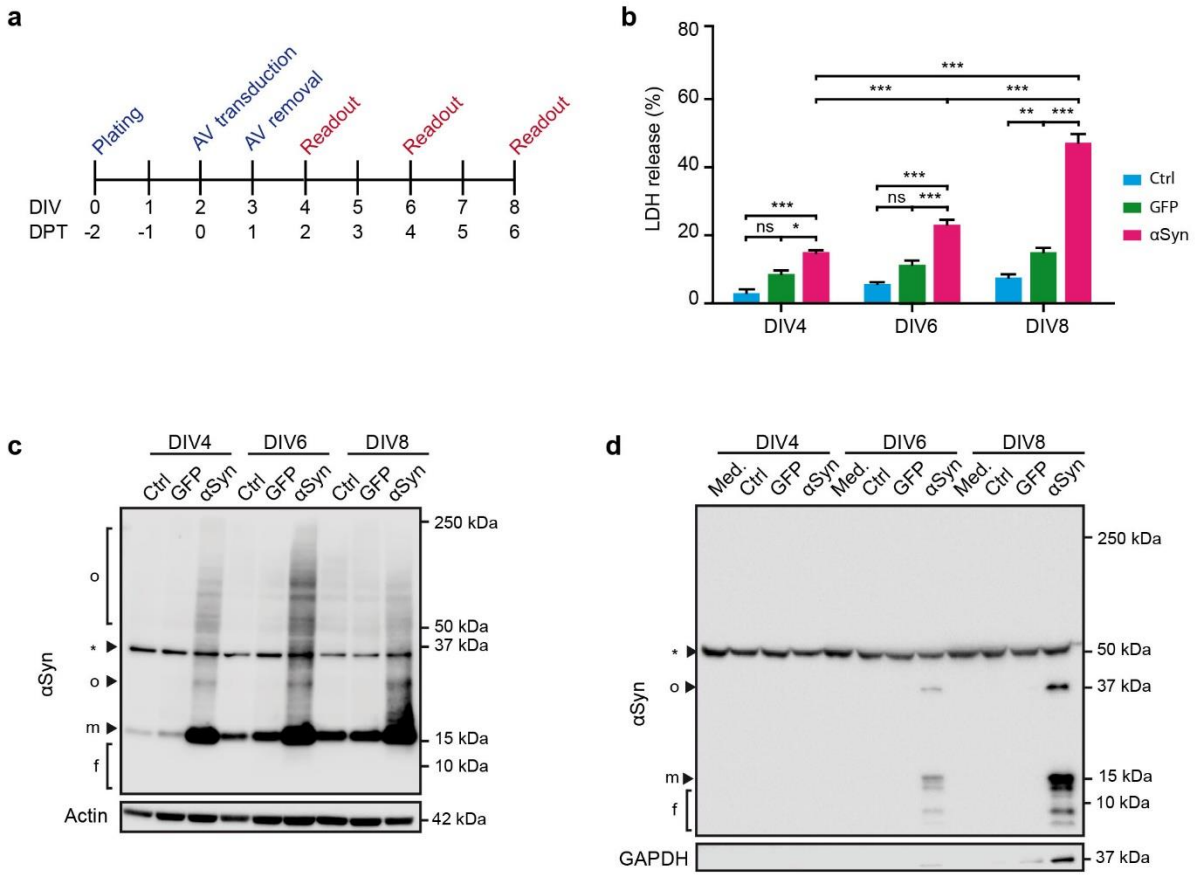

Figure 4.1. αSyn fragments in the conditioned medium of αSyn-overexpressing LUHMES neurons. (a) Experimental design. LUHMES cells were transduced with green fluorescent protein (GFP) or aSyn adenoviral vectors (AV) two days after plating. Viruses were removed 24 hours after transduction. Cells and conditioned medium (CM) were harvested at the indicated readout times. DIV: days *in vitro*. DPT: days post-transduction. (b) αSyn-mediated toxicity. Cellular toxicity was monitored by lactate dehydrogenase (LDH) activity in the CM at the indicated readout times. Cells were either left untreated (Ctrl), challenged with a control AV, expressing GFP or an AV expressing wild type αSyn. Data is presented as mean + standard error of the mean (SEM) from at least 3 biological repeats. ns: not significant, * $p < 0.05$, ** $p < 0.005$, *** $p < 0.001$; two-way ANOVA with Tukey's *post hoc* test. (c) Intracellular αSyn. Cell lysates analyzed at the indicated readout times by Western blot (WB) against αSyn. f: fragments; m: monomer; o: oligomer; *: unspecific band. Actin was used as loading control. (d) Extracellular αSyn. CM analyzed at the indicated time points by WB against αSyn. Medium incubated without cells (Med.) was used as control for unspecific bands. GAPDH was used as control for cytoplasmic content in the CM. f: fragments; m: monomer; o: oligomer; *: unspecific band. [modified from (Chakroun et al., 2020)]

The first 10 amino acids of the N-terminus were missing in all detected peptides suggesting that a truncation event took place at this site, whereas multiple truncation events appeared on the C-terminal side of αSyn (Figure 4.2). Importantly, the MS analysis allowed to confirm the bands below 15 kDa observed in the extracellular space (Figure 4.1d) as several αSyn fragments, and suggest that these fragments result from a proteolytic activity at multiple sites of αSyn. However, due to the margin of error inherent to peptide sequencing, it was not possible to identify precise cleavage sites which would have allowed to unambiguously delineate the protease(s) responsible for such a cleavage pattern in this model.

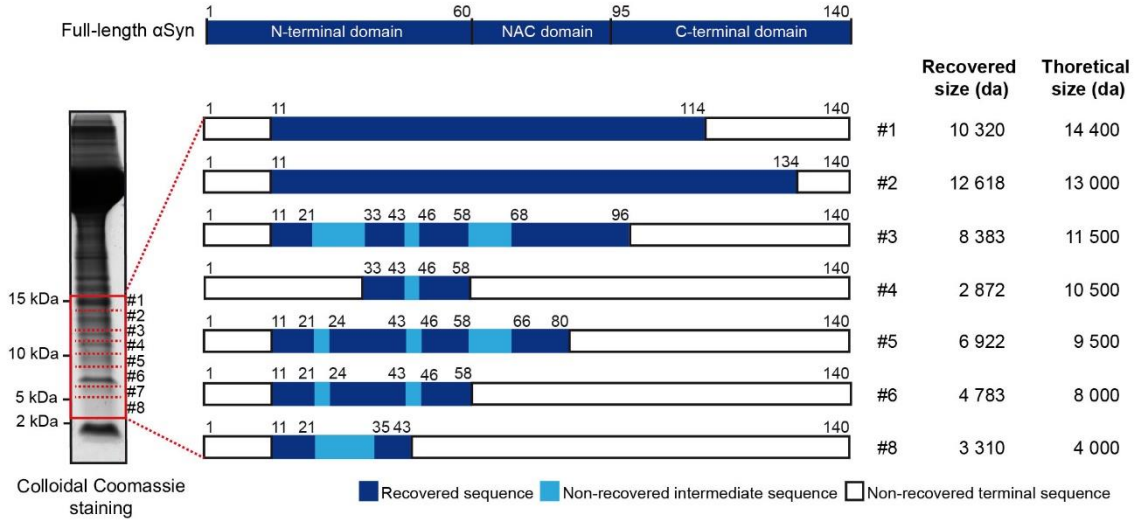

Figure 4.2. Identification of extracellular αSyn fragments. Schematic depiction of αSyn fragments detected in the CM of αSyn-overexpressing cells. CM of αSyn-overexpressing cells was separated by gel electrophoresis. Eight sections, containing proteins between 3 and 15 kDa, were excised (red boxes) and analyzed by mass spectrometry. Recovered peptide sequences (dark blue boxes), not recovered sequences within recovered sequences (light blue boxes), and not recovered edge sequences (white boxes) are shown. Recovered and expected molecular sizes (corresponding to molecular size on the gel) of αSyn are displayed. In section 7, no sequence could technically be recovered. [taken from (Chakroun et al., 2020)]

4.3. Fragments result from extracellularly processed full-length αSyn

Since WB analysis showed a complete intracellular absence and a clear extracellular presence of αSyn fragments (Figures 4.1c and 4.1d), I wanted to find out whether they are generated extracellularly.

To do so, I incubated recombinant FL-αSyn with unconcentrated conditioned cell culture medium. In this experimental design, CM-derived FL-αSyn and fragments were below detection limit. Therefore, only the added recombinant FL-αSyn and its cleavage products could be visualized. Unconditioned unsupplemented medium, as well as unconditioned medium containing either N2- or B27-supplements were used as controls to exclude that cleavage of αSyn in the medium was caused by the culture medium or by specific supplements (Figure 4.3a).

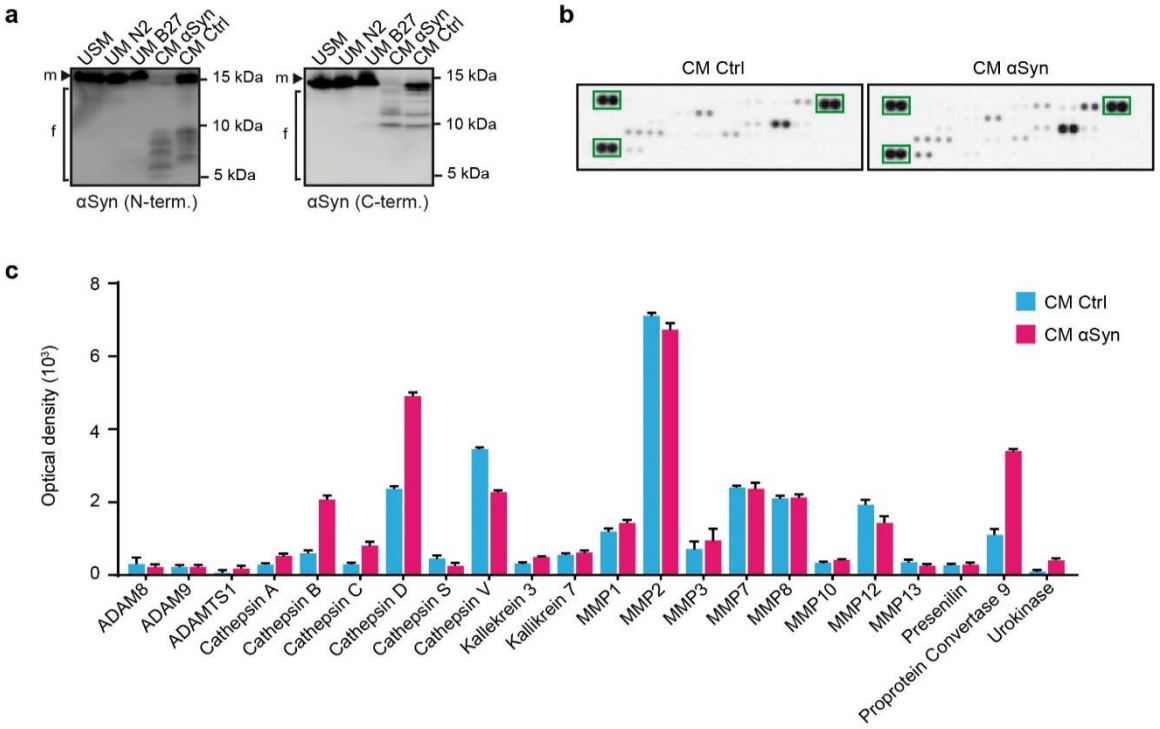

Figure 4.3. Extracellular generation of αSyn fragments and screening of proteases present in LUHMES cells CM. (a) Generation of αSyn fragments in CM. Recombinant FL-αSyn was added to CM from αSyn-overexpressing cells (CM αSyn) or from control cells (CM Ctrl). Unsupplemented medium (USM) and unconditioned medium supplemented with N2- (UM N2) or B27-supplement (UM B27) were used as controls. WB with N-terminal (N-term.) and C-terminal (C-term.) antibodies are shown. f: fragments, m: monomer. (b) Screening of proteases present in LUHMES cells CM. Dots in green rectangles are internal controls to insure the proper functioning of the array. Each protease is represented by dot duplicates and the array is able to screen up to 35 different proteases. Only proteases that showed a detectable positive signal in duplicates were considered present in CM of control and αSyn-overexpressing cells. (c) Levels of all the proteases detected by the protease array in CM of control and αSyn-overexpressing cells measured by optical density. [(a) taken from (Chakroun et al., 2020)]

WB analysis with N- and C-terminal αSyn antibodies revealed that cleavage of recombinant αSyn occurred in CM of both, αSyn-overexpressing cells and untransduced control cells. However, the medium alone and the tested supplements did not lead to the cleavage of αSyn. Although the cleavage observed in the αSyn-overexpression condition was significantly more pronounced than in the untransduced control condition, the presence of cleaved αSyn in untransduced controls indicates that αSyn is very likely cleaved in the extracellular space by a protease that is secreted by cells also under physiological conditions. Furthermore, the marked reduction of monomeric αSyn after incubation with CM from αSyn-overexpressing cells points to elevated levels of the implicated protease(s) by upregulating its/their secretion upon αSyn overexpression.

4.4. Several proteases are present in the conditioned medium of LUHMES cells

In order to identify proteases in the CM of LUHMES cells, I used a protease screening kit that targets a large variety of proteases. Antibodies against specific proteases are dotted on a nitrocellulose membrane. Upon incubation of the membranes with CM of control and αSyn-overexpressing cells, followed by development with an enhanced chemiluminescencereagent, a signal corresponding to the different proteases present in this system is revealed (Figure 4.3b). Positive signals were linked to the corresponding proteases using an identification overlay provided by the manufacturer, and signal levels were measured as optical densities (Figure 4.3c). The identity and the catalytic type of proteases that were present in both control and αSyn-overexpressing CM conditions are reported in table 4. Since previous results show an increased cleavage in the CM of αSyn-overexpressing cells, proteases that appear to be be increased under this condition are marked with an asterisk (Table 4).

4.5. The serine protease plasmin is involved in the cleavage of αSyn in the extracellular space

To further investigate which protease(s) are responsible for extracellular cleavage of αSyn, several protease inhibitors were selected based on the data obtained from the protease screening (Figure 4.3) and the literature. In addition to inhibitors of metalloproteases (EDTA and NNGH) and cathepsins (pepstatin), calpains (calpastatin) and caspases (Z-VAD-FMK) were included as well. A protease inhibitor cocktail (PIC) was used as a broad spectrum inhibitor. Surprisingly, none of the protease-specific inhibitors showed an effect on αSyn cleavage. The PIC however, seemed to reduce the proteolytic processing of αSyn in the extracellular space (Figure 4.4a). Next, the different components of the PIC were tested individually to determine which one is most effective

in blocking cleavage of αSyn. A second PIC (PIC2) from a different supplier was used to confirm the results obtained with the first one (PIC1). From the different individual components, only AEBSF and aprotinin most efficiently reduced the appearance of αSyn fragments in CM. Both have a serine protease inhibitor activity. This suggests a serine protease to be responsible for αSyn cleavage in the CM of LUHMES cells (Figure 4.4b).

Table 4. List of Proteases detected in CM of untreated control and αSyn-overexpressing cells

Ctrl CM	**αSyn CM**	**Activity**
ADAM8	ADAM8	Metalloprotease
ADAM9	ADAM9	Metalloprotease
ADAMTS1	ADAMTS1*	Metalloprotease
Cathepsin A	Cathepsin A*	Serine protease
Cathepsin B	Cathepsin B*	Cysteine protease
Cathepsin C	Cathepsin C*	Cysteine protease
Cathepsin D	Cathepsin D*	Aspartic protease
Cathepsin S	Cathepsin S	Cysteine protease
Cathepsin V	Cathepsin V	Cysteine protease
Kallikrein 7	Kallikrein 7*	Serine protease
MMP1	MMP1*	Metalloprotease
MMP2	MMP2 *	Metalloprotease
MMP3	MMP3*	Metalloprotease
MMP7	MMP7	Metalloprotease
MMP8	MMP8	Metalloprotease
MMP10	MMP10*	Metalloprotease
MMP12	MMP12	Metalloprotease
MMP13	MMP13	Metalloprotease
Presenilin	Presenilin	aspartic protease
Proprotein convertase 9	Proprotein convertase 9*	serine protease
Urokinase	Urokinase*	serine protease

* : Proteases with increased signal in the CM of αSyn-overexpressing cells.

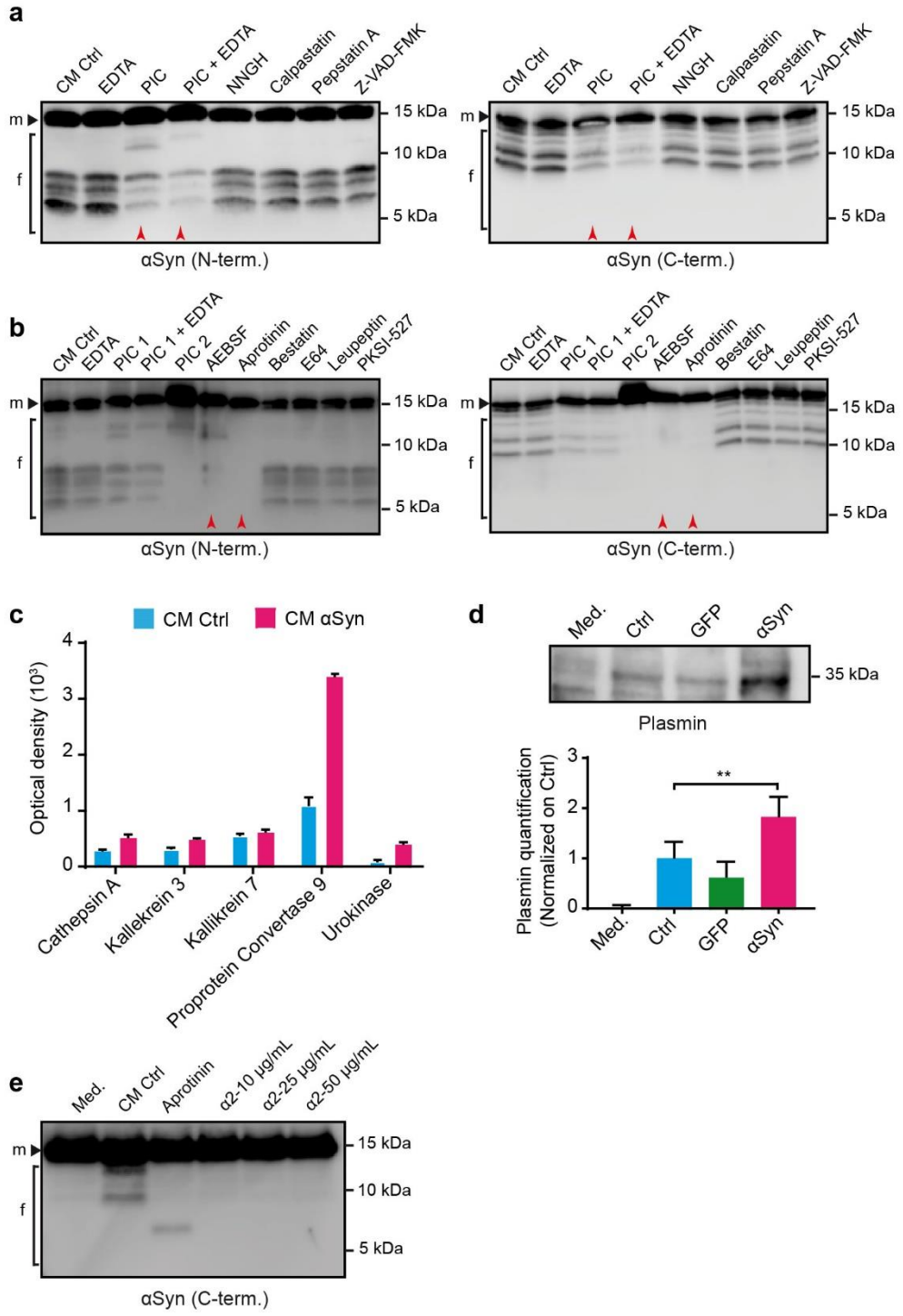

Figure 4.4. Identification of the responsible protease for extracellular αSyn cleavage. (a, b, e) Different protease inhibitors were added to CM from control LUHMES cells prior to addition of recombinant FL-αSyn. WB with N-terminal (N-term.) and/or C-terminal (C-term.) antibodies are shown. (a) shows a broad spectrum of inhibitors. (b) shows individual inhibitor components of the PIC, and (e) shows specific inhibition of plasmin. PIC: Protease inhibitor cocktail, Med.: Unconditioned medium, f: fragments, m: monomer. (c) Quantification of the optical density signal from the protease array corresponding to serine proteases in the CM of control and αSyn-overexpressing cells. (d) WB detection of plasmin in CM of LUHMES (upper panel). Quantification of plasmin bands detected by WB reveals an increase of plasmin in CM of both control and αSyn-overexpressing cells.

The protease array previously used (Figure 4.3b, c) allowed me to identify several serine proteases present in control CM with a tendency to increase in αSyn CM (Figure 4.4c, Table 4). A search on the MEROPS peptidase database tool (Rawlings et al., 2018) [https://www.ebi.ac.uk/merops/] showed however, that none of these proteases have a cleavage pattern that corresponds with αSyn sequence, which means that αSyn is not a direct substrate of any of them. Therefore, an intermediate protease is most likely involved. Therefore, I performed a literature search which revealed that only urokinase is a well established activator of plasminogen, the precursor form of plasmin. Plasmin has been shown to cleave αSyn on several sites (Kim et al., 2012). These correspond exactly to the ones identified by MS analysis (Figure 4.2, Table 5). Therefore, I performed a WB analysis of the CM to confirm the presence of plasmin, which showed that it only appeared when the medium was conditioned with control cells, and that it increases significantly under αSyn-overexpression condition (Figure 4.4d). Moreover, a very specific plasmin inhibitor (α2-antiplasmin) was able to effectively inbhibit αSyn cleavage in the CM (Figure 4.4e), confirming plasmin as the active protease in this experimental system that is involved in the appearance of different αSyn fragments in the extracellular space.

Table 5. Plasmin cleavage sites on αSyn (Kim et al., 2012).

	Cleaved bonds	**Cleavage position**	**Resulting fragments**
#1	GLSK ǂ AKEG	10 ǂ 11	1-10, 11-140
#2	AAGK ǂ TKEG	32 ǂ 33	1-32, 33-140
#3	VGSK ǂ TKEG	43 ǂ 44	1-43, 44-140
#4	VAEK ǂ TKEQ	58 ǂ 59	1-58, 59-140
#5	VAQK ǂ TVEG	80 ǂ 81	1-80, 81-140
#6	GFVK ǂ KDQL	96 ǂ 97	1-96, 97-140

ǂ : Cleavage site.

4.6. Extracellularly generated αSyn fragments can be taken up by naïve αSyn knockout cells

A major goal of my study was to investigate whether αSyn fragments can be involved in cell-to-cell spreading of αSyn pathology. Thus, I questioned whether the fragments generated in the extracellular space of αSyn-overexpressing cells are taken up by naïve cells.

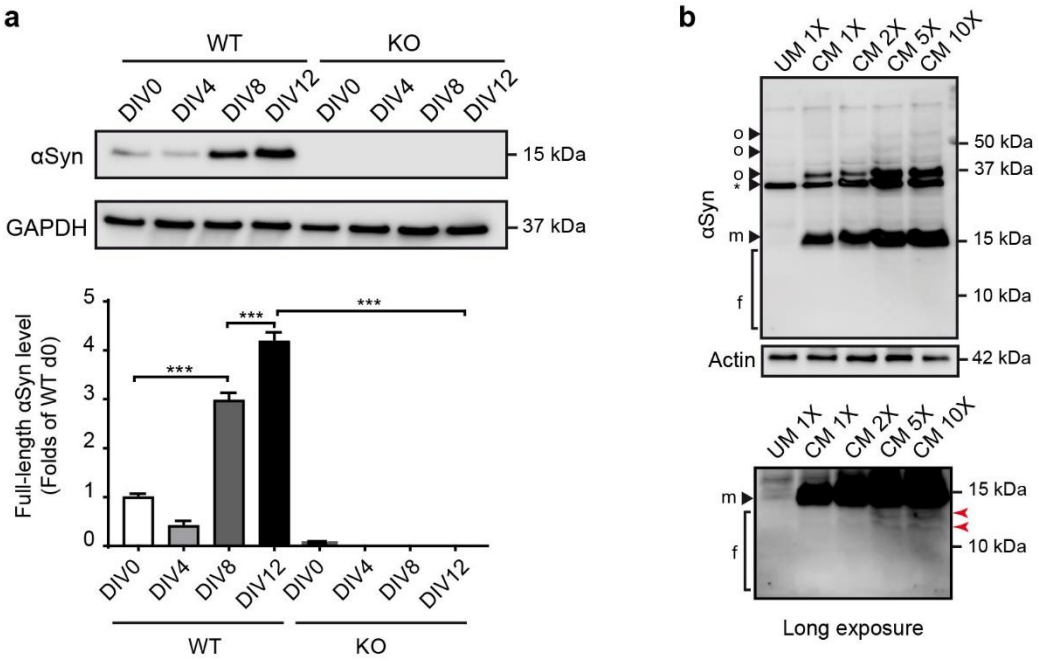

Figure 4.5. The αSyn knockout (KO) LUHMES cell line and uptake of CM-generated αSyn fragments. (a) Validation of CRISPR/Cas9 αSyn knockout (KO) LUHMES cells. Wild type (WT) and αSyn KO LUHMES cells were differentiated for the indicated amount of time and αSyn protein levels were assessed by Western blot. Top panel shows a Western blot of αSyn in WT and KO LUHMES cells at the indicated times. GAPDH was used as loading control. Lower panel shows a quantification of αSyn monomer levels normalized with GAPDH. Data is presented as mean + SEM from 3 biological repeats. *** $p < 0.001$; one-way ANOVA with Tukey's *post hoc* test. (b) αSyn KO cells were treated with different concentrations of CM of αSyn-overexpressing cells for 6 h. Medium was either used unconcentrated (CM 1X) or 2 (CM 2X), 5 (CM 5X), and 10 times (CM 10X) concentrated. Unconditioned medium (UM 1X) was used as negative control. Red arrowheads show αSyn fragments (bottom panel). f: fragments, m: monomer, o: oligomer, *: unspecific bands. [modified from (Chakroun et al., 2020)]

In order to exclusively observe the uptake of extracellular αSyn, I used αSyn knockout (KO) LUHMES neurons as recipient cells. An αSyn KO LUHMES cell line was generated by CRISPR/Cas9 genome editing. This cell line showed absence of αSyn even at an advanced differentiation stage (Figure 4.5a).

For the uptake experiment, naïve αSyn KO cells were incubated for 6 hours at DIV8 either with unconcentrated or 2, 5, and 10 times concentrated CM of wild-type (WT) αSyn-overexpressing cells and the uptake of extracellular αSyn was analyzed by WB. A dose-dependent uptake of monomeric FL-αSyn as well as an oligomeric species at 37 kDa was observed, but no presence of fragments could be detected upon short exposure time of the WB (Figure 4.5b, top panel). With a longer exposure time, however, a faint signal corresponding to an uptake of αSyn fragments was visible with the highest concentrations (5X and 10X) of CM (Figure 4.5b, lower panel). This

finding provides evidence that αSyn fragments can be taken-up by naïve cells. In these experimental conditions, the uptake of FL and oligomeric αSyn species seems predominate over fragmented αSyn. I therefore conducted further experiments with recombinant human αSyn fragments.

4.7. Recombinant αSyn fragments differentially influence the aggregation of FL-αSyn

To systematically characterize and compare the effects of αSyn fragments on FL-αSyn aggregation, distinct recombinant fragments containing one or two adjacent full domains of αSyn were selected for this study. Noteworthy, the fragments identified in sections #3 and #6 in the CM of αSyn-overexpressing cells (Figure 4.2) were similar to recombinant fragments 1-95 and 1-60 chosen for this study (Figure 4.6a).

In a cell-free aggregation assay, I used non-aggregated recombinant fragments as seeds and monomeric FL-αSyn as a substrate. αSyn preformed fibrils (PFFs) were used as a positive control for seeded aggregation due to their well-established capacity as highly efficient seeds (Volpicelli-Daley et al., 2011, Luk et al., 2012). To compare the seeding effiency of fragments, FL-αSyn (1-140) was set as the reference baseline of aggregation kinetics. The molar ratio of seed to substrate was 1 to 10, respectively, in all the reactions. Aggregation was monitored over time with thioflavin T (ThT).

To control for the seeds' own contribution to the overall ThT signal, reactions containing seeds without substrate were included (Figure 4.6b). In this regard, none of the tested seeds displayed a discernible increase in fluorescent signal within the monitored time window suggesting that they do not have a considerable influence on the aggregation curves when incubated without a substrate. However, when the substrate was added to the reactions, the ThT signal increased substantially, indicating that it corresponds primarily to the aggregation of FL-αSyn (Figure 4.6c).

Generally, the obtained ThT fluorescence curves had a characteristic sigmoidal amyloid-like aggregation shape (Figure 4.6c). The apparent lag time was reported as the time at which ThT signal reached 10% of its total increase, and growth rates were calculated as the difference in RFU per hour between 10% and 50% of the total ThT signal increase (Figure 4.3d).

Expectedly, PFFs prominently accelerated the aggregation with a reduced apparent lag time.

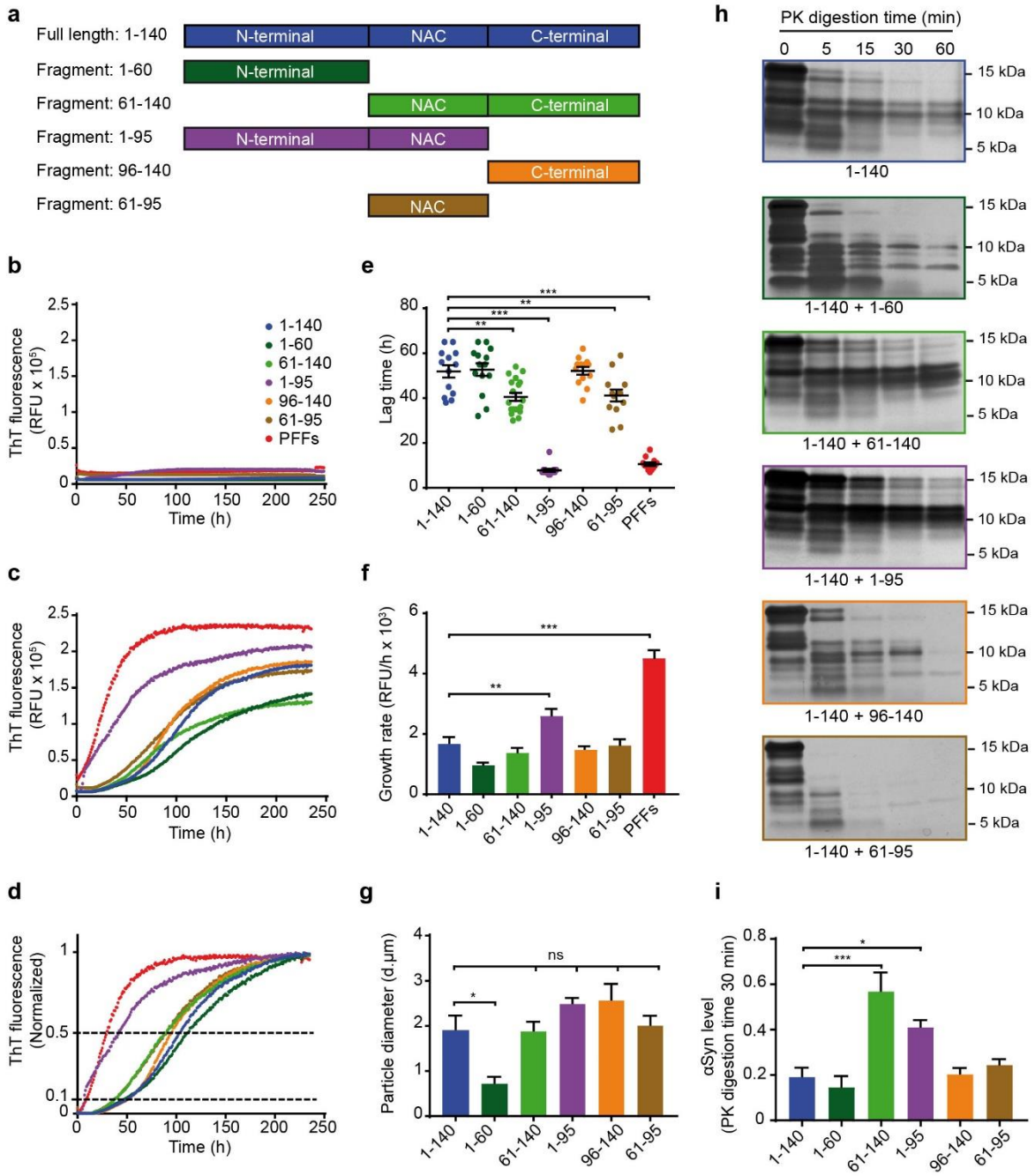

Figure 4.6: Recombinant αSyn fragments show distinct effects on aggregation of full-length αSyn in a cell-free aggregation assay. (a) Schematic overview of recombinant FL-αSyn and fragments used in this study. The same nomenclature and color codes are used in all the panels. (b-d) Seeding effect of recombinant αSyn fragments on recombinant FL-αSyn in a cell-free aggregation assay. Fragments described in (a) were used as seeds and FL-αSyn was used as a substrate at a molar ratio of 1:10, respectively. Aggregation kinetics were monitored with thioflavin T (ThT). Pre-formed fibrils (PFFs) were used as positive control for seeding. RFU: relative fluorescence unit. (b) Aggregation curves of αSyn fragments without addition of FL-αSyn substrate. (c) Aggregation curves with addition of FL-αSyn substrate as raw fluorescence data. (d) Normalized fluorescence ratio data from (c). The lower (0.1) and the upper (0.5) fluorescence thresholds of the total signal are shown with dotted lines. Aggregation curves are presented as mean from at least 3 independent repeats with 3 technical replicates each.

Figure 4.6 (continued legend) :
(e) Apparent lag time of aggregation. Lag times are presented as the time at which each curve reached 10% of the total fluorescence signal. Each dot of the scatter plot represents one aggregation curve. Data is presented as mean ± SEM from at least 3 repeats with 3 technical replicates each (black lines). ** $p < 0.005$, *** $p < 0.001$; one-way ANOVA with Tukey's *post hoc* test. (f) Growth rate of aggregation. Aggregation growth rate is presented as a measure of increased ThT fluorescence per hour. Data is presented as mean + SEM from at least 3 repeats with 3 technical replicates each. ** $p < 0.005$, *** $p < 0.001$; one-way ANOVA with Tukey's *post hoc* test. (g) Particle size of aggregates seeded with different αSyn fragments. Particle size of aggregates was measured with dynamic light scattering (DLS) after the aggregation reactions were finished. Data is presented as mean + SEM of particle diameter (d.µm) from at least 3 repeats. * $p < 0.05$; one-way ANOVA with Tukey's *post hoc* test. (h,i) Proteinase K (PK) resistance. Aggregation was carried out with the same molar ratio of seed to substrate (1:10). PK digestion was performed at 37 °C for the indicated amounts of time. (i) A normalized optical density quantification of αSyn digestion at 30 min. Data is presented as mean + SEM from at least 3 repeats. * $p < 0.05$, *** $p < 0.001$; one-way ANOVA with Tukey's *post hoc* test. [taken from (Chakroun et al., 2020)]

Strikingly, fragment 1-95 behaved similarly and reduced the apparent lag time to the same extent as PFFs. Fragments 61-140 and 61-95 also reduced the aggregation lag time significantly but more moderately.

The growth rate of seeded aggregation with PFFs was higher than the one seeded with fragment 1-95 implying that even though PFFs and fragment 1-95 initiated the aggregation elongation phase with a very similar efficiency, the aggregation seeded with fragment 1-95 required a longer time to reach a plateau as compared to PFFs. Similarly, fragments 61-140 and 61-95 reduced the lag time without detectable effect on the growth rate in comparison with monomeric FL-αSyn (1-140). Fragments 1-60 and 96-140, however, had no effect on aggregation kinetics (Figures 4.6e and f).

Next, I investigated whether aggregates seeded with different αSyn fragments would have distinct utrastructural properties. Dynamic light scattering was used to measure the particle diameter size of these aggregates (Figure 4.6g). No significant differences in particle size was observed across the tested aggregates, except for the ones seeded with fragment 1-60 which resulted in a significantly smaller average particule size. Subsequently, the PK resistant of the different aggregates was analyzed. Interestingly, aggregation seeded with both fragments 61-140 and 1-95 resulted in a higher PK resistant than all the other aggregates (Figure 4.6h and i). PFFs were not used as positive control in these latter experiments, since the aggregates formed by αSyn 1-140 are identical to PFFs.

Taken together, these data showed that the NAC domain is essential but not sufficient for aggregation. Indeed, non-aggregated αSyn fragments that contain the NAC domain flanked by

either the N- or the C-terminal domain are able to effectively seed the aggregation of FL-αSyn but with very different kinetics.

4.8. Aggregates generated with αSyn recombinant fragments have distinct seeding properties in a second aggregation cycle

As a further characterization step, aggregates resulting from seeding with the different αSyn recombinant fragments were used as seeds in a new cycle of aggregation. The 1-140 condition represents the aggregation kinetics reference to which the other conditions are compared, and the PFF positive control was omitted since it corresponds to the aggregates generated in the 1-140 condition in this experimental setup. As before, monomeric FL-αSyn was used as a substrate and the seed to substrate ratio used was 1:10. Expectingly, the no-substrate control conditions did not show a significant increase in ThT signal over time, meaning they are not aggregation competent by themselves and depend on monomeric substrate to further aggregate (Figure 4.7a). Once the substrate is added however, the aggregation kinetics seem to be very different than previously observed. In comparison with the first aggregation cycle, the 1-140 reference condition shows a strong decrease in apparent lag time in the second aggregation cycle (54h vs. 10h, respectively). This decrease was observed in all other conditions in the second aggregation cycle and there were no significant differences between their respective apparent lag times, indicating that all the aggregates tested were able to initiate the elongation phase with the same efficiency. Strikingly, the growth rates, especially for the 61-140 and the 1-95 conditions, showed very distinct aggregation kinetics. While the 61-140 fragment lead to a slow growth rate in the first cycle, the resulting aggregates induced a significantly higher growth rate in the second cycle. Oppositely, fragment 1-95 showed a significant growth rate increase in the first cycle, and a significant deacrease in the second cycle (Figure 4.7b). These surprising results may imply a dynamic progression of seeding properties of αSyn through several cycles of aggregation.

4.9. Recombinant αSyn fragments are taken up by LUHMES neurons

In order to assess the relevance of αSyn fragments in intercellular spreading, I addressed their uptake into human dopaminergic neurons. Recombinant FL-αSyn and the fragments were fluorescently labeled with ATTO-488. The labeling was verified with gel electrophoretic separation followed by fluorescence imaging (Figure 4.8a). Successful labeling was revealed by the appearance of a fluorescent signal at the expected molecular sizes for all the different αSyn forms tested.

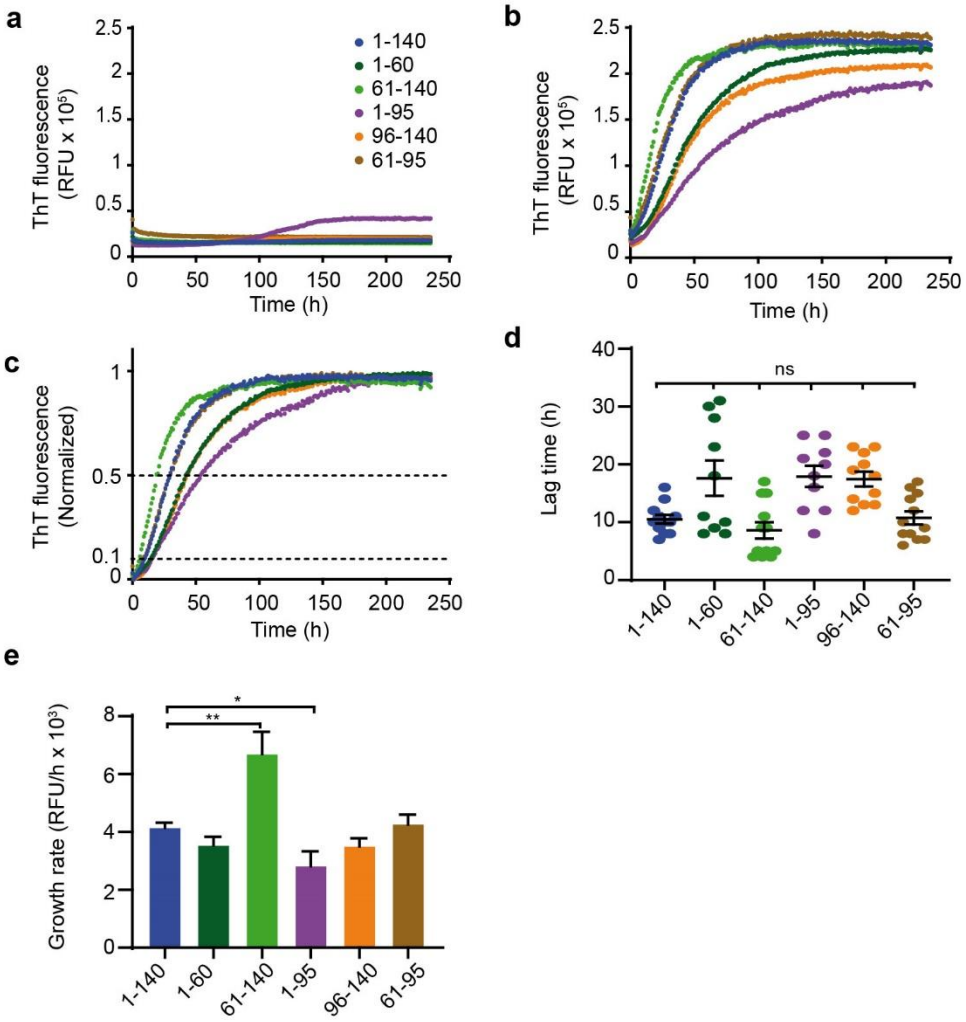

Figure 4.7. Seeding properties of aggregates generated with recombinant αSyn fragments in the second aggregation cycle. (a-c) Seeding effect of aggregates produced with αSyn fragments. Seeds and substrate were used as a substrate at a molar ratio of 1:10, respectively. RFU: relative fluorescence unit. (a) Aggregation curves of aggregates without addition of FL-αSyn substrate. (b) Aggregation curves with addition of FL-αSyn substrate as raw fluorescence data. (c) Normalized fluorescence ratio data from (b). Aggregation curves are presented as mean from at least 3 independent repeats with 3 technical replicates each. (d) Apparent lag time of aggregation. Each dot of the scatter plot represents one aggregation curve. Data is presented as mean ± SEM from at least 3 repeats with 3 technical replicates each (black lines). ns : not significant; one-way ANOVA with Tukey's *post hoc* test. (e) Growth rate of aggregation. Data is presented as mean + SEM from at least 3 repeats with 3 technical replicates each. ** $p < 0.005$, *** $p < 0.001$; one-way ANOVA with Tukey's *post hoc* test.

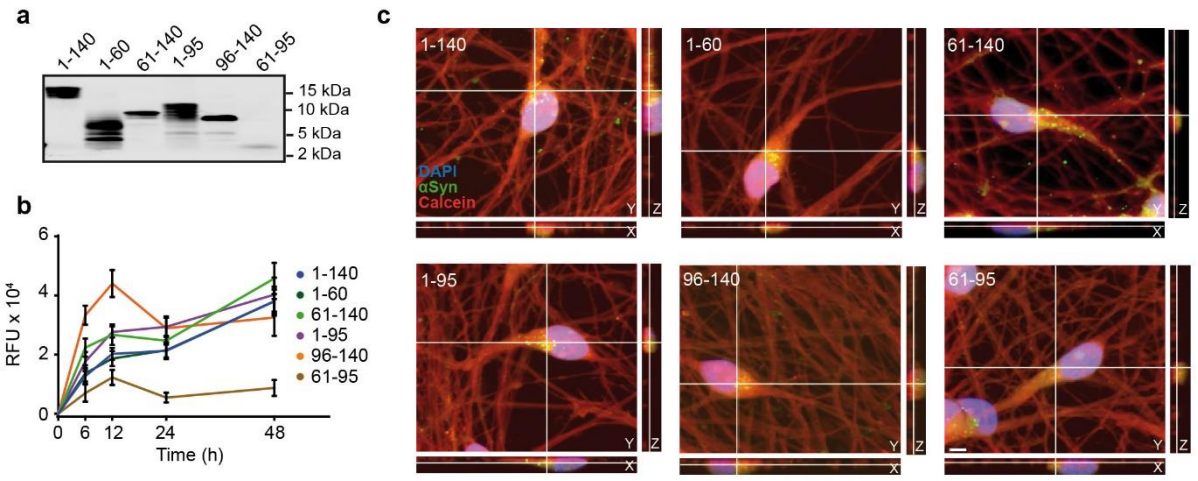

Figure 4.8. Uptake of recombinant αSyn fragments by naïve WT LUHMES neurons. (a) Fluorescent gel imaging of recombinant ATTO-488-labeled FL-αSyn and fragments (depicted in Figure 4.6a). (b**)** Uptake kinetics of recombinant FL-αSyn and fragments. Cells were treated with labeled αSyn at DIV4. At the indicated time points, intracellular fluorescence was measured. Extracellular fluorescence was quenched using trypan blue. RFU: relative fluorescence unit. (c) Uptake of ATTO-488-labeled αSyn fragments at 48 hours after treatment. Confocal images show orthogonal projections of Z-stacks. A calcein red-orange filling (red), DAPI staining (blue) and labeled recombinant αSyn (green) are shown. Scale bar: 5 µm. [taken from (Chakroun et al., 2020)]

The labeled material was used to treat cells at DIV4 for the indicated amounts of time. Uptake kinetics were monitored with an automated assay where extracellular fluorescence was quenched with trypan blue, followed by measuring of the intracellular fluorescence with plate reader (Figure 4.8b). The uptake kinetics of all labeled species were characterized by a rapid phase in the first 12 h, followed by slower phase and a plateau between 12 and 48 h. Overall, all the investigates species had a similar uptake pattern, with the exception of fragment 61-95, i.e. the NAC domain. The latter appears to be taken up less efficiently than all others which may be attributed to its highly hydrophobic nature and aggregated state.

I thereafter used confocal imaging with z-stack acquisition to ascertain that uptake took place. The cells were filled with a calcein stain to provide a visual contrast and delimitate the cell boundaries. The fluorescent signal corresponding to the different labeled αSyn species was indeed contained within the cells, thus showing their intracellular localization (Figure 4.8c).

4.10. αSyn fragments 1-95 and 61-140 result in different intracellular aggregation patterns

The next step in addressing the relevance of αSyn fragments in spreading would have to be the investigation of their capacity to seed intracellular aggregation after uptake. I had already established that fragments 61-140 and 1-95 influence aggregation kinetics and properties in a cell-free assay. In order to determine if they have a respective seeding potential on cell-endogenous FL-αSyn, 4 days differentiated LUHMES cells were treated with recombinant αSyn species (depicted in Figure 4.6a).

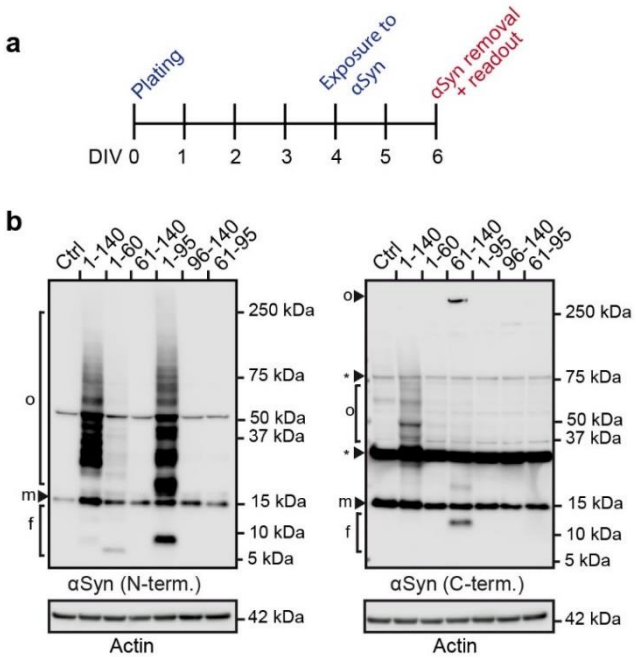

Figure 4.9. αSyn fragments induce different aggregation patterns in LUHMES neurons. (a) Experimental design. Cells were differentiated for 4 days then treated with recombinant FL-αSyn and fragments for 48 hours. (b) Intracellular seeding potency of recombinant FL-αSyn and fragments at DIV6. Western blot (WB) analysis was performed with antibodies targeting either the N-terminus (N-term.) or the C-terminus (C-term.) of αSyn. f: fragments, m: monomer, o: oligomer, *: unspecific bands. Actin was used as loading control. [modified from (Chakroun et al., 2020)]

The intracellular concentration of αSyn in neurons was previously estimated to lie between 30 to 60 µM. These values were obtained with a mathematical estimation model of the cubic volume of a neuronal cell, together with the observation that αSyn contitutes 0.5 to 1% of the total protein content in neurons (Iwai et al., 1995, Bodner et al., 2009, Kamp et al., 2010). Accordingly, I treated the cells with 3 µM recombinant FL-αSyn and fragments to maintain the previous 1:10 seed to substrate ratio. After 48 hours the treatments were removed and the cells were washed with trypsin

to remove extracellular αSyn. Intracellular αSyn was then examined by WB using antibodies targeting either the N- or C-terminus of αSyn (Figure 4.9a)

Convincing intracellular aggregation was only observed in cells exposed to FL-αSyn and fragments 1-95 and 61-140 and. Interestingly, the treatments resulted in very different patterns of intracellular aggregation, implying different aggregation pathways. Also, fragment 1-60 seemed to trigger another distinct aggregation pathway, showing, however, a less prominent pattern. Fragment 96-140 did not induce detectable intracellular aggregation, most likely due to the lack of the aggregation-prone NAC domain. Fragment 61-95 showed a lack of intracellular aggregation as well which may be explained by its highly insoluble state and inefficient uptake into cells (Figure 4.9b).

Intriguingly, while intracellular aggregation ensuing from FL-αSyn was detected by both N- and C-terminal antibodies, aggregates resulting from treatment with fragments 1-95 and 61-140 were only detectable by the N-terminal or the C-terminal antibody, respectively. This finding could imply that endogenous αSyn is recruited for aggregation and the resulting aggregates expose specific epitopes only detectable with antibodies targeting their respective seeding species. Alternatively, the observed intracellular aggregation may potentially be generated by self-aggregation of the different αSyn treatments.

4.11. Fragment-seeded intracellular aggregation requires endogenous αSyn

To determine whether endogenous αSyn is indeed recruited by fragments 61-140 and 1-95 for aggregation, I compared the intracellular seeding activity in WT and αSyn KO LUHMES cells. Two readout time points were chosen in order to analyze the immediate effects (DIV6) and the persistent effects after removal of recombinant αSyn (DIV10) (Figure 4.10a).

At DIV6, the characteristic aggregation patterns were present in WT cells as expected. However, they completely failed to appear for FL-αSyn and fragment 1-95, and were substantially reduced for fragment 61-140 in αSyn KO cells (Figure 4.10b). This indicates that endogenous αSyn is not merely recruited, but is a rather fundamental substrate for aggregation.

Furthermore, the fragment-seeded aggregation process continued to progress for at least four days after the removal of treatments in WT cells (Figure 4.10b). This further suggests that endogenous αSyn is an essential substrate for maintaining the aggregation progression. In addition, I analyzed the αSyn content in the MPER insoluble fraction extracted from cell lysates.

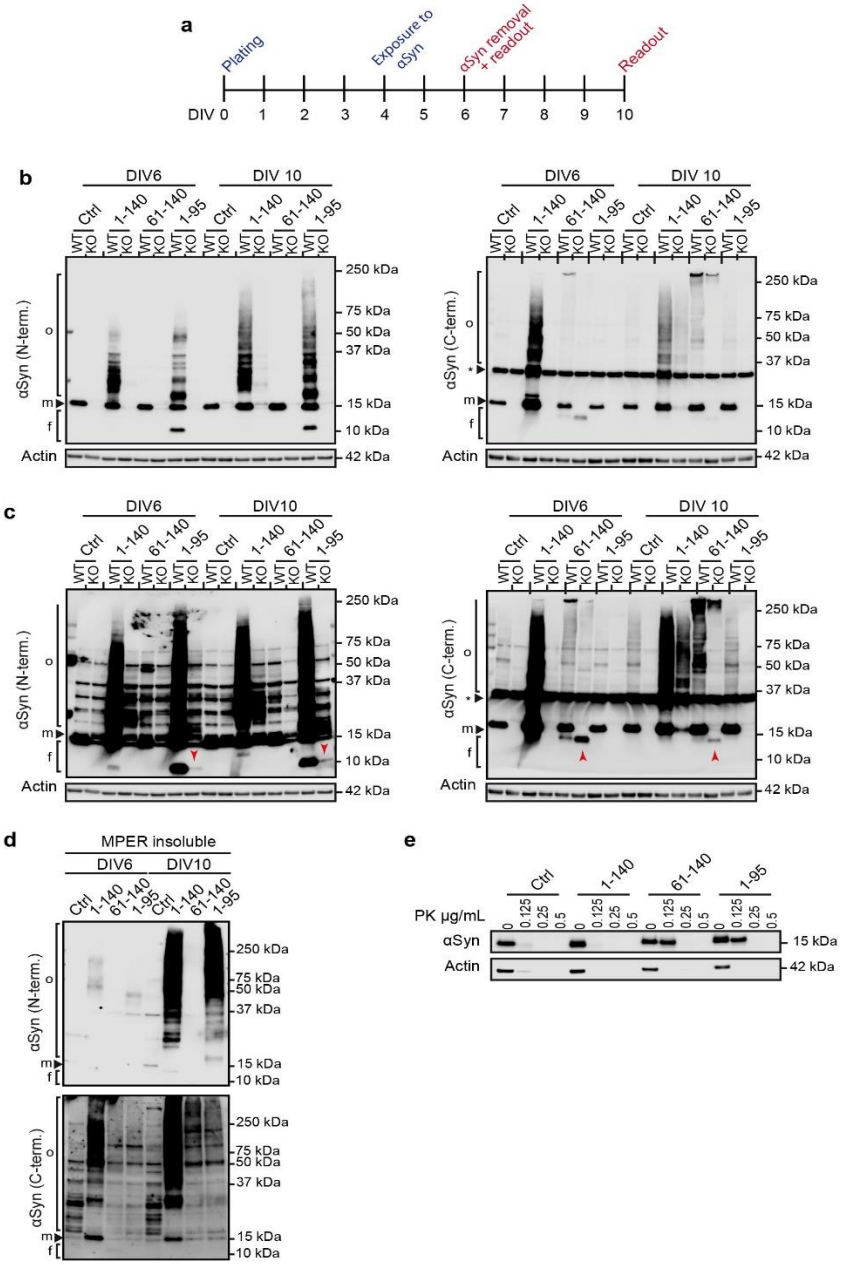

Figure 4.10. αSyn fragments recruit endogenous αSyn and induce long lasting aggregation. (a) Experimental design. Cells were differentiated for 4 days prior to treating with recombinant FL-αSyn and fragments for 48 hours. Readouts were performed at DIV6 and DIV10. (b) Intracellular seeding potency of recombinant FL-αSyn and fragments in wild type (WT) and αSyn knockout (KO) LUHMES cells. f: fragments, m: monomer, o: oligomer, *: unspecific bands. Actin was used as loading control. (c) Overexposed WB from (b). Red arrowheads show fragments in treated KO cells. (d) Evaluation of insoluble material in MPER-insoluble fractions of cell homogenates. 1% sarkosyl was used to solubilize the MPER insoluble material. f: fragments, m: monomer, o: oligomer, *: unspecific band. (e) Proteinase K (PK) resistance of intracellular aggregates produced by seeding with recombinant FL-αSyn and fragments. PK was added at the indicated concentrations to cell lysates from DIV10 cells and incubated at 37 °C for 30 min. Actin was used as control for both sample loading and PK digestion efficiency. [modified from (Chakroun et al., 2020)]

A clear shift from the soluble to the insoluble fraction between DIV6 and DIV10 provided supplementary evidence of the aggregation process continuing to take place after recombinant fragment treatments were removed (Figure 4.10d).

Notably, endogenous αSyn seems to influence either the uptake or the intracellular processing of recombinant αSyn fragments. In WT cells, recombinant FL-αSyn and fragments 61-140 and 1-95 were clearly visible in cell homogenates at the expected molecular size with short exposure times. In αSyn KO cells, longer exposure times were necessary to make them visable (Figure 4.10c). This points towards reduced intracellular amounts of recombinant fragments, most likely due to increased degradation of fragments, if they don't engage in aggregation, or alternatively to reduced uptake in KO cells.

Next, I examined the PK resistance of intracellularly induced aggregates. Cell homogenates were incubated with increasing concentrations of PK for 30 min and WB against total αSyn was performed. In accordance with previous findings in a cell-free context (Figure 4.6h and i), intracellular aggregates seeded by fragments 61-140 and 1-95 showed greater PK resistance than aggregates seeded with FL-αSyn (Figure 4.10e).

4.12. αSyn fragments 61-140 and 1-95 induce toxicity that can be prevented with domain-specific antibodies

To further establish the relevance for spreading of pathology, I examined whether these specific fragments induced toxicity subsequent to uptake and intracellular aggregation. Therefore, I treated LUHMES cells for 48 hours with different αSyn fragments and monitored the cellular toxicity by measuring LDH activity in the CM at three time points (Figure 4.11a). None of the treatments showed an immediate toxic effect at DIV6 and DIV9 (Figure 4.11b and c).

However, only fragments 61-140 and 1-95, but not FL-αSyn, induced toxicity that started to appear at DIV12 (Figure 4.11d). To further confirm this finding, the cells were fixed and stained with 4',6-diamidino-2-phenylindole (DAPI) at DIV12 to quantify the percentage of condensed nuclei (Figure 4.11e and f). This cell-based method reveals cells undergoing the final stage of apoptosis. It also showed an increased percentage of condensed nuclei in cells treated with fragments 61-140 and 1-95 in comparison to those treated with FL-αSyn and the untreated control.

The observations that the toxicity started with a delay and that it only appeared in conditions where PK-resistant intracellular aggregates were generated and accumulated overtime strongly suggest that the two events might be related.

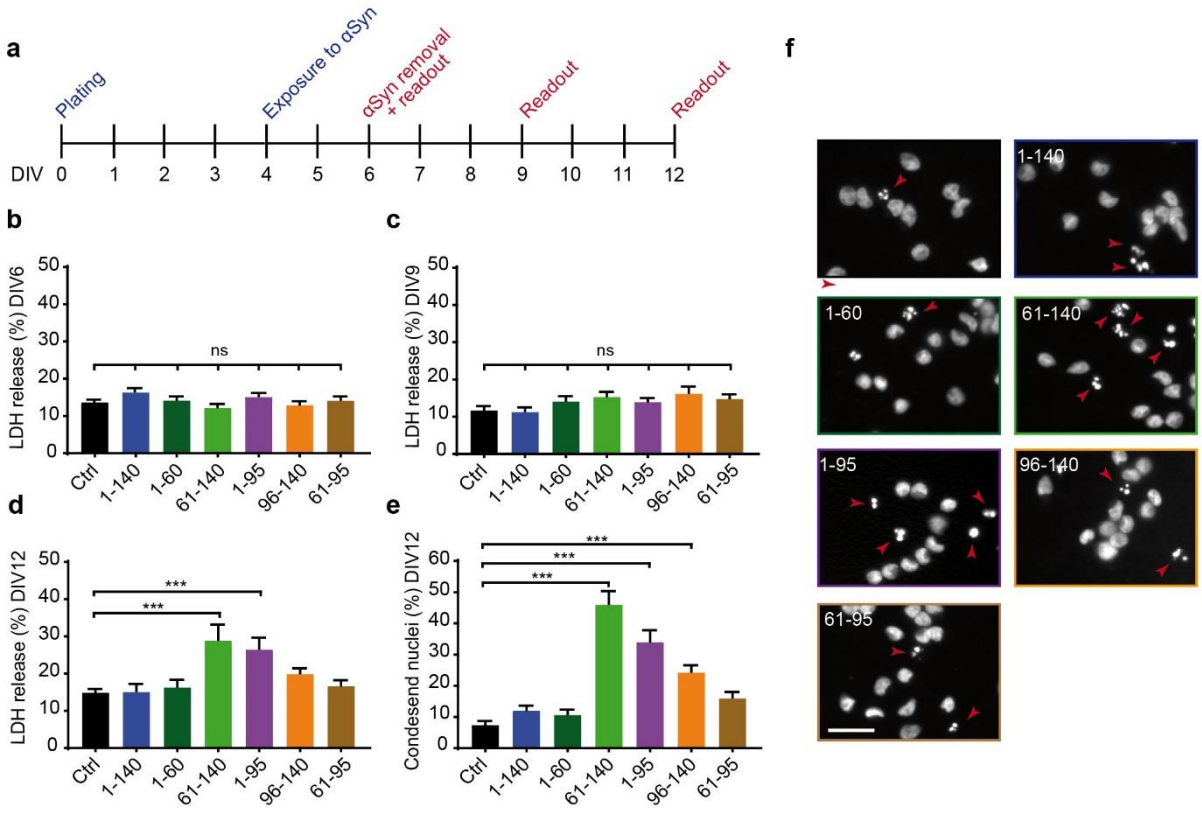

Figure 4.11. Intracellular seeding-potent αSyn fragments also induce toxicity. (a) Experimental design. Cells were differentiated for 4 days prior treatments to reach a stable level of endogenously expressed αSyn. Treatments with recombinant FL-αSyn and fragments were carried out for 48 h. Toxicity was assessed at three readout times. (b-d) Toxicity measured by LDH released from cells treated with recombinant FL-αSyn and fragments at DIV6 (b), DIV 9 (c), and DIV12 (d). Data is presented as mean + SEM from 4 biological repeats with at least 3 technical replicates each. ns: not significant, *** $p < 0.001$; one-way ANOVA with Tukey's *post hoc* test. (e-f) Percentage of condensed nuclei in cells treated with recombinant FL-αSyn and fragments at DIV12. Cells were fixed and nuclei were stained with DAPI. Data is presented as mean + SEM from 3 biological replicates with at least 3 technical repeats each and 3 pictures per technical repeat. *** $p < 0.001$; one-way ANOVA with Tukey's *post hoc* test. (f) Representative pictures of DAPI stained nuclei of cells treated with recombinant FL-αSyn and fragments at DIV12. Red arrowheads indicate condensed nuclei. Scale bar: 30 µm. [taken from (Chakroun et al., 2020)]

However, in order to conclude with certainty that toxicity observed with fragments 61-140 and 1-95 derives directly from their uptake and subsequent intracellular aggregation, αSyn antibodies were used prevent uptake of the two fragments into cells. Antibodies Syn303 and Syn211, targeting the N- and the C-terminal regions respectively (Figure 4.12a), were previously shown to functionally block the uptake of PFFs and into cultured cells (Tran et al., 2014). Similarly, Syn303 significantly reduced toxicity in cells treated with the 1-95 fragment and Syn211 reduced it in the

61-140 treated cells. Since both antibodies have the same isotype, and the N-terminal antibody failed to prevent C-terminal fragment induced toxicity and vice versa, each antibody seved as a negative control for the other.

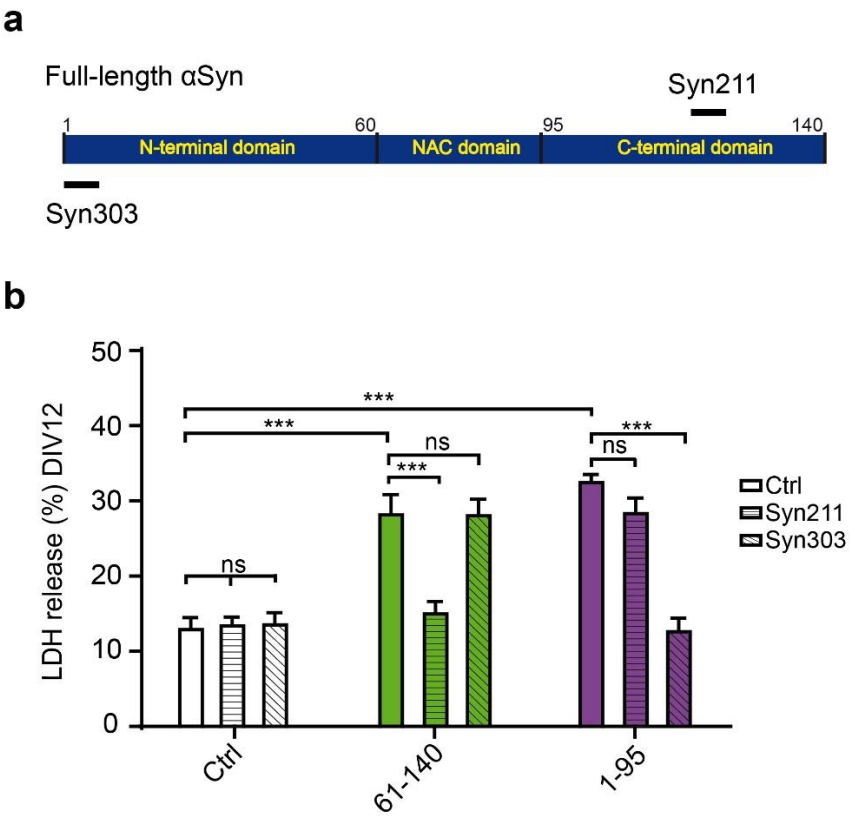

Figure 4.12. αSyn fragments-mediated toxicity can be rescued by domain specific antibodies. (a) Schematic depiction of full-length αSyn and the position of the epitopes recognized by antibodies Syn303 and Syn211. (b) Cells were differentiated for 4 days then treated with antibodies for 1h prior to addition of recombinant fragments. Co-incubation was carried out for 48 h. Toxicity was measured by LDH released from cells at DIV12. Data is presented as mean + SEM from 4 biological repeats with at least 3 technical replicates each. ns: not significant, *** $p < 0.001$; one-way ANOVA with Tukey's *post hoc* test.

5. DISCUSSION

While αSyn aggregation is well established to be a key process in various synucleinopathies, the specific role of different αSyn fragments in the formation of LBs and LNs remains rather elusive so far. The present investigation demonstrates that αSyn-mediated pathology leads to the generation of fragmented αSyn species in the extracellular space and proposes a proteolytic processing of FL-αSyn via plasmin. Although αSyn fragments 1-95 and 61-140 induced very distinct aggregation dynamics of FL-αSyn in a cell-free system, both resulted in aggregates that display increased PK-resistance. Moreover, both fragments were rapidly taken up into differentiated neurons, recruited endogenous FL-αSyn into a long-lasting formation of PK-resistant intracellular aggregates, and induced neurotoxicity. Notably, the aggregates induced by both fragments 1-95 and 61-140 were only immunoreactive to distinct antibodies, suggesting that fragments might be implicated in formation of different strains of αSyn aggregates.

5.1. Biological fragments versus recombinant fragments

As a first approach, I attempted to isolate and enrich the extracellularly generated αSyn fragments and further studied their relevance in seeding and spreading. However, this approach revealed a big number of technical challenges. These fragments were only available in extremely low amounts, and enriching, separating, and purifying them to obtain amounts sufficient to perform the necessary experiments were not realistically achievable. In addition, generating necessary amounts for analysis, would have resulted in exorbitant costs. The use of a set of clearly defined recombinant αSyn fragments seemed to be a more realistic approach to carry out further analyses. Eventhough the sequences of the selected recombinat fragments differ from the ones identified in the CM of αSyn-overexpressing LUHMES cells, they presented paramount advantages. First of all, they are unambiguously defined and were available in sufficient amounts to conduct the study in a satisfactory manner. Secondly, these recombinant fragments which alternatively combine all the main domains of αSyn, allowed to evaluate the effects of the major domains of αSyn, rather than the partially-cleaved domains that result from proteolytic cleavage. Admittedly, the sequences of the recombinant fragments that I used may not be considered ‘biologically accurate’, but the evalution of the effects of distinct αSyn domains and various domain combinations leads to a broader understanding of their role in aggregation and spreading nonetheless. Furthermore, the systematic comparision of different αSyn domain combinations did reveal valuable insights regarding their potential roles in several aspects of disease pathogenesis.

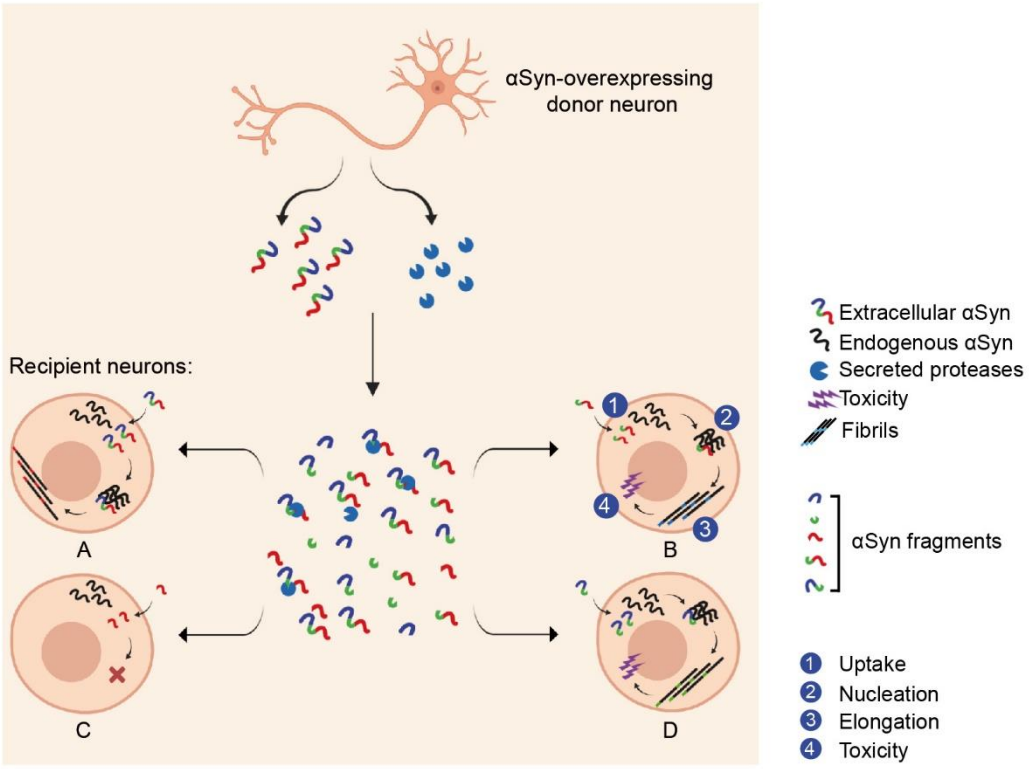

Figure 5.1. Summary of fragment generation and spreading model in LUHMES cells. Neurons affected by αSyn pathology release full-length αSyn (FL-αSyn) into the extracellular space, where it encounters secreted proteases and is subsequently processed by them. The various generated αSyn fragments are taken up by neighbouring healthy cells. These cells are labeled as recipient neurons A to D in the lower panel. Based on the findings of this study, each recipient neuron depicts a different outcome depending on the domain-composition of the internalized species. The studied spreading processes are labeled from 1 to 4 in order of occurence. Nucleation refers to first stages of aggregation where a seeding species recruits endogenous αSyn to form an aggregation nucleus. Elongation refers to the steady addition of monomers to the nucleus to form fibrils. In this particular model, FL-αSyn seeds aggregation but does not lead to toxicity within the time frame of this study (recipient neuron A). Fragments containing the NAC domain (green) in combination with either the N- or the C- terminal domain (blue and red, respectively) seed intracellular aggregation and induce toxicity (recipient neurons D and B, respectively). Fragments lacking the NAC domain do not seed aggregation (recipient neuron C).

5.2. Biological relevance of αSyn fragments

αSyn fragments have been detected both, in tissues and in biological fluids, indicating potential intracellular and extracellular functions. Indeed, intracellular cleavage of αSyn has been described in primary neurons and resulted in the production of a potent neurotoxic, N- and C-terminally cleaved αSyn species (Grassi et al., 2018). Notably, mass spectrometry data from human brain samples revealed fragments with the sequences 1-96 and 65-140 (Li et al., 2005, Kellie et al.,

2014), which highly correspond to fragments 1-95 and 61-140 used in this study. To my knowledge, the findings reported in the present thesis provide the first experimental evidence that these two specific truncated forms of αSyn might play a crucial role in seeding and further propagation of αSyn pathology. Interestingly, recombinant αSyn fragments 1-95 and 61-140 were found to impair the viability of primary microglia and increase the release of pro-inflammatory cytokines interleukin-6 and tumor necrosis factor alpha (Rabenstein et al., 2019). This further underlines the biological relevance of these two fragments since they might play synergetic pathological roles in both neurons and glial cells via distinct mechanisms.

Furthermore, the presence of αSyn in biological fluids has been well documented in the past (Miller et al., 2004, El-Agnaf et al., 2006, Mollenhauer et al., 2011). A number of studies showed several cleaved αSyn forms to be present in cerebrospinal fluid (Borghi et al., 2000, Hong et al., 2010), platelets, whole blood samples (Li et al., 2002, Michell et al., 2005, Hong et al., 2010), and saliva (Devic et al., 2011) of human subjects. However, most studies addressing the presence of αSyn in biological fluids focused mainly on purely quantitative methods (Malek et al., 2014), which do not allow to differentiate between truncated and FL-αSyn. Therefore, it is currently uncertain whether the presence of αSyn fragments in biological fluids plays a role in spreading of pathology in humans. Several truncated forms of αSyn were found in both, healthy and diseased human brain samples, suggesting that truncation of αSyn may occur under physiological and pathophysiological conditions (Oueslati et al., 2010). However, their role in pathological events is not clearly established thus far.

5.3. Spreading of αSyn fragments versus fibrils

When assessing the relevance of the different recombinant αSyn fragments for intercellular spreading in a human dopaminergic cell model, I established that all the tested fragments, except the highly hydrophobic NAC domain (fragment 61-95), were rapidly taken up by cells. Theoretically, if an extracellular αSyn species is efficiently and rapidly taken up by neighboring cells, it would have a higher potential to further spread the pathology. In this regard, some αSyn fragments appear to be strong candidates due to their small size and high solubility to facilitate their cellular uptake. Conversely, αSyn PFFs are substantially larger and less soluble hereby reducing their uptake propensity. Although the use of αSyn PFFs is a validated and well-established method in spreading models, they often have to be either sonicated beforehand to

reduce their size, and/or combined with transfection agents to artificially facilitate their uptake into cells (Nonaka et al., 2010, Polinski et al., 2018).

Disconcertingly, fibrils were found to be more prone to spreading and toxicity in comparison to soluble oligomers when injected in mice brains (Peelaerts et al., 2015). This unresolved paradox could however result from a simple timing matter. If fibrils are considered as final aggregation product, the fact that they lead to an eariler measurable spreading and toxicity does not exclude that smaller soluble species (i.e oligomers or fragments) are actively involved in seeding endogenous aggregation in the mean time, and would reach their pathological potential at a later stage. Furthermore, aggregates seeded with αSyn fragments seem to have dynamically evolved and acquired distinct aggregation characteristics between the first and the second aggregation cycles as suggested by the data displayed above (Figure 4.7).

5.4. Proteolytic cleavage of αSyn

The findings of the present thesis suggest that extracellular cleavage of αSyn involves plasmin in this particular experimental setup. However, several extracellular proteases were reported to cleave αSyn in other experimental models, e.g., plasmin (Kim et al., 2012), neurosin (Kasai et al., 2008, Tatebe et al., 2010), calpain (Games et al., 2014) and several metalloproteinases (Sung et al., 2005, Levin et al., 2009, Joo et al., 2010, Oh et al., 2017). Overall, two main outcomes for proteolytic cleavage of extracellular αSyn seem to emerge: a reduction of pathology upon the complete digestion of αSyn, or an exacerbation of pathology when the digestion was incomplete. Indeed, incomplete cleavage of extracellular αSyn resulted in the production of highly aggregation-prone C-terminally truncated forms that accelerated disease progression (Levin et al., 2009, Sung et al., 2005). Furthermore, a highly neurotoxic truncated αSyn species was shown to result from incomplete intracellular cleavage by the proteasome (Grassi et al., 2018). Here, I provide evidence that the absence of either the N- or the C-terminal end of αSyn can lead to pathology. Therefore, when considering the modulation of proteolytic activity as a therapeutic approach, it is essential to carefully consider the different domains and cleavage sites involved. Regarding the present findings, it might be most beneficial to inhibit proteolysis that occurs in the N- and C-terminal domains and promote proteolysis that targets more specifically the NAC domain of αSyn, since it seems detrimental for aggregation.

5.5. Aggregation characteristics of αSyn fragments

The aggregation-prone characteristic of C-terminally truncated αSyn has been well established (Murray et al., 2003, Ulusoy et al., 2010, Iyer et al., 2017, Ma et al., 2018, van der Wateren et al., 2018). However, very little is known about the aggregation activity of N-terminally truncated αSyn. The present study provides an innovative approach through a systematic direct comparison of the influence of all different non-aggregated αSyn domains and domain combinations on the aggregation of FL-αSyn. In a cell-free assay, fragments were used to seed the aggregation of FL-αSyn with a molar ratio similar to the one found in LBs (Baba et al., 1998, Lucking and Brice, 2000, Beyer and Ariza, 2013). My results show that absence of the N- or C-terminal domains of αSyn leads to more PK-resistant aggregates, despite of very different aggregation dynamics. This provides evidence that seeding of FL-αSyn aggregation with various fragments leads to different aggregates with distinct properties.

Furthermore, I found that recombinant FL-αSyn as well as fragments 1-95 and 61-140 are able to induce intracellular aggregation. Although all of them seem to recruit endogenous αSyn for aggregation, each one of them produced a different aggregation pattern further suggesting that they lead to different aggregates. Interestingly, endogenous αSyn was essential for aggregation initiation and progression, which has also recently been shown *in vivo* (Kim et al., 2019). Importantly, intracellular aggregates derived from seeding with fragments 1-95 and 61-140 were not only more PK-resistant, but also induced a higher cellular toxicity than the ones seeded with FL-αSyn. Together, these findings suggest that seeding with different fragments can potentially determine specific aggregation pathways, and therefore leads to different strains.

5.6. αSyn fragments and implications for strains

αSyn strains are emerging as a potential explanation for why αSyn pathology in various synucleinopathies affects different brain areas and cell types (Peng et al., 2018a). The discovery that recombinant αSyn monomers can form aggregates with variable conformations and biological activities (Guo et al., 2013) paved the way for more findings that propose αSyn strains as aggregates with very distinct physical and structural properties. More importantly, different strains have the ability to impose their structural and conformational properties on a new cycle of aggregation. Indeed, the examination of αSyn aggregates extracted from PD and MSA brains revealed distinct seeding characteristics that were conserved even after several cycles of aggregation (Yamasaki et al., 2019), further showing that αSyn strains might be responsible for the vast pathophysiological and clinical disparities between synucleinopathies. Currently, there is no clear evidence that αSyn fragments are implicated in the formation of different strains of

aggregates. Nonetheless, αSyn fragments were found to have variable solubilities in different synucleinopathies, which directly implicates their seeding activities. Indeed, in MSA brain samples, αSyn fragments seem to be more soluble than in PD and DLB (Campbell et al., 2001). Moreover, comparison across several studies reveals differences in αSyn fragment patterns between PD, DLB, and MSA brain samples. In PD, larger fragments (~12-13 kDa) seem to be enriched, whereas smaller fragments (~6-8 kDa) appear to be more abundant in DLB. Although αSyn fragments were also detected in MSA, their accumulation was less prominent than in PD and DLB (Campbell et al., 2001, Liu et al., 2005). Accordingly, the question arises whether differential proteolytic activities might be a driving mechanism that can determine the pathogenesis of different synucleinopathies. More recently, it was shown that fibrils prepared with homogenous N- or C-terminally truncated αSyn species exhibited distinct prion-like cross-seeding activities in WT mice (Terada et al., 2018). These data together with my findings strongly implicate the contribution of αSyn fragments in the formation of different strains of aggregates. A systematic comparison of human samples with different confirmed synucleinopathies needs to be performed, however, ideally with several antibodies. In relation to my data, further characterization, e.g., more detailed examination of structural and conformational changes, as well as the ability to maintain the same characteristics throughout several cycles of aggregation, would provide a deeper understanding of whether αSyn fragments effectively lead to formation of different strains. However, assuming that αSyn fragments indeed lead to different strains of aggregates, the already complex etiology of various synucleinopathies could be implemented with another aspect to further complicate these pathogeneses. Especially, considering that in a biological context, initial aggregation events might trigger proteolytic cleavage of αSyn as an attempt to attenuate or inhibit the pathophysiological process (Mishizen-Eberz et al., 2005, Sung et al., 2005). Should such a cleavage produce several aggregation-competent fragments, and if each one of them proceeds to induce different types of aggregates, it is conceivable that a specific combination of diverse strains might in fact be involved in the pathogenesis of individual synucleinopathies.

5.7. Immunoreactivity of fragment-induced aggregates: implications for immunotherapeutical approaches

Most intriguingly, I showed that the aggregates seeded with fragments 1-95 and 61-140 were only detectable with antibodies that target either the N- or the C-terminal domains of αSyn, respectively. Regarding the strong evidence that endogenous FL-αSyn is part of such aggregates, it would be expected that they should be recognized by both antibodies. However, the formed aggregates only

showed immunoreactivity toward antibodies that targeted their corresponding seeding species. Thus, the unrecognized epitopes are either hidden or missing. Accordingly, depending on the seed type, different conformations of FL-αSyn could be formed so that only epitopes of the added seeds are exposed during the aggregation. Alternatively, it might be possible that fragments are able to trigger the activation of certain proteases to cleave endogenous FL-αSyn and convert it into fragmented forms containing only the epitope of the seed. Consistent with this explanation, it was shown that treating cells with recombinant fibrils produced with C-terminally truncated αSyn resulted in the activation of caspase 1, which in turn cleaved endogenous FL-αSyn into the same C-terminally truncated form (Ma et al., 2018).

These findings might have tremendous implications for immunotherapeutic approaches. Currently, immunotherapy is considered as one of the most promising disease-modifying strategies for synucleinopathies (Brundin et al., 2017). Efficacious therapeutic antibodies would act by targetting extracellular αSyn species and preventing them from spreading to neighbouring cells. Thus, it is crucial to thoroughly characterize the spreading of αSyn species and subsequently raise antibodies that recognize them with high specificity and affinity. Here, I describe different aggregates for which certain commonly used antibodies are completely unable to bind. Thus, a comprehensive screening for a variety of epitopes on several forms of patient-derived αSyn would be the most effective approach to achieve a better estimation on specific species to target in order to scavenge them more efficiently. Moreover, it may be even necessary to turn towards disease-, or even patient-specific customized antibody mixtures as a future approach.

6. SUMMARY AND SIGNIFICANCE

This work provides novel experimental evidence for the relevance of distinct αSyn fragments as probable interneuron spreading species. In a dopaminergic neuron cell model, I showed that fragments containing the central NAC domain flanked by either the N- or C-terminus of αSyn, namley fragments 61-140 and 1-95, have the capacity to enter cells. Subsequently, they recruit endogenous FL-αSyn for aggregation, and seem to impose specific aggregation pathways as well. Indeed, they result in very distict aggregation patterns with seed-dependant immunoreactivities. In addition, seeding with these fragments resulted in different aggregation kinetics and an enhanced proteinase K resistance. Importantly, fragments 61-140 and 1-95 were shown as slowly acting neurotoxic elements. Their toxicity could however be significanlty reduced with domain-specific antibodies.

Immunotherapy has emerged as a promising avenue to block αSyn spreading (Wong and Krainc, 2017). A key prerequisite for safe and efficacious immunotherapy is to target specific disease-relevant αSyn species with well-defined epitopes. In the view of targeting pathological αSyn with immunotherapy, opinions are still conflicting, given the considerable number of different species. In any case, there is an urgent need to identify and characterize optimal αSyn species as therapeutic targets. In this regard, my findings provide important new insights on the possible involvement of αSyn fragments in differential strain formation, and therefore, in the pathogenesis of different synucleinopathies. Moreover, the seed-specific immunoreactivity of different aggregates might have considerable implications on future imuunotherapeutical approaches. Furthermore, my study revealed that αSyn fragments are species that may very likely occur as an early upstream event under pathological conditions, which places differential protease activity in the center of pathological mechanisms of synucleinopathies. The selective modulation of distinct proteases might therefore be strongly considered as potential disease-modifying strategy as well.

7. ACKNOWLEDGEMENT

First and foremost, i would like to thank my parents and brothers for their unlimited support and unconditional love throughout my whole life. My husband for his patience, support, and understanding. And my son for being my sunshine and always putting a smile on my face.

I want also to sincerely thank Prof. Günter Höglinger, my doctoral advisor, for welcoming me in his team and for his support and guidance, which allowed me to grow and push my limits as a scientist. I would like to thank my co-advisor, Prof. Aphrodite Kapurniotu, and my mentor, Dr. Karin Danzer as well for their help and input. To my supervisor, Dr. Thomas Rösler, you have my sincerest gratitute for your help, support, and all the animated discussions as well.

Also, a special thanks to the postdocs in the team: Dr. Matthias Höllerhage, Dr. Niko-Petteri Nykänen, Dr. Thomas Koegelsperger, and Dr. Sigrid Schwarz for their constant help and collaboration.

To Elisabeth, Valentin, Tabea, Niko, and Lena, thank you for your friendship, trustworthiness and sense of humor that made the difficult times bearable, and the fun times funnier.

In addition, i want to express a special thanks to Mr. Robin Konhaeuser, Dr. Julius Bruch, Dr. Hong Xu, Ms. Magda Baba-Berjas, and Ms. Natascha Fussi for their valuable help and guidance when I first arrived at the lab. Last but not least, I would like to extend my deepest gratitude to all the colleagues from the German center for neurodegenerative diseases (DZNE) and Institute for stroke and dementia research (ISD) that always had time to help, discuss and guide.

8. DECLARATION OF CONTRIBUTIONS

The mass spectrometry experiments and related data analysis was performed by Dr. Andreas schmidt. Protein Analysis Unit (ZfP), Biomedical Center (BMC), University of Munich, 82152, Planegg, Germany.

The LUHMES alpha-synuclein knockout cell line was designed and created by Mr. Valentin Evsyukov. Department of Translational Neurodegeneration, German Center for Neurodegenerative Diseases (DZNE), 81377, Munich, Germany. Department of Neurology, School of Medicine, Technical University of Munich, 81675, Munich, Germany.

The german translation of the abstract was done with the valuable help of Ms. Elisabeth Findeiss. Department of Translational Neurodegeneration, German Center for Neurodegenerative Diseases (DZNE), 81377, Munich, Germany. Department of Neurology, School of Medicine, Technical University of Munich, 81675, Munich, Germany.

Proofreeding of the thesis was done with the valuable help of Dr. Thomas Rösler. Department of Translational Neurodegeneration, German Center for Neurodegenerative Diseases (DZNE), 81377, Munich, Germany. Department of Neurology, School of Medicine, Technical University of Munich, 81675, Munich, Germany.

9. REFERENCES

ABELIOVICH, A., SCHMITZ, Y., FARINAS, I., CHOI-LUNDBERG, D., HO, W. H., CASTILLO, P. E., SHINSKY, N., VERDUGO, J. M., ARMANINI, M., RYAN, A., HYNES, M., PHILLIPS, H., SULZER, D. & ROSENTHAL, A. 2000. Mice lacking alpha-synuclein display functional deficits in the nigrostriatal dopamine system. *Neuron,* 25**,** 239-52.

AHN, K. J., PAIK, S. R., CHUNG, K. C. & KIM, J. 2006. Amino acid sequence motifs and mechanistic features of the membrane translocation of alpha-synuclein. *J Neurochem,* 97**,** 265-79.

ALEGRE-ABARRATEGUI, J., BRIMBLECOMBE, K. R., ROBERTS, R. F., VELENTZA-ALMPANI, E., TILLEY, B. S., BENGOA-VERGNIORY, N. & PROUKAKIS, C. 2019. Selective vulnerability in alpha-synucleinopathies. *Acta Neuropathol,* 138**,** 681-704.

ALVES DA COSTA, C., DUPLAN, E. & CHECLER, F. 2017. alpha-synuclein and p53 functional interplay in physiopathological contexts. *Oncotarget,* 8**,** 9001-9002.

ANDERSON, J. P., WALKER, D. E., GOLDSTEIN, J. M., DE LAAT, R., BANDUCCI, K., CACCAVELLO, R. J., BARBOUR, R., HUANG, J., KLING, K., LEE, M., DIEP, L., KEIM, P. S., SHEN, X., CHATAWAY, T., SCHLOSSMACHER, M. G., SEUBERT, P., SCHENK, D., SINHA, S., GAI, W. P. & CHILCOTE, T. J. 2006. Phosphorylation of Ser-129 is the dominant pathological modification of alpha-synuclein in familial and sporadic Lewy body disease. *J Biol Chem,* 281**,** 29739-52.

APPEL-CRESSWELL, S., VILARINO-GUELL, C., ENCARNACION, M., SHERMAN, H., YU, I., SHAH, B., WEIR, D., THOMPSON, C., SZU-TU, C., TRINH, J., AASLY, J. O., RAJPUT, A., RAJPUT, A. H., JON STOESSL, A. & FARRER, M. J. 2013. Alpha-synuclein p.H50Q, a novel pathogenic mutation for Parkinson's disease. *Mov Disord,* 28**,** 811-3.

BABA, M., NAKAJO, S., TU, P. H., TOMITA, T., NAKAYA, K., LEE, V. M., TROJANOWSKI, J. Q. & IWATSUBO, T. 1998. Aggregation of alpha-synuclein in Lewy bodies of sporadic Parkinson's disease and dementia with Lewy bodies. *Am J Pathol,* 152**,** 879-84.

BACH, J. P., ZIEGLER, U., DEUSCHL, G., DODEL, R. & DOBLHAMMER-REITER, G. 2011. Projected numbers of people with movement disorders in the years 2030 and 2050. *Mov Disord,* 26**,** 2286-90.

BEN-SHLOMO, Y., WENNING, G. K., TISON, F. & QUINN, N. P. 1997. Survival of patients with pathologically proven multiple system atrophy: a meta-analysis. *Neurology,* 48**,** 384-93.

BERNAL-CONDE, L. D., RAMOS-ACEVEDO, R., REYES-HERNANDEZ, M. A., BALBUENA-OLVERA, A. J., MORALES-MORENO, I. D., ARGUERO-SANCHEZ, R., SCHULE, B. & GUERRA-CRESPO, M. 2019. Alpha-Synuclein Physiology and Pathology: A Perspective on Cellular Structures and Organelles. *Front Neurosci,* 13**,** 1399.

BEYER, K. & ARIZA, A. 2013. alpha-Synuclein posttranslational modification and alternative splicing as a trigger for neurodegeneration. *Mol Neurobiol,* 47**,** 509-24.

BEYER, K., DOMINGO-SABAT, M., HUMBERT, J., CARRATO, C., FERRER, I. & ARIZA, A. 2008. Differential expression of alpha-synuclein, parkin, and synphilin-1 isoforms in Lewy body disease. *Neurogenetics,* 9**,** 163-72.

BEYER, K., LAO, J. I., CARRATO, C., MATE, J. L., LOPEZ, D., FERRER, I. & ARIZA, A. 2004. Differential expression of alpha-synuclein isoforms in dementia with Lewy bodies. *Neuropathol Appl Neurobiol,* 30**,** 601-7.

BILLINGSLEY, K. J., BANDRES-CIGA, S., SAEZ-ATIENZAR, S. & SINGLETON, A. B. 2018. Genetic risk factors in Parkinson's disease. *Cell Tissue Res,* 373**,** 9-20.

BODNER, C. R., DOBSON, C. M. & BAX, A. 2009. Multiple tight phospholipid-binding modes of alpha-synuclein revealed by solution NMR spectroscopy. *J Mol Biol,* 390**,** 775-90.

BORGHI, R., MARCHESE, R., NEGRO, A., MARINELLI, L., FORLONI, G., ZACCHEO, D., ABBRUZZESE, G. & TABATON, M. 2000. Full length alpha-synuclein is present in cerebrospinal fluid from Parkinson's disease and normal subjects. *Neurosci Lett,* 287**,** 65-7.

BOUSSET, L., PIERI, L., RUIZ-ARLANDIS, G., GATH, J., JENSEN, P. H., HABENSTEIN, B., MADIONA, K., OLIERIC, V., BOCKMANN, A., MEIER, B. H. & MELKI, R. 2013. Structural and functional characterization of two alpha-synuclein strains. *Nat Commun,* 4**,** 2575.

BOWER, J. H., MARAGANORE, D. M., MCDONNELL, S. K. & ROCCA, W. A. 1997. Incidence of progressive supranuclear palsy and multiple system atrophy in Olmsted County, Minnesota, 1976 to 1990. *Neurology,* 49**,** 1284-8.

BRAAK, H., DEL TREDICI, K., RUB, U., DE VOS, R. A., JANSEN STEUR, E. N. & BRAAK, E. 2003. Staging of brain pathology related to sporadic Parkinson's disease. *Neurobiol Aging,* 24**,** 197-211.

BREYDO, L., WU, J. W. & UVERSKY, V. N. 2012. Alpha-synuclein misfolding and Parkinson's disease. *Biochim Biophys Acta,* 1822**,** 261-85.

BRUINSMA, I. B., BRUGGINK, K. A., KINAST, K., VERSLEIJEN, A. A., SEGERS-NOLTEN, I. M., SUBRAMANIAM, V., KUIPERIJ, H. B., BOELENS, W., DE WAAL, R. M. & VERBEEK, M. M. 2011. Inhibition of alpha-synuclein aggregation by small heat shock proteins. *Proteins,* 79**,** 2956-67.

BRUNDIN, P., DAVE, K. D. & KORDOWER, J. H. 2017. Therapeutic approaches to target alpha-synuclein pathology. *Exp Neurol,* 298**,** 225-235.

BUNGEROTH, M., APPENZELLER, S., REGULIN, A., VOLKER, W., LORENZEN, I., GROTZINGER, J., PENDZIWIAT, M. & KUHLENBAUMER, G. 2014. Differential aggregation properties of alpha-synuclein isoforms. *Neurobiol Aging,* 35**,** 1913-9.

BURAI, R., AIT-BOUZIAD, N., CHIKI, A. & LASHUEL, H. A. 2015. Elucidating the Role of Site-Specific Nitration of alpha-Synuclein in the Pathogenesis of Parkinson's Disease via Protein Semisynthesis and Mutagenesis. *J Am Chem Soc,* 137**,** 5041-52.

BURRE, J., SHARMA, M. & SUDHOF, T. C. 2012. Systematic mutagenesis of alpha-synuclein reveals distinct sequence requirements for physiological and pathological activities. *J Neurosci,* 32**,** 15227-42.

BURRE, J., SHARMA, M., TSETSENIS, T., BUCHMAN, V., ETHERTON, M. R. & SUDHOF, T. C. 2010. Alpha-synuclein promotes SNARE-complex assembly in vivo and in vitro. *Science,* 329**,** 1663-7.

CAMPBELL, B. C., MCLEAN, C. A., CULVENOR, J. G., GAI, W. P., BLUMBERGS, P. C., JAKALA, P., BEYREUTHER, K., MASTERS, C. L. & LI, Q. X. 2001. The solubility of alpha-synuclein in multiple system atrophy differs from that of dementia with Lewy bodies and Parkinson's disease. *J Neurochem,* 76**,** 87-96.

CAPPAI, R., LECK, S. L., TEW, D. J., WILLIAMSON, N. A., SMITH, D. P., GALATIS, D., SHARPLES, R. A., CURTAIN, C. C., ALI, F. E., CHERNY, R. A., CULVENOR, J. G., BOTTOMLEY, S. P., MASTERS, C. L., BARNHAM, K. J. & HILL, A. F. 2005. Dopamine promotes alpha-synuclein aggregation into SDS-resistant soluble oligomers via a distinct folding pathway. *FASEB J,* 19**,** 1377-9.

CAUGHEY, B. & LANSBURY, P. T. 2003. Protofibrils, pores, fibrils, and neurodegeneration: separating the responsible protein aggregates from the innocent bystanders. *Annu Rev Neurosci,* 26**,** 267-98.

CHAKROUN, T., EVSYUKOV, V., NYKANEN, N. P., HOLLERHAGE, M., SCHMIDT, A., KAMP, F., RUF, V. C., WURST, W., ROSLER, T. W. & HOGLINGER, G. U. 2020. Alpha-synuclein fragments trigger distinct aggregation pathways. *Cell Death Dis,* 11**,** 84.

CHANG, D., NALLS, M. A., HALLGRIMSDOTTIR, I. B., HUNKAPILLER, J., VAN DER BRUG, M., CAI, F., INTERNATIONAL PARKINSON'S DISEASE GENOMICS, C., ANDME RESEARCH, T., KERCHNER, G. A., AYALON, G., BINGOL, B., SHENG, M., HINDS, D., BEHRENS, T. W., SINGLETON, A. B., BHANGALE, T. R. & GRAHAM, R. R. 2017. A meta-analysis of genome-wide association studies identifies 17 new Parkinson's disease risk loci. *Nat Genet,* 49**,** 1511-1516.

CHARCOT, J. M., BOURNEVILLE & FOWLER, E. P. 1878. *Lectures on localization in diseases of the brain,* New York,, W. Wood & co.

CHARTIER-HARLIN, M. C., KACHERGUS, J., ROUMIER, C., MOUROUX, V., DOUAY, X., LINCOLN, S., LEVECQUE, C., LARVOR, L., ANDRIEUX, J., HULIHAN, M., WAUCQUIER, N., DEFEBVRE, L., AMOUYEL, P., FARRER, M. & DESTEE, A. 2004. Alpha-synuclein locus duplication as a cause of familial Parkinson's disease. *Lancet,* 364**,** 1167-9.

CHIBA-FALEK, O. & NUSSBAUM, R. L. 2001. Effect of allelic variation at the NACP-Rep1 repeat upstream of the alpha-synuclein gene (SNCA) on transcription in a cell culture luciferase reporter system. *Hum Mol Genet,* 10**,** 3101-9.

CLAYTON, D. F. & GEORGE, J. M. 1999. Synucleins in synaptic plasticity and neurodegenerative disorders. *J Neurosci Res,* 58**,** 120-9.

COLLA, E., COUNE, P., LIU, Y., PLETNIKOVA, O., TRONCOSO, J. C., IWATSUBO, T., SCHNEIDER, B. L. & LEE, M. K. 2012. Endoplasmic reticulum stress is important for the manifestations of alpha-synucleinopathy in vivo. *J Neurosci,* 32**,** 3306-20.

CROWTHER, R. A., JAKES, R., SPILLANTINI, M. G. & GOEDERT, M. 1998. Synthetic filaments assembled from C-terminally truncated alpha-synuclein. *FEBS Lett,* 436**,** 309-12.

CUERVO, A. M., STEFANIS, L., FREDENBURG, R., LANSBURY, P. T. & SULZER, D. 2004. Impaired degradation of mutant alpha-synuclein by chaperone-mediated autophagy. *Science,* 305**,** 1292-5.

DAHER, J. P., YING, M., BANERJEE, R., MCDONALD, R. S., HAHN, M. D., YANG, L., FLINT BEAL, M., THOMAS, B., DAWSON, V. L., DAWSON, T. M. & MOORE, D. J. 2009. Conditional transgenic mice expressing C-terminally truncated human alpha-synuclein (alphaSyn119) exhibit reduced striatal dopamine without loss of nigrostriatal pathway dopaminergic neurons. *Mol Neurodegener,* 4**,** 34.

DANZER, K. M., KRANICH, L. R., RUF, W. P., CAGSAL-GETKIN, O., WINSLOW, A. R., ZHU, L., VANDERBURG, C. R. & MCLEAN, P. J. 2012. Exosomal cell-to-cell transmission of alpha synuclein oligomers. *Mol Neurodegener,* 7**,** 42.

DANZER, K. M., KREBS, S. K., WOLFF, M., BIRK, G. & HENGERER, B. 2009. Seeding induced by alpha-synuclein oligomers provides evidence for spreading of alpha-synuclein pathology. *J Neurochem,* 111**,** 192-203.

DENG, W. W., MAO, L., YU, G. T., BU, L. L., MA, S. R., LIU, B., GUTKIND, J. S., KULKARNI, A. B., ZHANG, W. F. & SUN, Z. J. 2016. LAG-3 confers poor prognosis and its blockade reshapes antitumor response in head and neck squamous cell carcinoma. *Oncoimmunology,* 5**,** e1239005.

DEVIC, I., HWANG, H., EDGAR, J. S., IZUTSU, K., PRESLAND, R., PAN, C., GOODLETT, D. R., WANG, Y., ARMALY, J., TUMAS, V., ZABETIAN, C. P., LEVERENZ, J. B., SHI, M. & ZHANG, J. 2011. Salivary alpha-synuclein and DJ-1: potential biomarkers for Parkinson's disease. *Brain,* 134**,** e178.

DEWITT, D. C. & RHOADES, E. 2013. alpha-Synuclein can inhibit SNARE-mediated vesicle fusion through direct interactions with lipid bilayers. *Biochemistry,* 52**,** 2385-7.

DI MAIO, R., BARRETT, P. J., HOFFMAN, E. K., BARRETT, C. W., ZHARIKOV, A., BORAH, A., HU, X., MCCOY, J., CHU, C. T., BURTON, E. A., HASTINGS, T. G. & GREENAMYRE, J. T. 2016. alpha-Synuclein binds to TOM20 and inhibits mitochondrial protein import in Parkinson's disease. *Sci Transl Med,* 8**,** 342ra78.

DRESCHER, M. 2012. EPR in protein science : intrinsically disordered proteins. *Top Curr Chem,* 321**,** 91-119.

EHRNHOEFER, D. E., BIESCHKE, J., BOEDDRICH, A., HERBST, M., MASINO, L., LURZ, R., ENGEMANN, S., PASTORE, A. & WANKER, E. E. 2008. EGCG redirects amyloidogenic polypeptides into unstructured, off-pathway oligomers. *Nat Struct Mol Biol,* 15**,** 558-66.

EL-AGNAF, O. M., SALEM, S. A., PALEOLOGOU, K. E., CURRAN, M. D., GIBSON, M. J., COURT, J. A., SCHLOSSMACHER, M. G. & ALLSOP, D. 2006. Detection of oligomeric forms of alpha-synuclein protein in human plasma as a potential biomarker for Parkinson's disease. *FASEB J,* 20**,** 419-25.

ELIEZER, D., KUTLUAY, E., BUSSELL, R., JR. & BROWNE, G. 2001. Conformational properties of alpha-synuclein in its free and lipid-associated states. *J Mol Biol,* 307**,** 1061-73.

EMAMZADEH, F. N. 2016. Alpha-synuclein structure, functions, and interactions. *J Res Med Sci,* 21**,** 29.

FANCIULLI, A. & WENNING, G. K. 2015. Multiple-system atrophy. *N Engl J Med,* 372**,** 1375-6.

FRANCO, R., LI, S., RODRIGUEZ-ROCHA, H., BURNS, M. & PANAYIOTIDIS, M. I. 2010. Molecular mechanisms of pesticide-induced neurotoxicity: Relevance to Parkinson's disease. *Chem Biol Interact,* 188**,** 289-300.

FUJIWARA, H., HASEGAWA, M., DOHMAE, N., KAWASHIMA, A., MASLIAH, E., GOLDBERG, M. S., SHEN, J., TAKIO, K. & IWATSUBO, T. 2002. alpha-Synuclein is phosphorylated in synucleinopathy lesions. *Nat Cell Biol,* 4**,** 160-4.

FUSSI, N., HÖLLERHAGE, M., CHAKROUN, T., NYKANEN, N. P., RÖSLER, T. W., KOEGLSPERGER, T., WURST, W., BEHRENDS, C. & HÖGLINGER, G. U. 2018. Exosomal secretion of alpha-synuclein as protective mechanism after upstream blockage of macroautophagy. *Cell Death Dis,* 9**,** 757.

GALLEGOS, S., PACHECO, C., PETERS, C., OPAZO, C. M. & AGUAYO, L. G. 2015. Features of alpha-synuclein that could explain the progression and irreversibility of Parkinson's disease. *Front Neurosci,* 9**,** 59.

GAMES, D., VALERA, E., SPENCER, B., ROCKENSTEIN, E., MANTE, M., ADAME, A., PATRICK, C., UBHI, K., NUBER, S., SACAYON, P., ZAGO, W., SEUBERT, P., BARBOUR, R., SCHENK, D. & MASLIAH, E. 2014. Reducing C-terminal-truncated alpha-synuclein by immunotherapy attenuates neurodegeneration and propagation in Parkinson's disease-like models. *J Neurosci,* 34**,** 9441-54.

GAMEZ-VALERO, A. & BEYER, K. 2018. Alternative Splicing of Alpha- and Beta-Synuclein Genes Plays Differential Roles in Synucleinopathies. *Genes (Basel),* 9.

GEORGE, J. M. 2002. The synucleins. *Genome Biol,* 3**,** REVIEWS3002.

GIASSON, B. I., MURRAY, I. V., TROJANOWSKI, J. Q. & LEE, V. M. 2001. A hydrophobic stretch of 12 amino acid residues in the middle of alpha-synuclein is essential for filament assembly. *J Biol Chem,* 276**,** 2380-6.

GOERS, J., MANNING-BOG, A. B., MCCORMACK, A. L., MILLETT, I. S., DONIACH, S., DI MONTE, D. A., UVERSKY, V. N. & FINK, A. L. 2003. Nuclear localization of alpha-synuclein and its interaction with histones. *Biochemistry,* 42**,** 8465-71.

GOMEZ-TORTOSA, E., NEWELL, K., IRIZARRY, M. C., SANDERS, J. L. & HYMAN, B. T. 2000. alpha-Synuclein immunoreactivity in dementia with Lewy bodies: morphological staging and comparison with ubiquitin immunostaining. *Acta Neuropathol,* 99**,** 352-7.

GONCALVES, S. & OUTEIRO, T. F. 2013. Assessing the subcellular dynamics of alpha-synuclein using photoactivation microscopy. *Mol Neurobiol,* 47**,** 1081-92.

GRASSI, D., HOWARD, S., ZHOU, M., DIAZ-PEREZ, N., URBAN, N. T., GUERRERO-GIVEN, D., KAMASAWA, N., VOLPICELLI-DALEY, L. A., LOGRASSO, P. & LASMEZAS, C. I. 2018. Identification of a highly neurotoxic alpha-synuclein species inducing mitochondrial damage and mitophagy in Parkinson's disease. *Proc Natl Acad Sci U S A,* 115**,** E2634-E2643.

GROZDANOV, V. & DANZER, K. M. 2018. Release and uptake of pathologic alpha-synuclein. *Cell Tissue Res,* 373**,** 175-182.

GUO, J. L., COVELL, D. J., DANIELS, J. P., IBA, M., STIEBER, A., ZHANG, B., RIDDLE, D. M., KWONG, L. K., XU, Y., TROJANOWSKI, J. Q. & LEE, V. M. 2013. Distinct alpha-synuclein strains differentially promote tau inclusions in neurons. *Cell,* 154**,** 103-17.

HALLIDAY, G. M., SONG, Y. J. & HARDING, A. J. 2011. Striatal beta-amyloid in dementia with Lewy bodies but not Parkinson's disease. *J Neural Transm (Vienna),* 118**,** 713-9.

HAMPTON, R. Y. 2000. ER stress response: getting the UPR hand on misfolded proteins. *Curr Biol,* 10**,** R518-21.

HARDY, J. 2005. Expression of normal sequence pathogenic proteins for neurodegenerative disease contributes to disease risk: 'permissive templating' as a general mechanism underlying neurodegeneration. *Biochem Soc Trans,* 33**,** 578-81.

HASEGAWA, M., FUJIWARA, H., NONAKA, T., WAKABAYASHI, K., TAKAHASHI, H., LEE, V. M., TROJANOWSKI, J. Q., MANN, D. & IWATSUBO, T. 2002. Phosphorylated alpha-synuclein is ubiquitinated in alpha-synucleinopathy lesions. *J Biol Chem,* 277**,** 49071-6.

HAUSER, R. A. 2010. Early pharmacologic treatment in Parkinson's disease. *Am J Manag Care,* 16 Suppl Implications**,** S100-7.

HOFER, A., BERG, D., ASMUS, F., NIWAR, M., RANSMAYR, G., RIEMENSCHNEIDER, M., BONELLI, S. B., STEFFELBAUER, M., CEBALLOS-BAUMANN, A., HAUSSERMANN, P., BEHNKE, S., KRUGER, R., PRESTEL, J., SHARMA, M., ZIMPRICH, A., RIESS, O. & GASSER, T. 2005. The role of alpha-synuclein gene multiplications in early-onset Parkinson's disease and dementia with Lewy bodies. *J Neural Transm (Vienna),* 112**,** 1249-54.

HÖLLERHAGE, M., FUSSI, N., RÖSLER, T. W., WURST, W., BEHRENDS, C. & HÖGLINGER, G. U. 2019. Multiple molecular pathways stimulating macroautophagy protect from alpha-synuclein-induced toxicity in human neurons. *Neuropharmacology,* 149**,** 13-26.

HÖLLERHAGE, M., GOEBEL, J. N., DE ANDRADE, A., HILDEBRANDT, T., DOLGA, A., CULMSEE, C., OERTEL, W. H., HENGERER, B. & HÖGLINGER, G. U. 2014. Trifluoperazine rescues human dopaminergic cells from wild-type alpha-synuclein-induced toxicity. *Neurobiol Aging,* 35**,** 1700-11.

HONG, Z., SHI, M., CHUNG, K. A., QUINN, J. F., PESKIND, E. R., GALASKO, D., JANKOVIC, J., ZABETIAN, C. P., LEVERENZ, J. B., BAIRD, G., MONTINE, T. J., HANCOCK, A. M., HWANG, H., PAN, C.,

BRADNER, J., KANG, U. J., JENSEN, P. H. & ZHANG, J. 2010. DJ-1 and alpha-synuclein in human cerebrospinal fluid as biomarkers of Parkinson's disease. *Brain,* 133**,** 713-26.

HOYER, W., ANTONY, T., CHERNY, D., HEIM, G., JOVIN, T. M. & SUBRAMANIAM, V. 2002. Dependence of alpha-synuclein aggregate morphology on solution conditions. *J Mol Biol,* 322**,** 383-93.

IBANEZ, P., BONNET, A. M., DEBARGES, B., LOHMANN, E., TISON, F., POLLAK, P., AGID, Y., DURR, A. & BRICE, A. 2004. Causal relation between alpha-synuclein gene duplication and familial Parkinson's disease. *Lancet,* 364**,** 1169-71.

IWAI, A., MASLIAH, E., YOSHIMOTO, M., GE, N., FLANAGAN, L., DE SILVA, H. A., KITTEL, A. & SAITOH, T. 1995. The precursor protein of non-A beta component of Alzheimer's disease amyloid is a presynaptic protein of the central nervous system. *Neuron,* 14**,** 467-75.

IWATA, A., MARUYAMA, M., AKAGI, T., HASHIKAWA, T., KANAZAWA, I., TSUJI, S. & NUKINA, N. 2003. Alpha-synuclein degradation by serine protease neurosin: implication for pathogenesis of synucleinopathies. *Hum Mol Genet,* 12**,** 2625-35.

IYER, A., ROETERS, S. J., KOGAN, V., WOUTERSEN, S., CLAESSENS, M. & SUBRAMANIAM, V. 2017. C-Terminal Truncated alpha-Synuclein Fibrils Contain Strongly Twisted beta-Sheets. *J Am Chem Soc,* 139**,** 15392-15400.

JAKES, R., SPILLANTINI, M. G. & GOEDERT, M. 1994. Identification of two distinct synucleins from human brain. *FEBS Lett,* 345**,** 27-32.

JANECZEK, P. & LEWOHL, J. M. 2013. The role of alpha-synuclein in the pathophysiology of alcoholism. *Neurochem Int,* 63**,** 154-62.

JANKOVIC, J. 2008. Parkinson's disease: clinical features and diagnosis. *J Neurol Neurosurg Psychiatry,* 79**,** 368-76.

JI, H., LIU, Y. E., JIA, T., WANG, M., LIU, J., XIAO, G., JOSEPH, B. K., ROSEN, C. & SHI, Y. E. 1997. Identification of a breast cancer-specific gene, BCSG1, by direct differential cDNA sequencing. *Cancer Res,* 57**,** 759-64.

JIN, H., KANTHASAMY, A., GHOSH, A., YANG, Y., ANANTHARAM, V. & KANTHASAMY, A. G. 2011. alpha-Synuclein negatively regulates protein kinase Cdelta expression to suppress apoptosis in dopaminergic neurons by reducing p300 histone acetyltransferase activity. *J Neurosci,* 31**,** 2035-51.

JOO, S. H., KWON, K. J., KIM, J. W., KIM, J. W., HASAN, M. R., LEE, H. J., HAN, S. H. & SHIN, C. Y. 2010. Regulation of matrix metalloproteinase-9 and tissue plasminogen activator activity by alpha-synuclein in rat primary glial cells. *Neurosci Lett,* 469**,** 352-6.

KALIVENDI, S. V., YEDLAPUDI, D., HILLARD, C. J. & KALYANARAMAN, B. 2010. Oxidants induce alternative splicing of alpha-synuclein: Implications for Parkinson's disease. *Free Radic Biol Med,* 48**,** 377-83.

KAMP, F., EXNER, N., LUTZ, A. K., WENDER, N., HEGERMANN, J., BRUNNER, B., NUSCHER, B., BARTELS, T., GIESE, A., BEYER, K., EIMER, S., WINKLHOFER, K. F. & HAASS, C. 2010. Inhibition of mitochondrial fusion by alpha-synuclein is rescued by PINK1, Parkin and DJ-1. *EMBO J,* 29**,** 3571-89.

KARPOWICZ, R. J., JR., HANEY, C. M., MIHAILA, T. S., SANDLER, R. M., PETERSSON, E. J. & LEE, V. M. 2017. Selective imaging of internalized proteopathic alpha-synuclein seeds in primary neurons reveals mechanistic insight into transmission of synucleinopathies. *J Biol Chem,* 292**,** 13482-13497.

KASAI, T., TOKUDA, T., YAMAGUCHI, N., WATANABE, Y., KAMETANI, F., NAKAGAWA, M. & MIZUNO, T. 2008. Cleavage of normal and pathological forms of alpha-synuclein by neurosin in vitro. *Neurosci Lett,* 436**,** 52-6.

KELLIE, J. F., HIGGS, R. E., RYDER, J. W., MAJOR, A., BEACH, T. G., ADLER, C. H., MERCHANT, K. & KNIERMAN, M. D. 2014. Quantitative measurement of intact alpha-synuclein proteoforms from post-mortem control and Parkinson's disease brain tissue by intact protein mass spectrometry. *Sci Rep,* 4**,** 5797.

KIELY, A. P., ASI, Y. T., KARA, E., LIMOUSIN, P., LING, H., LEWIS, P., PROUKAKIS, C., QUINN, N., LEES, A. J., HARDY, J., REVESZ, T., HOULDEN, H. & HOLTON, J. L. 2013. alpha-Synucleinopathy associated with G51D SNCA mutation: a link between Parkinson's disease and multiple system atrophy? *Acta Neuropathol,* 125**,** 753-69.

KIM, K. S., CHOI, Y. R., PARK, J. Y., LEE, J. H., KIM, D. K., LEE, S. J., PAIK, S. R., JOU, I. & PARK, S. M. 2012. Proteolytic cleavage of extracellular alpha-synuclein by plasmin: implications for Parkinson disease. *J Biol Chem,* 287**,** 24862-72.

KIM, S., KWON, S. H., KAM, T. I., PANICKER, N., KARUPPAGOUNDER, S. S., LEE, S., LEE, J. H., KIM, W. R., KOOK, M., FOSS, C. A., SHEN, C., LEE, H., KULKARNI, S., PASRICHA, P. J., LEE, G., POMPER, M. G., DAWSON, V. L., DAWSON, T. M. & KO, H. S. 2019. Transneuronal Propagation of Pathologic alpha-Synuclein from the Gut to the Brain Models Parkinson's Disease. *Neuron,* 103**,** 627-641 e7.

KIRIK, D., GEORGIEVSKA, B., BURGER, C., WINKLER, C., MUZYCZKA, N., MANDEL, R. J. & BJORKLUND, A. 2002. Reversal of motor impairments in parkinsonian rats by continuous intrastriatal delivery of L-dopa using rAAV-mediated gene transfer. *Proc Natl Acad Sci U S A,* 99**,** 4708-13.

KORDOWER, J. H., CHU, Y., HAUSER, R. A., FREEMAN, T. B. & OLANOW, C. W. 2008a. Lewy body-like pathology in long-term embryonic nigral transplants in Parkinson's disease. *Nat Med,* 14**,** 504-6.

KORDOWER, J. H., CHU, Y., HAUSER, R. A., OLANOW, C. W. & FREEMAN, T. B. 2008b. Transplanted dopaminergic neurons develop PD pathologic changes: a second case report. *Mov Disord,* 23**,** 2303-6.

KRÜGER, R., KUHN, W., MULLER, T., WOITALLA, D., GRAEBER, M., KOSEL, S., PRZUNTEK, H., EPPLEN, J. T., SCHOLS, L. & RIESS, O. 1998. Ala30Pro mutation in the gene encoding alpha-synuclein in Parkinson's disease. *Nat Genet,* 18**,** 106-8.

LAI, Y., KIM, S., VARKEY, J., LOU, X., SONG, J. K., DIAO, J., LANGEN, R. & SHIN, Y. K. 2014. Nonaggregated alpha-synuclein influences SNARE-dependent vesicle docking via membrane binding. *Biochemistry,* 53**,** 3889-96.

LAVEDAN, C., LEROY, E., DEHEJIA, A., BUCHHOLTZ, S., DUTRA, A., NUSSBAUM, R. L. & POLYMEROPOULOS, M. H. 1998. Identification, localization and characterization of the human gamma-synuclein gene. *Hum Genet,* 103**,** 106-12.

LEE, B. R. & KAMITANI, T. 2011. Improved immunodetection of endogenous alpha-synuclein. *PLoS One,* 6**,** e23939.

LEE, F. J., LIU, F., PRISTUPA, Z. B. & NIZNIK, H. B. 2001. Direct binding and functional coupling of alpha-synuclein to the dopamine transporters accelerate dopamine-induced apoptosis. *FASEB J,* 15**,** 916-26.

LEE, H. J., PATEL, S. & LEE, S. J. 2005. Intravesicular localization and exocytosis of alpha-synuclein and its aggregates. *J Neurosci,* 25**,** 6016-24.

LEE, H. J., SUK, J. E., BAE, E. J., LEE, J. H., PAIK, S. R. & LEE, S. J. 2008a. Assembly-dependent endocytosis and clearance of extracellular alpha-synuclein. *Int J Biochem Cell Biol,* 40**,** 1835-49.

LEE, H. J., SUK, J. E., BAE, E. J. & LEE, S. J. 2008b. Clearance and deposition of extracellular alpha-synuclein aggregates in microglia. *Biochem Biophys Res Commun,* 372**,** 423-8.

LESAGE, S. & BRICE, A. 2009. Parkinson's disease: from monogenic forms to genetic susceptibility factors. *Hum Mol Genet,* 18**,** R48-59.

LEVIN, J., GIESE, A., BOETZEL, K., ISRAEL, L., HOGEN, T., NUBLING, G., KRETZSCHMAR, H. & LORENZL, S. 2009. Increased alpha-synuclein aggregation following limited cleavage by certain matrix metalloproteinases. *Exp Neurol,* 215**,** 201-8.

LI, J. Y., ENGLUND, E., HOLTON, J. L., SOULET, D., HAGELL, P., LEES, A. J., LASHLEY, T., QUINN, N. P., REHNCRONA, S., BJORKLUND, A., WIDNER, H., REVESZ, T., LINDVALL, O. & BRUNDIN, P. 2008. Lewy bodies in grafted neurons in subjects with Parkinson's disease suggest host-to-graft disease propagation. *Nat Med,* 14**,** 501-3.

LI, J. Y., ENGLUND, E., WIDNER, H., REHNCRONA, S., BJORKLUND, A., LINDVALL, O. & BRUNDIN, P. 2010. Characterization of Lewy body pathology in 12- and 16-year-old intrastriatal mesencephalic grafts surviving in a patient with Parkinson's disease. *Mov Disord,* 25**,** 1091-6.

LI, Q. X., CAMPBELL, B. C., MCLEAN, C. A., THYAGARAJAN, D., GAI, W. P., KAPSA, R. M., BEYREUTHER, K., MASTERS, C. L. & CULVENOR, J. G. 2002. Platelet alpha- and gamma-synucleins in Parkinson's disease and normal control subjects. *J Alzheimers Dis,* 4**,** 309-15.

LI, W., WEST, N., COLLA, E., PLETNIKOVA, O., TRONCOSO, J. C., MARSH, L., DAWSON, T. M., JAKALA, P., HARTMANN, T., PRICE, D. L. & LEE, M. K. 2005. Aggregation promoting C-terminal truncation of alpha-synuclein is a normal cellular process and is enhanced by the familial Parkinson's disease-linked mutations. *Proc Natl Acad Sci U S A,* 102**,** 2162-7.

LIANI, E., EYAL, A., AVRAHAM, E., SHEMER, R., SZARGEL, R., BERG, D., BORNEMANN, A., RIESS, O., ROSS, C. A., ROTT, R. & ENGELENDER, S. 2004. Ubiquitylation of synphilin-1 and alpha-synuclein by SIAH and its presence in cellular inclusions and Lewy bodies imply a role in Parkinson's disease. *Proc Natl Acad Sci U S A,* 101**,** 5500-5.

LIM, K. L., DAWSON, V. L. & DAWSON, T. M. 2002. The genetics of Parkinson's disease. *Curr Neurol Neurosci Rep,* 2**,** 439-46.

LIU, C. W., GIASSON, B. I., LEWIS, K. A., LEE, V. M., DEMARTINO, G. N. & THOMAS, P. J. 2005. A precipitating role for truncated alpha-synuclein and the proteasome in alpha-synuclein aggregation: implications for pathogenesis of Parkinson disease. *J Biol Chem,* 280**,** 22670-8.

LONGHENA, F., FAUSTINI, G., SPILLANTINI, M. G. & BELLUCCI, A. 2019. Living in Promiscuity: The Multiple Partners of Alpha-Synuclein at the Synapse in Physiology and Pathology. *Int J Mol Sci,* 20.

LOTHARIUS, J., BARG, S., WIEKOP, P., LUNDBERG, C., RAYMON, H. K. & BRUNDIN, P. 2002. Effect of mutant alpha-synuclein on dopamine homeostasis in a new human mesencephalic cell line. *J Biol Chem,* 277**,** 38884-94.

LOTHARIUS, J. & BRUNDIN, P. 2002. Pathogenesis of Parkinson's disease: dopamine, vesicles and alpha-synuclein. *Nat Rev Neurosci,* 3**,** 932-42.

LOTHARIUS, J., FALSIG, J., VAN BEEK, J., PAYNE, S., DRINGEN, R., BRUNDIN, P. & LEIST, M. 2005. Progressive degeneration of human mesencephalic neuron-derived cells triggered by

dopamine-dependent oxidative stress is dependent on the mixed-lineage kinase pathway. *J Neurosci,* 25**,** 6329-42.

LUCKING, C. B. & BRICE, A. 2000. Alpha-synuclein and Parkinson's disease. *Cell Mol Life Sci,* 57**,** 1894-908.

LUK, K. C., KEHM, V., CARROLL, J., ZHANG, B., O'BRIEN, P., TROJANOWSKI, J. Q. & LEE, V. M. 2012. Pathological alpha-synuclein transmission initiates Parkinson-like neurodegeneration in nontransgenic mice. *Science,* 338**,** 949-53.

MA, K. L., SONG, L. K., YUAN, Y. H., ZHANG, Y., HAN, N., GAO, K. & CHEN, N. H. 2014. The nuclear accumulation of alpha-synuclein is mediated by importin alpha and promotes neurotoxicity by accelerating the cell cycle. *Neuropharmacology,* 82**,** 132-42.

MA, L., YANG, C., ZHANG, X., LI, Y., WANG, S., ZHENG, L. & HUANG, K. 2018. C-terminal truncation exacerbates the aggregation and cytotoxicity of alpha-Synuclein: A vicious cycle in Parkinson's disease. *Biochim Biophys Acta Mol Basis Dis,* 1864**,** 3714-3725.

MACLEAN, B. X., PRATT, B. S., EGERTSON, J. D., MACCOSS, M. J., SMITH, R. D. & BAKER, E. S. 2018. Using Skyline to Analyze Data-Containing Liquid Chromatography, Ion Mobility Spectrometry, and Mass Spectrometry Dimensions. *J Am Soc Mass Spectrom,* 29**,** 2182-2188.

MALEK, N., SWALLOW, D., GROSSET, K. A., ANICHTCHIK, O., SPILLANTINI, M. & GROSSET, D. G. 2014. Alpha-synuclein in peripheral tissues and body fluids as a biomarker for Parkinson's disease - a systematic review. *Acta Neurol Scand,* 130**,** 59-72.

MANNING-BOG, A. B., MCCORMACK, A. L., LI, J., UVERSKY, V. N., FINK, A. L. & DI MONTE, D. A. 2002. The herbicide paraquat causes up-regulation and aggregation of alpha-synuclein in mice: paraquat and alpha-synuclein. *J Biol Chem,* 277**,** 1641-4.

MAROTEAUX, L., CAMPANELLI, J. T. & SCHELLER, R. H. 1988. Synuclein: a neuron-specific protein localized to the nucleus and presynaptic nerve terminal. *J Neurosci,* 8**,** 2804-15.

MARTIN, L. J., PAN, Y., PRICE, A. C., STERLING, W., COPELAND, N. G., JENKINS, N. A., PRICE, D. L. & LEE, M. K. 2006. Parkinson's disease alpha-synuclein transgenic mice develop neuronal mitochondrial degeneration and cell death. *J Neurosci,* 26**,** 41-50.

MASLIAH, E., ROCKENSTEIN, E., VEINBERGS, I., MALLORY, M., HASHIMOTO, M., TAKEDA, A., SAGARA, Y., SISK, A. & MUCKE, L. 2000. Dopaminergic loss and inclusion body formation in alpha-synuclein mice: implications for neurodegenerative disorders. *Science,* 287**,** 1265-9.

MASUDA, M., SUZUKI, N., TANIGUCHI, S., OIKAWA, T., NONAKA, T., IWATSUBO, T., HISANAGA, S., GOEDERT, M. & HASEGAWA, M. 2006. Small molecule inhibitors of alpha-synuclein filament assembly. *Biochemistry,* 45**,** 6085-94.

MATSUMOTO, L., TAKUMA, H., TAMAOKA, A., KURISAKI, H., DATE, H., TSUJI, S. & IWATA, A. 2010. CpG demethylation enhances alpha-synuclein expression and affects the pathogenesis of Parkinson's disease. *PLoS One,* 5**,** e15522.

MAZZITELLI, S., FILIPELLO, F., RASILE, M., LAURANZANO, E., STARVAGGI-CUCUZZA, C., TAMBORINI, M., POZZI, D., BARAJON, I., GIORGINO, T., NATALELLO, A. & MATTEOLI, M. 2016. Amyloid-beta 1-24 C-terminal truncated fragment promotes amyloid-beta 1-42 aggregate formation in the healthy brain. *Acta Neuropathol Commun,* 4**,** 110.

MCCARTHY, J. J., LINNERTZ, C., SAUCIER, L., BURKE, J. R., HULETTE, C. M., WELSH-BOHMER, K. A. & CHIBA-FALEK, O. 2011. The effect of SNCA 3' region on the levels of SNCA-112 splicing variant. *Neurogenetics,* 12**,** 59-64.

MCKEITH, I. G., GALASKO, D., KOSAKA, K., PERRY, E. K., DICKSON, D. W., HANSEN, L. A., SALMON, D. P., LOWE, J., MIRRA, S. S., BYRNE, E. J., LENNOX, G., QUINN, N. P., EDWARDSON, J. A., INCE, P. G., BERGERON, C., BURNS, A., MILLER, B. L., LOVESTONE, S., COLLERTON, D., JANSEN, E. N., BALLARD, C., DE VOS, R. A., WILCOCK, G. K., JELLINGER, K. A. & PERRY, R. H. 1996. Consensus guidelines for the clinical and pathologic diagnosis of dementia with Lewy bodies (DLB): report of the consortium on DLB international workshop. *Neurology,* 47**,** 1113-24.

MENG, X., MUNISHKINA, L. A., FINK, A. L. & UVERSKY, V. N. 2010. Effects of Various Flavonoids on the alpha-Synuclein Fibrillation Process. *Parkinsons Dis,* 2010**,** 650794.

MICHELL, A. W., LUHESHI, L. M. & BARKER, R. A. 2005. Skin and platelet alpha-synuclein as peripheral biomarkers of Parkinson's disease. *Neurosci Lett,* 381**,** 294-8.

MILLER, D. W., HAGUE, S. M., CLARIMON, J., BAPTISTA, M., GWINN-HARDY, K., COOKSON, M. R. & SINGLETON, A. B. 2004. Alpha-synuclein in blood and brain from familial Parkinson disease with SNCA locus triplication. *Neurology,* 62**,** 1835-8.

MISHIZEN-EBERZ, A. J., NORRIS, E. H., GIASSON, B. I., HODARA, R., ISCHIROPOULOS, H., LEE, V. M., TROJANOWSKI, J. Q. & LYNCH, D. R. 2005. Cleavage of alpha-synuclein by calpain: potential role in degradation of fibrillized and nitrated species of alpha-synuclein. *Biochemistry,* 44**,** 7818-29.

MOLLENHAUER, B., CULLEN, V., KAHN, I., KRASTINS, B., OUTEIRO, T. F., PEPIVANI, I., NG, J., SCHULZ-SCHAEFFER, W., KRETZSCHMAR, H. A., MCLEAN, P. J., TRENKWALDER, C., SARRACINO, D. A., VONSATTEL, J. P., LOCASCIO, J. J., EL-AGNAF, O. M. & SCHLOSSMACHER, M. G. 2008. Direct quantification of CSF alpha-synuclein by ELISA and first cross-sectional study in patients with neurodegeneration. *Exp Neurol,* 213**,** 315-25.

MOLLENHAUER, B., LOCASCIO, J. J., SCHULZ-SCHAEFFER, W., SIXEL-DORING, F., TRENKWALDER, C. & SCHLOSSMACHER, M. G. 2011. alpha-Synuclein and tau concentrations in cerebrospinal fluid of patients presenting with parkinsonism: a cohort study. *Lancet Neurol,* 10**,** 230-40.

MOSHAROV, E. V., LARSEN, K. E., KANTER, E., PHILLIPS, K. A., WILSON, K., SCHMITZ, Y., KRANTZ, D. E., KOBAYASHI, K., EDWARDS, R. H. & SULZER, D. 2009. Interplay between cytosolic dopamine, calcium, and alpha-synuclein causes selective death of substantia nigra neurons. *Neuron,* 62**,** 218-29.

MULLER, C. M., DE VOS, R. A., MAURAGE, C. A., THAL, D. R., TOLNAY, M. & BRAAK, H. 2005. Staging of sporadic Parkinson disease-related alpha-synuclein pathology: inter- and intra-rater reliability. *J Neuropathol Exp Neurol,* 64**,** 623-8.

MULTIPLE-SYSTEM ATROPHY RESEARCH, C. 2013. Mutations in COQ2 in familial and sporadic multiple-system atrophy. *N Engl J Med,* 369**,** 233-44.

MURRAY, I. V., GIASSON, B. I., QUINN, S. M., KOPPAKA, V., AXELSEN, P. H., ISCHIROPOULOS, H., TROJANOWSKI, J. Q. & LEE, V. M. 2003. Role of alpha-synuclein carboxy-terminus on fibril formation in vitro. *Biochemistry,* 42**,** 8530-40.

NAKAJO, S., SHIODA, S., NAKAI, Y. & NAKAYA, K. 1994. Localization of phosphoneuroprotein 14 (PNP 14) and its mRNA expression in rat brain determined by immunocytochemistry and in situ hybridization. *Brain Res Mol Brain Res,* 27**,** 81-6.

NAKAMURA, K., NEMANI, V. M., AZARBAL, F., SKIBINSKI, G., LEVY, J. M., EGAMI, K., MUNISHKINA, L., ZHANG, J., GARDNER, B., WAKABAYASHI, J., SESAKI, H., CHENG, Y., FINKBEINER, S., NUSSBAUM, R. L., MASLIAH, E. & EDWARDS, R. H. 2011. Direct membrane association drives

mitochondrial fission by the Parkinson disease-associated protein alpha-synuclein. *J Biol Chem,* 286**,** 20710-26.

NARHI, L., WOOD, S. J., STEAVENSON, S., JIANG, Y., WU, G. M., ANAFI, D., KAUFMAN, S. A., MARTIN, F., SITNEY, K., DENIS, P., LOUIS, J. C., WYPYCH, J., BIERE, A. L. & CITRON, M. 1999. Both familial Parkinson's disease mutations accelerate alpha-synuclein aggregation. *J Biol Chem,* 274**,** 9843-6.

NARKIEWICZ, J., GIACHIN, G. & LEGNAME, G. 2014. In vitro aggregation assays for the characterization of alpha-synuclein prion-like properties. *Prion,* 8**,** 19-32.

NONAKA, T., WATANABE, S. T., IWATSUBO, T. & HASEGAWA, M. 2010. Seeded aggregation and toxicity of {alpha}-synuclein and tau: cellular models of neurodegenerative diseases. *J Biol Chem,* 285**,** 34885-98.

OH, S. H., KIM, H. N., PARK, H. J., SHIN, J. Y., KIM, D. Y. & LEE, P. H. 2017. The Cleavage Effect of Mesenchymal Stem Cell and Its Derived Matrix Metalloproteinase-2 on Extracellular alpha-Synuclein Aggregates in Parkinsonian Models. *Stem Cells Transl Med,* 6**,** 949-961.

OKOCHI, M., WALTER, J., KOYAMA, A., NAKAJO, S., BABA, M., IWATSUBO, T., MEIJER, L., KAHLE, P. J. & HAASS, C. 2000. Constitutive phosphorylation of the Parkinson's disease associated alpha-synuclein. *J Biol Chem,* 275**,** 390-7.

ORME, T., GUERREIRO, R. & BRAS, J. 2018. The Genetics of Dementia with Lewy Bodies: Current Understanding and Future Directions. *Curr Neurol Neurosci Rep,* 18**,** 67.

OTTOLINI, D., CALI, T., SZABO, I. & BRINI, M. 2017. Alpha-synuclein at the intracellular and the extracellular side: functional and dysfunctional implications. *Biol Chem,* 398**,** 77-100.

OUESLATI, A. 2016. Implication of Alpha-Synuclein Phosphorylation at S129 in Synucleinopathies: What Have We Learned in the Last Decade? *J Parkinsons Dis,* 6**,** 39-51.

OUESLATI, A., FOURNIER, M. & LASHUEL, H. A. 2010. Role of post-translational modifications in modulating the structure, function and toxicity of alpha-synuclein: implications for Parkinson's disease pathogenesis and therapies. *Prog Brain Res,* 183**,** 115-45.

PAPP, M. I., KAHN, J. E. & LANTOS, P. L. 1989. Glial cytoplasmic inclusions in the CNS of patients with multiple system atrophy (striatonigral degeneration, olivopontocerebellar atrophy and Shy-Drager syndrome). *J Neurol Sci,* 94**,** 79-100.

PARKINSON, J. 1817. An essay on the shaking palsy. 1817. *J Neuropsychiatry Clin Neurosci,* 14**,** 223-36; discussion 222.

PASANEN, P., MYLLYKANGAS, L., SIITONEN, M., RAUNIO, A., KAAKKOLA, S., LYYTINEN, J., TIENARI, P. J., POYHONEN, M. & PAETAU, A. 2014. Novel alpha-synuclein mutation A53E associated with atypical multiple system atrophy and Parkinson's disease-type pathology. *Neurobiol Aging,* 35**,** 2180 e1-5.

PEELAERTS, W., BOUSSET, L., VAN DER PERREN, A., MOSKALYUK, A., PULIZZI, R., GIUGLIANO, M., VAN DEN HAUTE, C., MELKI, R. & BAEKELANDT, V. 2015. alpha-Synuclein strains cause distinct synucleinopathies after local and systemic administration. *Nature,* 522**,** 340-4.

PENG, C., GATHAGAN, R. J., COVELL, D. J., MEDELLIN, C., STIEBER, A., ROBINSON, J. L., ZHANG, B., PITKIN, R. M., OLUFEMI, M. F., LUK, K. C., TROJANOWSKI, J. Q. & LEE, V. M. 2018a. Cellular milieu imparts distinct pathological alpha-synuclein strains in alpha-synucleinopathies. *Nature,* 557**,** 558-563.

PENG, C., GATHAGAN, R. J. & LEE, V. M. 2018b. Distinct alpha-Synuclein strains and implications for heterogeneity among alpha-Synucleinopathies. *Neurobiol Dis,* 109**,** 209-218.

PERIQUET, M., FULGA, T., MYLLYKANGAS, L., SCHLOSSMACHER, M. G. & FEANY, M. B. 2007. Aggregated alpha-synuclein mediates dopaminergic neurotoxicity in vivo. *J Neurosci,* 27**,** 3338-46.

POLINSKI, N. K., VOLPICELLI-DALEY, L. A., SORTWELL, C. E., LUK, K. C., CREMADES, N., GOTTLER, L. M., FROULA, J., DUFFY, M. F., LEE, V. M. Y., MARTINEZ, T. N. & DAVE, K. D. 2018. Best Practices for Generating and Using Alpha-Synuclein Pre-Formed Fibrils to Model Parkinson's Disease in Rodents. *J Parkinsons Dis,* 8**,** 303-322.

POLYMEROPOULOS, M. H., LAVEDAN, C., LEROY, E., IDE, S. E., DEHEJIA, A., DUTRA, A., PIKE, B., ROOT, H., RUBENSTEIN, J., BOYER, R., STENROOS, E. S., CHANDRASEKHARAPPA, S., ATHANASSIADOU, A., PAPAPETROPOULOS, T., JOHNSON, W. G., LAZZARINI, A. M., DUVOISIN, R. C., DI IORIO, G., GOLBE, L. I. & NUSSBAUM, R. L. 1997. Mutation in the alpha-synuclein gene identified in families with Parkinson's disease. *Science,* 276**,** 2045-7.

RABENSTEIN, M., BESONG AGBO, D., WOLF, E., DAMS, J., NICOLAI, M., ROEDER, A., BACHER, M., DODEL, R. C. & NOELKER, C. 2019. Effect of naturally occurring alpha-synuclein-antibodies on toxic alpha-synuclein-fragments. *Neurosci Lett,* 704**,** 181-188.

RAWLINGS, N. D., BARRETT, A. J., THOMAS, P. D., HUANG, X., BATEMAN, A. & FINN, R. D. 2018. The MEROPS database of proteolytic enzymes, their substrates and inhibitors in 2017 and a comparison with peptidases in the PANTHER database. *Nucleic Acids Res,* 46**,** D624-D632.

REYES, J. F., OLSSON, T. T., LAMBERTS, J. T., DEVINE, M. J., KUNATH, T. & BRUNDIN, P. 2015. A cell culture model for monitoring alpha-synuclein cell-to-cell transfer. *Neurobiol Dis,* 77**,** 266-75.

ROSTOVTSEVA, T. K., GURNEV, P. A., PROTCHENKO, O., HOOGERHEIDE, D. P., YAP, T. L., PHILPOTT, C. C., LEE, J. C. & BEZRUKOV, S. M. 2015. alpha-Synuclein Shows High Affinity Interaction with Voltage-dependent Anion Channel, Suggesting Mechanisms of Mitochondrial Regulation and Toxicity in Parkinson Disease. *J Biol Chem,* 290**,** 18467-77.

ROTT, R., SZARGEL, R., HASKIN, J., SHANI, V., SHAINSKAYA, A., MANOV, I., LIANI, E., AVRAHAM, E. & ENGELENDER, S. 2008. Monoubiquitylation of alpha-synuclein by seven in absentia homolog (SIAH) promotes its aggregation in dopaminergic cells. *J Biol Chem,* 283**,** 3316-28.

ROTT, R., SZARGEL, R., SHANI, V., HAMZA, H., SAVYON, M., ABD ELGHANI, F., BANDOPADHYAY, R. & ENGELENDER, S. 2017. SUMOylation and ubiquitination reciprocally regulate alpha-synuclein degradation and pathological aggregation. *Proc Natl Acad Sci U S A,* 114**,** 13176-13181.

SAVICA, R., GROSSARDT, B. R., BOWER, J. H., AHLSKOG, J. E. & ROCCA, W. A. 2013. Incidence and pathology of synucleinopathies and tauopathies related to parkinsonism. *JAMA Neurol,* 70**,** 859-66.

SCHERZER, C. R., GRASS, J. A., LIAO, Z., PEPIVANI, I., ZHENG, B., EKLUND, A. C., NEY, P. A., NG, J., MCGOLDRICK, M., MOLLENHAUER, B., BRESNICK, E. H. & SCHLOSSMACHER, M. G. 2008. GATA transcription factors directly regulate the Parkinson's disease-linked gene alpha-synuclein. *Proc Natl Acad Sci U S A,* 105**,** 10907-12.

SCHILDKNECHT, S., KARREMAN, C., POLTL, D., EFREMOVA, L., KULLMANN, C., GUTBIER, S., KRUG, A., SCHOLZ, D., GERDING, H. R. & LEIST, M. 2013. Generation of genetically-modified human differentiated cells for toxicological tests and the study of neurodegenerative diseases. *ALTEX,* 30**,** 427-44.

SCHOLZ, D., POLTL, D., GENEWSKY, A., WENG, M., WALDMANN, T., SCHILDKNECHT, S. & LEIST, M. 2011. Rapid, complete and large-scale generation of post-mitotic neurons from the human LUHMES cell line. *J Neurochem,* 119**,** 957-71.

SCOTT, D. & ROY, S. 2012. alpha-Synuclein inhibits intersynaptic vesicle mobility and maintains recycling-pool homeostasis. *J Neurosci,* 32**,** 10129-35.

SEVCSIK, E., TREXLER, A. J., DUNN, J. M. & RHOADES, E. 2011. Allostery in a disordered protein: oxidative modifications to alpha-synuclein act distally to regulate membrane binding. *J Am Chem Soc,* 133**,** 7152-8.

SEVLEVER, D., JIANG, P. & YEN, S. H. 2008. Cathepsin D is the main lysosomal enzyme involved in the degradation of alpha-synuclein and generation of its carboxy-terminally truncated species. *Biochemistry,* 47**,** 9678-87.

SHIBAYAMA-IMAZU, T., OKAHASHI, I., OMATA, K., NAKAJO, S., OCHIAI, H., NAKAI, Y., HAMA, T., NAKAMURA, Y. & NAKAYA, K. 1993. Cell and tissue distribution and developmental change of neuron specific 14 kDa protein (phosphoneuroprotein 14). *Brain Res,* 622**,** 17-25.

SHIN, Y., KLUCKEN, J., PATTERSON, C., HYMAN, B. T. & MCLEAN, P. J. 2005. The co-chaperone carboxyl terminus of Hsp70-interacting protein (CHIP) mediates alpha-synuclein degradation decisions between proteasomal and lysosomal pathways. *J Biol Chem,* 280**,** 23727-34.

SOMA, H., YABE, I., TAKEI, A., FUJIKI, N., YANAGIHARA, T. & SASAKI, H. 2006. Heredity in multiple system atrophy. *J Neurol Sci,* 240**,** 107-10.

SPILLANTINI, M. G., CROWTHER, R. A., JAKES, R., CAIRNS, N. J., LANTOS, P. L. & GOEDERT, M. 1998a. Filamentous alpha-synuclein inclusions link multiple system atrophy with Parkinson's disease and dementia with Lewy bodies. *Neurosci Lett,* 251**,** 205-8.

SPILLANTINI, M. G., CROWTHER, R. A., JAKES, R., HASEGAWA, M. & GOEDERT, M. 1998b. alpha-Synuclein in filamentous inclusions of Lewy bodies from Parkinson's disease and dementia with lewy bodies. *Proc Natl Acad Sci U S A,* 95**,** 6469-73.

SPILLANTINI, M. G., SCHMIDT, M. L., LEE, V. M., TROJANOWSKI, J. Q., JAKES, R. & GOEDERT, M. 1997. Alpha-synuclein in Lewy bodies. *Nature,* 388**,** 839-40.

SUNG, J. Y., PARK, S. M., LEE, C. H., UM, J. W., LEE, H. J., KIM, J., OH, Y. J., LEE, S. T., PAIK, S. R. & CHUNG, K. C. 2005. Proteolytic cleavage of extracellular secreted {alpha}-synuclein via matrix metalloproteinases. *J Biol Chem,* 280**,** 25216-24.

TATEBE, H., WATANABE, Y., KASAI, T., MIZUNO, T., NAKAGAWA, M., TANAKA, M. & TOKUDA, T. 2010. Extracellular neurosin degrades alpha-synuclein in cultured cells. *Neurosci Res,* 67**,** 341-6.

TEHRANIAN, R., MONTOYA, S. E., VAN LAAR, A. D., HASTINGS, T. G. & PEREZ, R. G. 2006. Alpha-synuclein inhibits aromatic amino acid decarboxylase activity in dopaminergic cells. *J Neurochem,* 99**,** 1188-96.

TERADA, M., SUZUKI, G., NONAKA, T., KAMETANI, F., TAMAOKA, A. & HASEGAWA, M. 2018. The effect of truncation on prion-like properties of alpha-synuclein. *J Biol Chem,* 293**,** 13910-13920.

TOBE, T., NAKAJO, S., TANAKA, A., MITOYA, A., OMATA, K., NAKAYA, K., TOMITA, M. & NAKAMURA, Y. 1992. Cloning and characterization of the cDNA encoding a novel brain-specific 14-kDa protein. *J Neurochem,* 59**,** 1624-9.

TOFARIS, G. K., GARCIA REITBOCK, P., HUMBY, T., LAMBOURNE, S. L., O'CONNELL, M., GHETTI, B., GOSSAGE, H., EMSON, P. C., WILKINSON, L. S., GOEDERT, M. & SPILLANTINI, M. G. 2006. Pathological changes in dopaminergic nerve cells of the substantia nigra and olfactory bulb in

mice transgenic for truncated human alpha-synuclein(1-120): implications for Lewy body disorders. *J Neurosci,* 26**,** 3942-50.

TOFARIS, G. K., KIM, H. T., HOUREZ, R., JUNG, J. W., KIM, K. P. & GOLDBERG, A. L. 2011. Ubiquitin ligase Nedd4 promotes alpha-synuclein degradation by the endosomal-lysosomal pathway. *Proc Natl Acad Sci U S A,* 108**,** 17004-9.

TRAN, H. T., CHUNG, C. H., IBA, M., ZHANG, B., TROJANOWSKI, J. Q., LUK, K. C. & LEE, V. M. 2014. Alpha-synuclein immunotherapy blocks uptake and templated propagation of misfolded alpha-synuclein and neurodegeneration. *Cell Rep,* 7**,** 2054-65.

TU, P. H., GALVIN, J. E., BABA, M., GIASSON, B., TOMITA, T., LEIGHT, S., NAKAJO, S., IWATSUBO, T., TROJANOWSKI, J. Q. & LEE, V. M. 1998. Glial cytoplasmic inclusions in white matter oligodendrocytes of multiple system atrophy brains contain insoluble alpha-synuclein. *Ann Neurol,* 44**,** 415-22.

TYANOVA, S., TEMU, T. & COX, J. 2016. The MaxQuant computational platform for mass spectrometry-based shotgun proteomics. *Nat Protoc,* 11**,** 2301-2319.

ULUSOY, A., FEBBRARO, F., JENSEN, P. H., KIRIK, D. & ROMERO-RAMOS, M. 2010. Co-expression of C-terminal truncated alpha-synuclein enhances full-length alpha-synuclein-induced pathology. *Eur J Neurosci,* 32**,** 409-22.

UVERSKY, V. N. 2003. A protein-chameleon: conformational plasticity of alpha-synuclein, a disordered protein involved in neurodegenerative disorders. *J Biomol Struct Dyn,* 21**,** 211-34.

UVERSKY, V. N., LI, J. & FINK, A. L. 2001a. Evidence for a partially folded intermediate in alpha-synuclein fibril formation. *J Biol Chem,* 276**,** 10737-44.

UVERSKY, V. N., LI, J. & FINK, A. L. 2001b. Metal-triggered structural transformations, aggregation, and fibrillation of human alpha-synuclein. A possible molecular NK between Parkinson's disease and heavy metal exposure. *J Biol Chem,* 276**,** 44284-96.

UVERSKY, V. N., LI, J. & FINK, A. L. 2001c. Pesticides directly accelerate the rate of alpha-synuclein fibril formation: a possible factor in Parkinson's disease. *FEBS Lett,* 500**,** 105-8.

UVERSKY, V. N., LI, J., SOUILLAC, P., MILLETT, I. S., DONIACH, S., JAKES, R., GOEDERT, M. & FINK, A. L. 2002. Biophysical properties of the synucleins and their propensities to fibrillate: inhibition of alpha-synuclein assembly by beta- and gamma-synucleins. *J Biol Chem,* 277**,** 11970-8.

VAN DER WATEREN, I. M., KNOWLES, T. P. J., BUELL, A. K., DOBSON, C. M. & GALVAGNION, C. 2018. C-terminal truncation of alpha-synuclein promotes amyloid fibril amplification at physiological pH. *Chem Sci,* 9**,** 5506-5516.

VAN HEESBEEN, H. J. & SMIDT, M. P. 2019. Entanglement of Genetics and Epigenetics in Parkinson's Disease. *Front Neurosci,* 13**,** 277.

VARGAS, K. J., SCHROD, N., DAVIS, T., FERNANDEZ-BUSNADIEGO, R., TAGUCHI, Y. V., LAUGKS, U., LUCIC, V. & CHANDRA, S. S. 2017. Synucleins Have Multiple Effects on Presynaptic Architecture. *Cell Rep,* 18**,** 161-173.

VINNAKOTA, R. L., YEDLAPUDI, D., MANDA, K. M., BHAMIDIPATI, K., BOMMAKANTI, K. T., RANGALAKSHMI, G. S. & KALIVENDI, S. V. 2018. Identification of an Alternatively Spliced alpha-Synuclein Isoform That Generates a 41-Amino Acid N-Terminal Truncated Peptide, 41-syn: Role in Dopamine Homeostasis. *ACS Chem Neurosci,* 9**,** 2948-2958.

VLAD, C., LINDNER, K., KARREMAN, C., SCHILDKNECHT, S., LEIST, M., TOMCZYK, N., RONTREE, J., LANGRIDGE, J., DANZER, K., CIOSSEK, T., PETRE, A., GROSS, M. L., HENGERER, B. & PRZYBYLSKI,

M. 2011. Autoproteolytic fragments are intermediates in the oligomerization/aggregation of the Parkinson's disease protein alpha-synuclein as revealed by ion mobility mass spectrometry. *Chembiochem,* 12**,** 2740-4.

VOLPICELLI-DALEY, L. A., GAMBLE, K. L., SCHULTHEISS, C. E., RIDDLE, D. M., WEST, A. B. & LEE, V. M. 2014. Formation of alpha-synuclein Lewy neurite-like aggregates in axons impedes the transport of distinct endosomes. *Mol Biol Cell,* 25**,** 4010-23.

VOLPICELLI-DALEY, L. A., LUK, K. C., PATEL, T. P., TANIK, S. A., RIDDLE, D. M., STIEBER, A., MEANEY, D. F., TROJANOWSKI, J. Q. & LEE, V. M. 2011. Exogenous alpha-synuclein fibrils induce Lewy body pathology leading to synaptic dysfunction and neuron death. *Neuron,* 72**,** 57-71.

WANG, W., NGUYEN, L. T., BURLAK, C., CHEGINI, F., GUO, F., CHATAWAY, T., JU, S., FISHER, O. S., MILLER, D. W., DATTA, D., WU, F., WU, C. X., LANDERU, A., WELLS, J. A., COOKSON, M. R., BOXER, M. B., THOMAS, C. J., GAI, W. P., RINGE, D., PETSKO, G. A. & HOANG, Q. Q. 2016. Caspase-1 causes truncation and aggregation of the Parkinson's disease-associated protein alpha-synuclein. *Proc Natl Acad Sci U S A,* 113**,** 9587-92.

WEINREB, P. H., ZHEN, W., POON, A. W., CONWAY, K. A. & LANSBURY, P. T., JR. 1996. NACP, a protein implicated in Alzheimer's disease and learning, is natively unfolded. *Biochemistry,* 35**,** 13709-15.

WERSINGER, C. & SIDHU, A. 2003. Attenuation of dopamine transporter activity by alpha-synuclein. *Neurosci Lett,* 340**,** 189-92.

WHITTAKER, H. T., QUI, Y., BETTENCOURT, C. & HOULDEN, H. 2017. Multiple system atrophy: genetic risks and alpha-synuclein mutations. *F1000Res,* 6**,** 2072.

WINSLOW, A. R., CHEN, C. W., CORROCHANO, S., ACEVEDO-AROZENA, A., GORDON, D. E., PEDEN, A. A., LICHTENBERG, M., MENZIES, F. M., RAVIKUMAR, B., IMARISIO, S., BROWN, S., O'KANE, C. J. & RUBINSZTEIN, D. C. 2010. alpha-Synuclein impairs macroautophagy: implications for Parkinson's disease. *J Cell Biol,* 190**,** 1023-37.

WONG, Y. C. & KRAINC, D. 2016. Lysosomal trafficking defects link Parkinson's disease with Gaucher's disease. *Mov Disord,* 31**,** 1610-1618.

WONG, Y. C. & KRAINC, D. 2017. alpha-synuclein toxicity in neurodegeneration: mechanism and therapeutic strategies. *Nat Med,* 23**,** 1-13.

XU, W., TAN, L. & YU, J. T. 2015. Link between the SNCA gene and parkinsonism. *Neurobiol Aging,* 36**,** 1505-18.

YAMASAKI, T. R., HOLMES, B. B., FURMAN, J. L., DHAVALE, D. D., SU, B. W., SONG, E. S., CAIRNS, N. J., KOTZBAUER, P. T. & DIAMOND, M. I. 2019. Parkinson's disease and multiple system atrophy have distinct alpha-synuclein seed characteristics. *J Biol Chem,* 294**,** 1045-1058.

ZARRANZ, J. J., ALEGRE, J., GOMEZ-ESTEBAN, J. C., LEZCANO, E., ROS, R., AMPUERO, I., VIDAL, L., HOENICKA, J., RODRIGUEZ, O., ATARES, B., LLORENS, V., GOMEZ TORTOSA, E., DEL SER, T., MUNOZ, D. G. & DE YEBENES, J. G. 2004. The new mutation, E46K, of alpha-synuclein causes Parkinson and Lewy body dementia. *Ann Neurol,* 55**,** 164-73.

ZHANG, J., LI, X. & LI, J. D. 2019. The Roles of Post-translational Modifications on alpha-Synuclein in the Pathogenesis of Parkinson's Diseases. *Front Neurosci,* 13**,** 381.

10. LIST OF PUBLICATIONS

Chakroun T, Evsyukov V, Nykänen NP, Höllerhage M, Schmidt A, Kamp F, Ruf VC, Wurst W, Rösler TW, Höglinger GU. Alpha-synuclein fragments trigger different aggregation pathways. Cell Death Dis. **11,** 84 (2020) doi:10.1038/s41419-020-2285-7.

Yi Tan, Carmelo Sgobio, Thomas Arzberger, Felix Machleid, Qilin Tang, Elisabeth Findeis, Jorg Tost, **Tasnim Chakroun**, Pan Gao, Mathias Höllerhage, Kai Bötzel, Jochen Herms, Günter Höglinger, Thomas Koeglsperger. Loss of fragile X mental retardation protein precedes Lewy pathology in Parkinson's disease. Acta Neuropathol (2019) doi:10.1007/s00401-019-02099-5

Fussi N, Höllerhage M, **Chakroun T**, Nykänen NP, Rösler TW, Koeglsperger T, Wurst W, Behrends C, Höglinger GU.Exosomal secretion of α-synuclein as protective mechanism after upstream blockage of macroautophagy. Cell Death Dis. 2018 Jul 9;9(7):757. doi: 10.1038/s41419-018-0816-2.

Höllerhage M , Moebius C, Melms J, Chiu WH, Goebel JN, **Chakroun T**, Koeglsperger T, Oertel WH, Rösler TW, Bickle M, Höglinger GU.Protective efficacy of phosphodiesterase-1 inhibition against alpha-synuclein toxicity revealed by compound screening in LUHMES cells. Sci Rep. 2017 Sep 13;7(1):11469. doi: 10.1038/s41598-017-11664-5.